ADVANCED PROCESS ANALYSIS SYSTEM

VOL. I

A Thesis

Submitted to the Graduate Faculty of the
Louisiana State University and
Agriculture and Mechanical College
in partial fulfillment of the
requirements for the degree of
Master of Science in Chemical Engineering

in

The Department of Chemical Engineering

by
Kedar Shivanand Telang
B.S., Indian Institute of Technology, Bombay, 1996
December 1998

ACKNOWLEDGMENTS

The author wishes to express his appreciation and gratitude to Professor Ralph W. Pike for giving him the opportunity to participate in this research work. His guidance and assistance are deeply appreciated. The examining committee members, Professor F. Carl Knopf and Professor Karsten Thompson are recognized for their efforts in reviewing and evaluating this research.

The cooperation of engineers and managers of the IMC Agrico Company was invaluable in this research. The assistance of Mr. Thomas A. Hertwig of IMC Agrico is especially acknowledged for providing the detailed information and data for the sulfuric acid process. In addition, the assistance of Ms. Gayathri Srinivasan and Mr. Tai Lee in Visual Basic programming was invaluable.

The financial support for this research by the Environment Protection Agency is gratefully acknowledged. Also, the Department of Chemical Engineering at Louisiana State University is recognized for its assistance and support.

Finally, the author would like to acknowledge the support and encouragement of friends and family during his post graduate study.

TABLE OF CONTENTS

VOLUME I

LIST OF TABLES

LIST OF FIGURES

CHAPTER 1 INTRODUCTION

This chapter introduces the Advanced Process Analysis System and its component programs. Also, it describes the framework used for energy conservation and pollution prevention in chemical plants and refineries.

A. An Overview of the Advanced Process Analysis System

An Advanced Process Analysis System is a powerful tool for use by process and plant engineers to perform comprehensive and in-depth evaluations of economic, environmental, safety and hazard analysis projects. This system is based on chemical engineering fundamentals such as stoichiometry, thermodynamics, fluid dynamics, heat transfer, mass transfer, reactor design and optimization. It identifies pollutants in chemical processes and petroleum refineries and develops innovative, economically viable designs to eliminate their generation. It aims at waste minimization and pollution prevention in chemical plants, in addition to increased profit and improved efficiency of operations.

The methodology of the Advanced Process Analysis System is based on the framework shown in Figure 1.1. The main components of this system are an on-line optimization program, a flowsheeting program for process material and energy balances, a chemical reactor analysis program, a heat exchanger network design program, and a pollution assessment module. A Windows interface is used to integrate these programs into one user-friendly application.

B. The Component Programs

B-1. Flowsheeting

Process flowsheeting programs perform steady-state material and energy balances

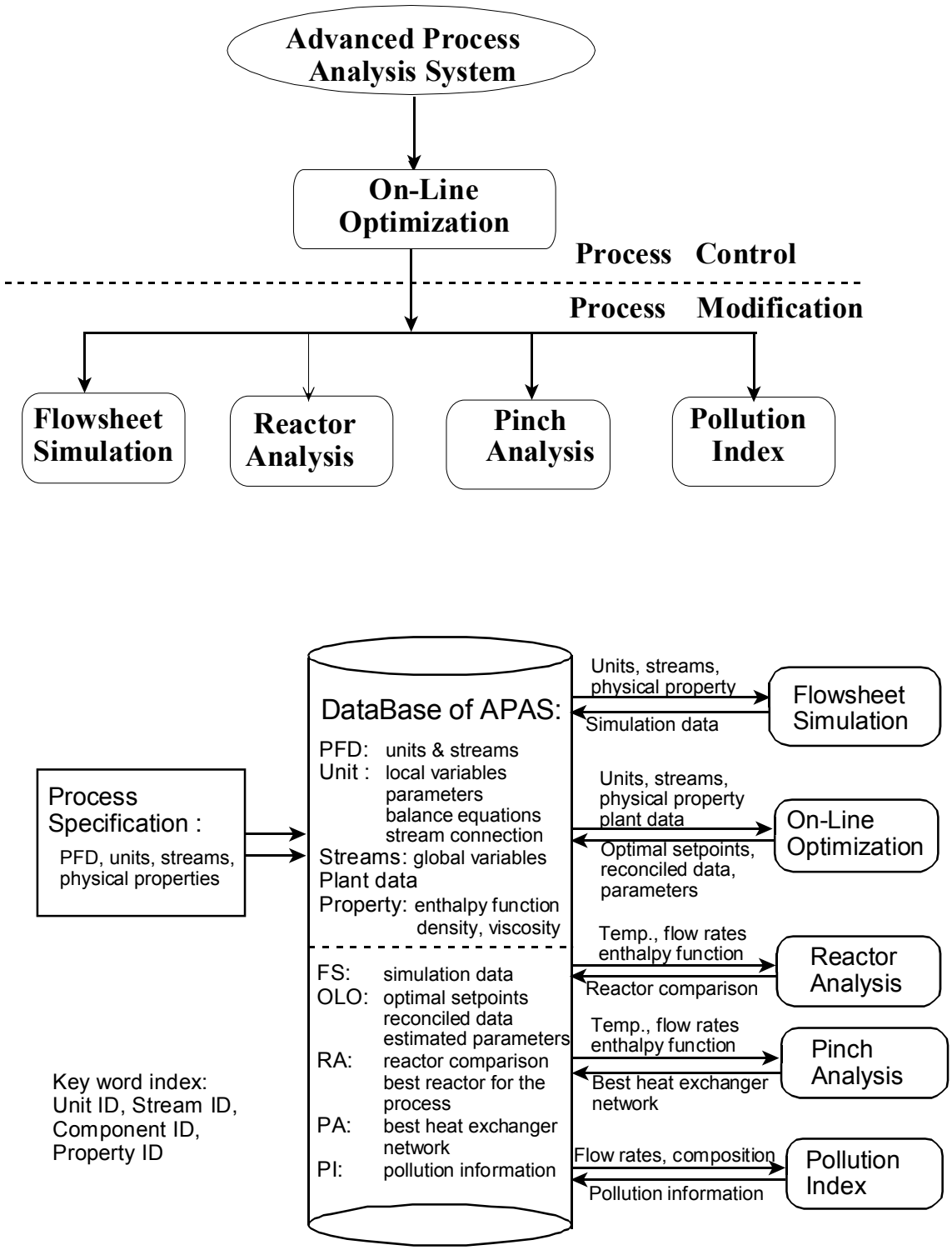

Figure 1.1: The Framework of the Advanced Process Analysis System

on a plant as specified by the process flow diagram and information about feeds and products. They contain sophisticated subroutines for predicting physical and thermodynamic properties of species in the process, and they can size separation units and simple chemical reactors. Many have the capability of estimating the various costs for construction of a new plant based on the process flow diagram and perform discounted cash flow calculations for economic evaluations. Also, many incorporate an optimization algorithm to predict the material and energy flows and equipment sizes for minimum cost. Although typically used for process design, they can be used effectively for process simulation of existing plants to conduct retrofit and debottlenecking evaluations. They can be used as the process simulation for on-line optimization. They contain efficient algorithms for solving large sets of non-linear algebraic equations. Newer features include interactive user interfaces that allow the engineer to assemble the process flow diagram graphically and perform the material and energy balance calculations. The result of this program gives composition and properties of all the process streams and information about operation of the individual units. ASPEN, HYSIM and PROII are some of the widely used flowsheeting programs.

B-2. Chemical Reactor Design Program

Process flowsheeting programs have limited capability to simulate complex chemical reactors. Consequently, the chemical reactor design is done on a case-by-case basis. The chemical reactor analysis program is a comprehensive, interactive computer simulation for three-phase catalytic gas-liquid reactors and their subsets, and an outline is shown in Figure 1.2. It has been developed by Professor Hopper and his research group at Lamar University (Saleh et al., 1995). It has a wide range of applications such as oxidation,

hydrogenation, hydrodesulfurization, hydrocracking and Fischer-Tropsch synthesis. This program interactively guides the engineer to select the best reactor design for the reacting system based on the characteristics of ten different types of industrial catalytic gas-liquid reactors which includes catalyst particle diameter and loading, diffusivities, flow regimes, gas-liquid and liquid-solid mass transfer rates, gas and liquid dispersions, heat transfer, holdup among others. The program solves the conservation equations and it has checks for the validity of the design, e.g., not allowing a complete catalyst-wetting factor if the liquid flowrate is not sufficient. A complete user's manual is available.

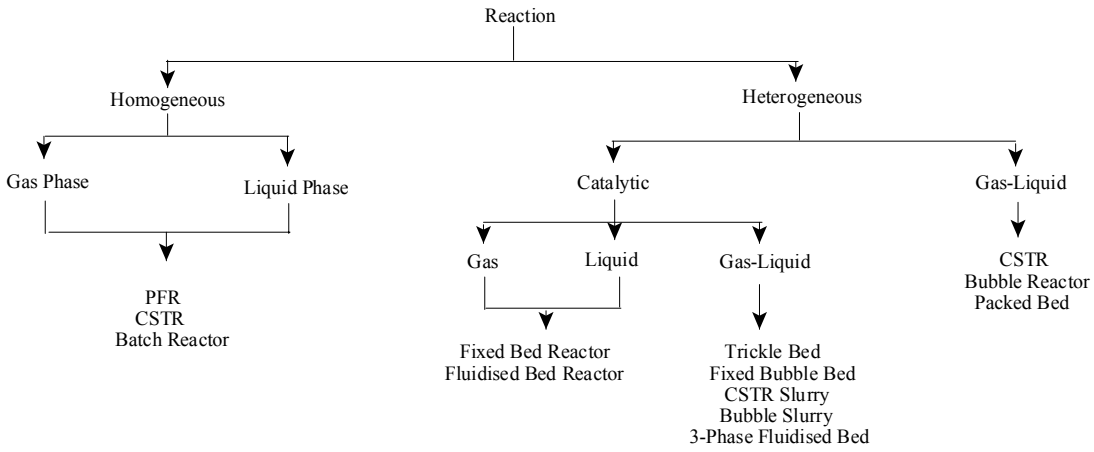

Figure 1.2: The Reactor Design Program Outline

B-3. Heat Exchanger Network Optimization

Heat exchanger network optimization deals with minimizing the use of external utilities by increasing the energy recovery in the process. Also, it aims at synthesizing a network that is feasible and has a low investment cost.

Pinch technology was developed in the late 1970's as a method for the design of heat exchanger networks, and it has since been extended to site energy integration including distillation and utility systems, mass exchangers and a number of other

applications. It employs three concepts: the composite curves, the grid diagram of process streams and the pinch point; and these are applied to minimize energy use in the process. Illustrations of composite curves and the grid diagram are shown in Figure 1.3 and Figure 1.4 respectively. The composite curves are plots of temperatures as a function of enthalpy from the material and energy balances for the streams that need to be heated called cold streams and those that need to be cooled called hot streams. From the composite curves of the hot and cold streams, the potential for energy exchange between the hot and cold streams can be determined as well as the process requirements for external heating and cooling from utilities such as steam and cooling water. The network grid diagram graphically shows the heaters, coolers and heat exchangers arrangement in the system. This can be helpful in selection of utilities and appropriate placement of boilers, turbines, distillation columns, evaporators and furnaces.

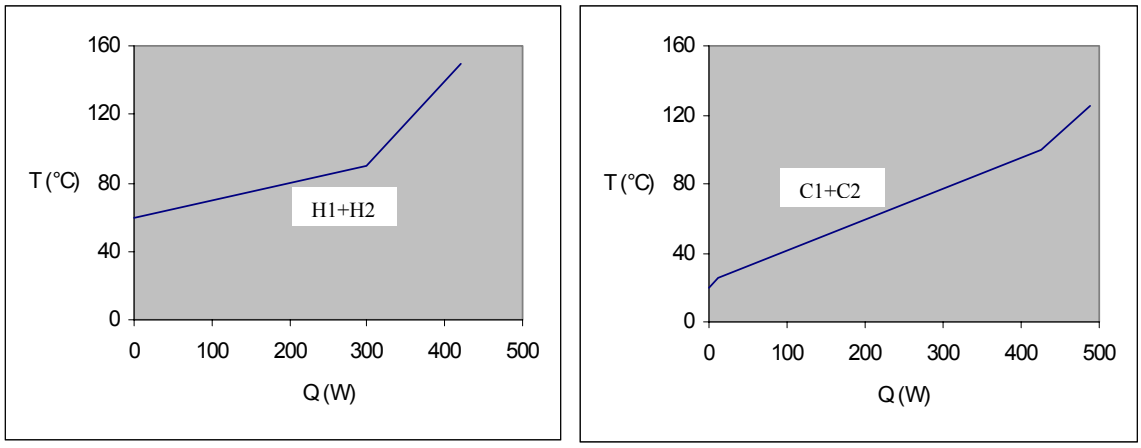

Figure 1.3: The Composite Curves for Hot Streams (on the left side) and Cold Streams (on the right side) for the Simple Process

HEXTRAN, SUPERTARGET and ASPEN PINCH are some of the commonly used commercial heat exchanger design programs. Also, newer approaches in the subject of heat exchanger network design are based on mathematical programming techniques. These have

been made possible by advances in computer science in both software and hardware. These methods formulate the network design as a linear or nonlinear optimization problem, which is solved using a package like GAMS (General Algebraic Modeling System).

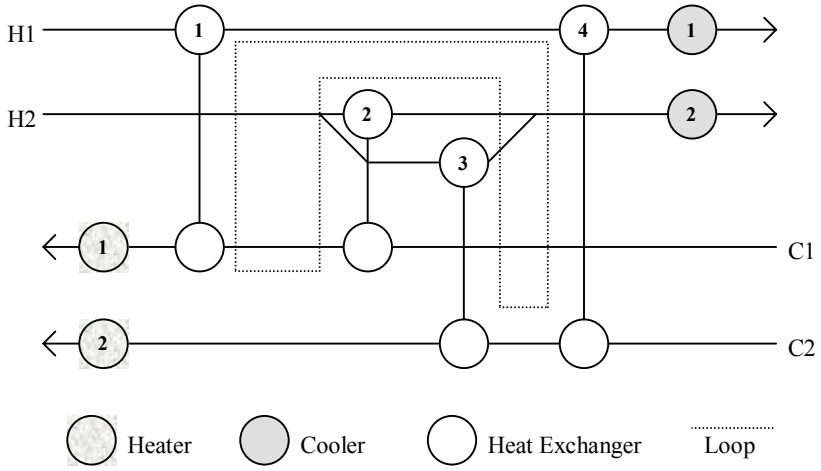

Figure 1.4: The Grid Diagram

B-4. Online Optimization

On-line optimization is the use of an automated system which adjusts the operation of a plant based on product scheduling and production control to maximize profit and minimize emissions by providing setpoints to the distributed control system. This is illustrated in Figure 1.5. Plant data is sampled from the distributed control system, and gross errors are removed from it. Then, the data is reconciled to be consistent with the material and energy balances of the process. An economic model is used to compute the profit for the plant and the plant model is used to determine the operating conditions, e.g. temperatures, pressures, flowrates of the various streams. These are variables in the material and energy balance of the plant model. The plant and economic model are together used with an optimization algorithm to determine the best operating conditions (e.g.

temperatures, pressures etc.) which maximizes the profit. These optimal operating

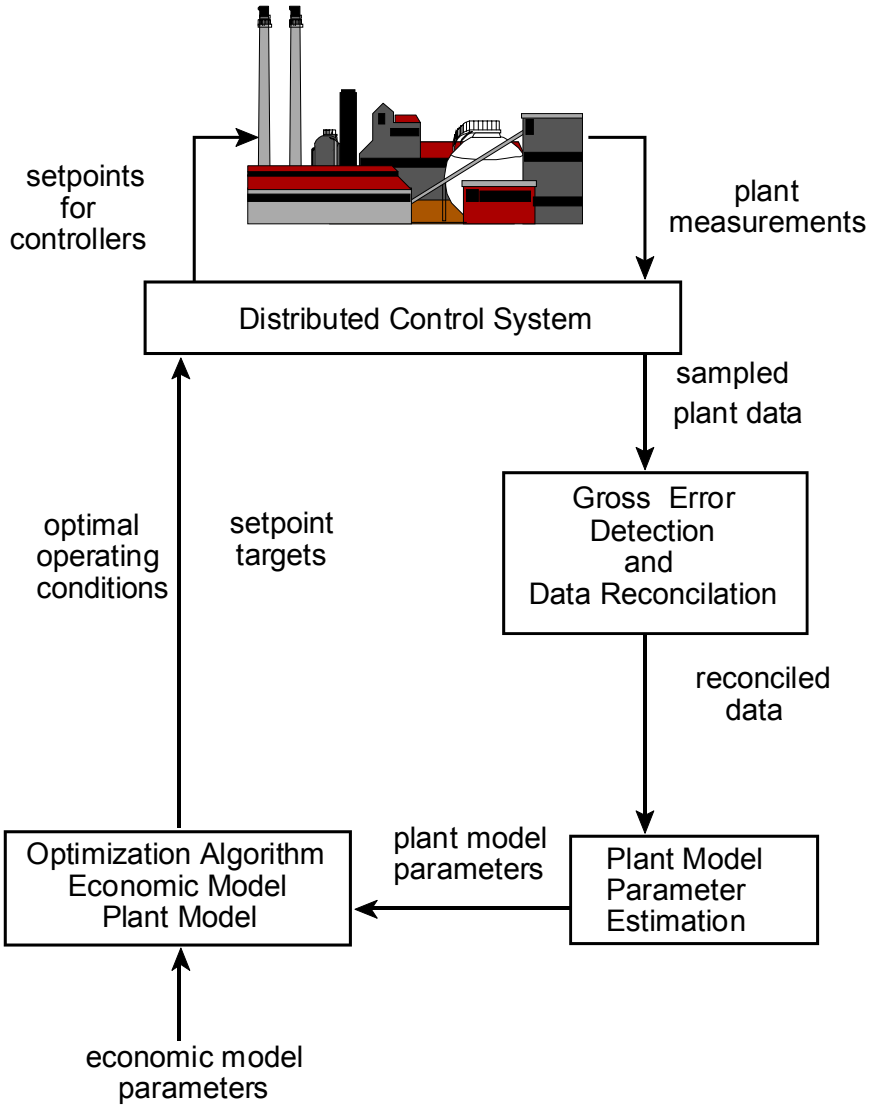

Figure 1.5: Simplified Structure of Online Optimization

conditions are then sent to the distributed control system to provide setpoints for the controllers.

B-5. Pollution Assessment Module

The pollution assessment program measures the pollution impact of a chemical

process on the environment. Coupled with an optimization package, it can be used to aid in pollution prevention in many different areas. There is a wealth of information available on pollution prevention methods for chemical and refinery processes. Some of the newer methods being developed are Clean Process Advisory System (CPAS), the Waste Reduction Algorithm (WAR), the Program for Assisting the Replacement of Industrial Solvents (Paris Algorithm), the Mass Exchange Network Methodology (MEN), and the Environmentally Acceptable Reaction Methodology (EAR). The pollution assessment module of the Advanced Process Analysis System is called as the 'Pollution Index Program' and it is based on the Waste Reduction Algorithm (WAR).

C. Summary

Thus, the Advanced Process Analysis System offers a combination of powerful process design and modification tools. The windows interface integrates all of these into one system and makes the application very user-friendly. It minimizes the load on the process engineer by automating most of the tasks but at the same time, it offers him complete control over the system.

The next chapter reviews the current status of literature on the techniques incorporated in the Advanced Process Analysis System with a focus on the methods for Heat Exchanger Network Synthesis (HENS) and the Waste Reduction Algorithm (WAR).

CHAPTER 2 LITERATURE REVIEW

This chapter will review the current status of the methodology and literature for the methods used in the Advanced Process Analysis System. Also, it gives a detailed description of the advances in heat exchanger network design methods and the WAR algorithm for pollution prevention.

A. Advanced Process Analysis System

The Advanced Process Analysis System based on the framework given in Figure 1.1 includes chemical reactor analysis, process flowsheeting, pinch analysis and on-line optimization. Currently, all of these are done using separate computer programs developed specifically for each of these purposes. However, all of these programs use the same information including a plant simulation (material and energy balances, rate equations and equilibrium relations). So, a more advanced and integrated approach is required for process analysis.

There are several descriptions in the literature of the need for an integrated approach to process analysis. Van Reeuwijk et al. (1993) proposed having a team of computer aided process engineering expert and a process engineer with technology knowledge to develop energy efficient chemical processes. A process engineer software environment is described by Ballinger et al. (1994) called '*epee'* whose goal is have to a user interface to create and manipulate objects such as processes, streams and components with sharing of data among process engineering applications in an open distributed environment. The Clean Process Advisory System (CPAS) has been described by Baker et al.(1995) as a computer based pollution prevention process and product design system that contains ten PC software tools being developed by an

industry-government-university team. This includes technology selection and sizing, potential and designs, physical property data, materials locators and regulatory guidance information. An article by Shaney (1995) describes the various modeling software and databases available for process analysis and design. A review of computer aided process engineering by Winter (1992) predicts linking various applications will result in better quality of process design, better plant operations and increased productivity. It also describes the PRODABAS concept, which focuses on capturing information from multiple sources into a common multi-user framework for analysis, process definition and process engineering documentation rather than the original concept of a common user interface and datastore linked with a range of applications computing tools. Thus, an Advanced Process Analysis System has potential for effective implementation of energy conservation and pollution prevention methods.

B. Energy Conservation

Heat Exchanger Network Synthesis (HENS) for maximum heat recovery is the key to energy conservation in a chemical plant. The problem of design and optimization of heat exchanger networks has received considerable attention over the last two decades.

The problem of HENS can be defined as the determination of cost-effective network to exchange heat among a set of process streams where any heating and cooling that is not satisfied by exchange among these streams must be provided by external utilities (Shenoy, 1995). Also, a minimum temperature difference is required between streams exchanging heat. This is called as the Minimum Approach Temperature.

B-1. Heuristic Approaches

The above HENS problem was first formulated by Masso and Rudd (1969). At that time, the design methods were generally based on heuristic approaches. One of the commonly used rules was to match the hottest stream with the coldest stream. Several other methods were based on tree search techniques (Lee et al., 1970). This generally led to feasible but non-optimal solutions.

B-2. Pinch Analysis

Hohmann (1971) made significant contributions to the development of the thermodynamic approach. In the late 1970s, Linnhoff and Hindmarsh (Linnhoff et al., 1979) first introduced Pinch Analysis; a method based on thermodynamic principles. They also introduced a number of important concepts, which formed the basis for further research. These concepts have been reviewed by Gundersen et al. (1987). Some of the important ones are discussed below.

C. Concepts

C-1. Temperature Intervals

The process is divided into a number of temperature intervals as shown in Figure 2.1 for an example process. The division is based on the supply and target temperatures of the various hot and cold streams, and the minimum approach temperature (ΔT_{min}). The limits of these intervals are calculated as follows.

ΔT_{min} /2 is subtracted from the hot stream temperatures and ΔT_{min} /2 is added to the cold stream temperatures. These temperatures are then sorted in descending order, omitting temperatures common to both hot and cold streams. These temperatures form the limits of the intervals.

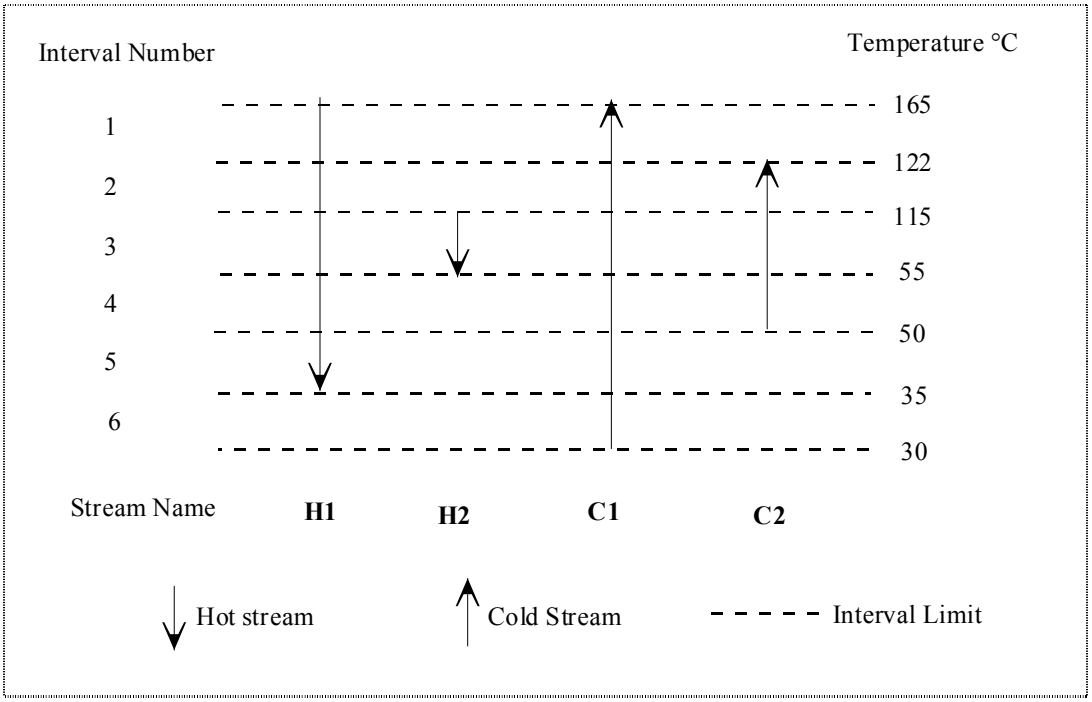

Figure 2.1 The Temperature Intervals

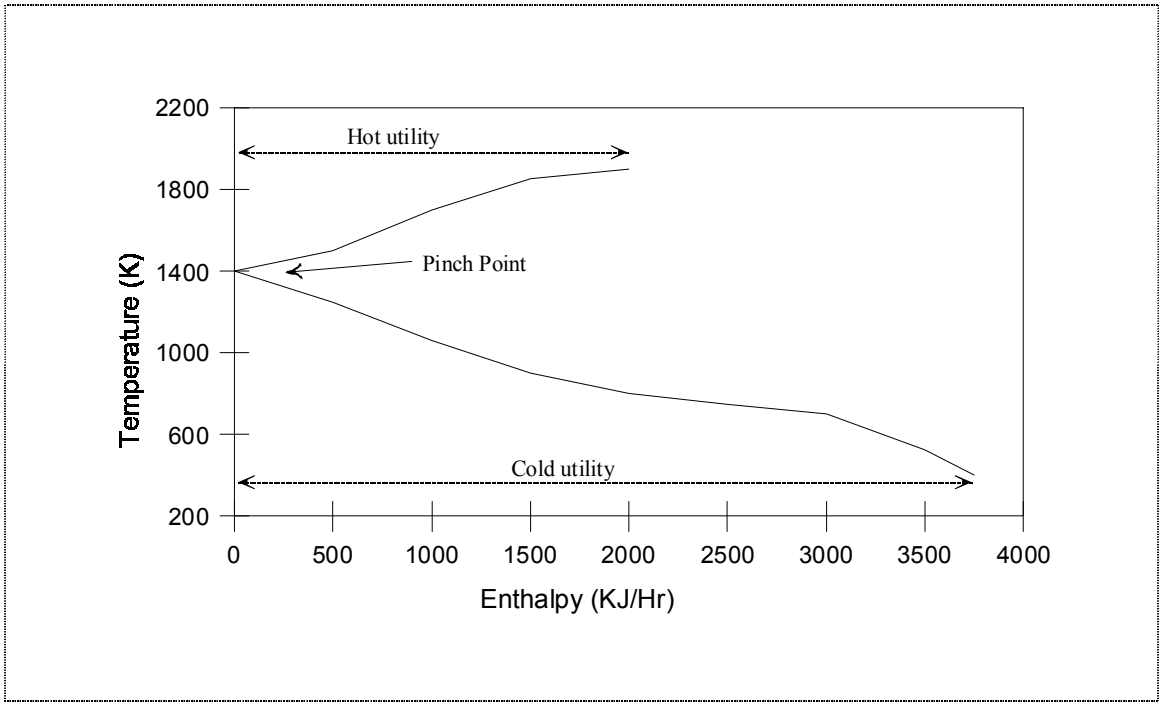

Figure 2.2 The Grand Composite Curve

C-2. Heat Cascade Diagram

In each temperature interval, the amount of enthalpy surplus is calculated by subtracting the enthalpy deficit of the cold streams from the enthalpy excess of the hot streams. The enthalpy surplus in each interval is cascaded down to the intervals below. This cascading is based on the simple thermodynamic principle that heat can only be transferred from a higher temperature to lower temperature. The representation of the heat cascade diagram in form of a table is also called as 'Problem Table Algorithm'.

C-3. Grand Composite Curve

The heat cascade diagram gives the amount of net surplus enthalpy in each interval after cascading. A plot of these cascaded heat amounts versus the interval temperatures is called as the 'Grand Composite Curve' (GCC) as shown in Figure 2.2. It is a complete representation of the heat flows in the process. The region of the GCC with a positive slope shows the process segment which needs external heat supply whereas the region with a negative slope shows the segment that needs to reject heat. It shows not only the amount of hot and cold utility required but also their temperature levels, which is useful in deciding the appropriate placement of the utilities.

C-4. Heat Recovery Pinch

This is the single most important concept in the methodology of pinch analysis. The point on the Grand Composite Curve where the heat flow is equal to zero is called the Pinch Point, and the corresponding temperature is called the Pinch Temperature. The pinch divides the process into two thermodynamically separate regions called 'above the pinch' and 'below the pinch'. Above the pinch, only hot utility is required and below the pinch, only cold utility is required. Any cooling provided above the pinch

results in an equal increase in the heating requirement below the pinch, thus incurring a double penalty.

C-5. Stream Grid Diagram

This is a convenient way of representing the hot and cold streams, the process and utility pinches and the heat exchanger network, and an example is shown in Figure 1.4. It illustrates heat load loops and paths, stream splitting and mixing in a very convenient manner.

D. Targeting

In addition to these concepts, Linnhoff and coworkers proposed a number of 'Targeting' algorithms. Targeting means predicting what is the best performance that can possibly be achieved by the system before attempting to achieve it. The targeting procedure allows the engineer to determine the minimum utility requirement, number of units, area of heat exchangers and the investment cost prior to the actual design of the network for a specified minimum approach temperature. These procedures are briefly summarized below.

D-1. Utility (Linnhoff and Flower, 1978)

The utility targets can be read off simply from the Grand Composite Curve. The amount of heat flow at the highest temperature level in the process corresponds to the amount of minimum hot utility. The amount of heat flow at the lowest temperature level corresponds to the amount of minimum cold utility. A heat exchanger network that uses the minimum amount of both, hot and cold utilities is called a 'Maximum Energy Recovery' network (MER).

D-2. Number of units (Linnhoff et al., 1979)

The minimum number of units needed to achieve a MER network can be calculated based on Euler's Network Theorem from the graph theory. The theorem can be stated in the context of HENS as follows: (Linnhoff et al., 1979)

$$N_u = N_s + N_l - N_p \quad (2.1)$$

where N_u is the minimum number of units, N_s is the number of process and utility streams, N_l is the number of loops and N_p is the number of independent sub-problems. A loop is any path in the network that starts at some point and returns to the same point. A sub-problem is a set of streams, which is perfectly matched (i.e. the streams which are in enthalpy balance with each other).

For an MER network, the number of independent sub-problems (N_p) is equal to 2 because the pinch point divides the problem into two thermodynamically separate regions, above the pinch and below the pinch. We apply equation 2.1 to each of the sub-problems. The sub-problems don't have any loops and can not be divided into smaller independent parts. Therefore, for the sub-problems, N_l is equal to 0 and N_p is equal to 1. Substituting these values into equation 2.1, we get the following equations

$$N_{u,a} = N_a - 1 \quad \text{and} \quad N_{u,b} = N_b - 1 \quad (2.2)$$

where $N_{u,a}$ is the minimum number of units required above the pinch, $N_{u,b}$ is the minimum number units below the pinch, N_a is the number of streams (process and utility) present above the stream and N_b is the number of streams (process and utility) present below the pinch.

The minimum number of units needed for the entire process is equal to the addition of the number of units needed for the sub-problems. Therefore, the minimum number of units for the process is given by the following equation.

$$N_{u,mer} = N_{u,a} + N_{u,b} = N_a + N_b - 2 \quad (2.3)$$

D-3. Heat Exchanger Area (Townsend and Linnhoff, 1984)

Area targeting involves calculation of the minimum surface area for heat transfer among hot streams, cold streams and utilities in a HEN that is to be designed. Townsend and Linnhoff (1984) introduced a new area targeting method, which takes into account individual heat transfer coefficients for the process streams. In this method, the process is first divided into a number of temperature intervals based on the pinch temperature as explained earlier. Next the log mean temperature difference is calculated as for each of the intervals as follows.

For temperature interval i, let $T_{u,i}$ be the upper limit and $T_{l,i}$ be the lower limit. ΔT_{min} /2 is added to both the limits to obtain the hot stream temperatures ($T_{hu,i}$ and $T_{hl,i}$). Similarly, ΔT_{min} /2 is subtracted from both the limits to obtain the cold stream temperatures ($T_{cu,i}$ and $T_{cl,i}$).

$$T_{hu,i} = T_{u,i} + \Delta T_{min}/2, \quad T_{hl,i} = T_{l,i} + \Delta T_{min}/2$$

$$T_{cu,i} = T_{u,i} - \Delta T_{min}/2, \quad T_{cl,i} = T_{l,i} - \Delta T_{min}/2 \quad (2.4)$$

The log mean temperature difference for interval i, ΔT_{LMi} can be calculated using the following equation.

$$\Delta T_{LM_i} = \frac{(T_{hu,i} - T_{cu,i}) - (T_{hl,i} - T_{cl,i})}{\log(\frac{T_{hu,i} - T_{cu,i}}{T_{hl,i} - T_{cl,i}})} \quad (2.5)$$

Each of the temperature intervals has some hot streams (process and utility) and some cold streams (process and utility). It is assumed that each hot stream exchanges heat with each cold stream in the same interval. Each of these matches corresponds to a heat exchanger in that interval. So, if temperature interval i has nh number of hot streams and nc number of cold streams, it has nh*nc number of heat exchangers. Let R_i denote the set of hot streams in the interval i and let S_i denote the set of cold streams. The heat exchanger between hot stream r ($r \in R$) and cold stream s ($s \in S$) has area equal to

$$A_{r,s} = \frac{1}{\Delta T_{LM_i}} * \frac{Q_{r,s}}{U_{r,s}} \tag{2.6}$$

where Q_{rs} is the amount of heat exchange in the exchanger and U_{rs} is the overall heat transfer coefficient of the exchanger.

The overall heat transfer coefficient U_{rs} can be approximated by the equation

$$\frac{1}{U_{rs}} = \frac{1}{h_r} + \frac{1}{h_s} \tag{2.7}$$

where h_r is the film heat transfer coefficient of stream r and h_s is the film heat transfer coefficient of stream s.

Substitution of equation 2.7 in equation 2.6 gives the following equation

$$A_{r,s} = \frac{1}{\Delta T_{LM_i}} * Q_{rs} * (\frac{1}{h_r} + \frac{1}{h_s}) \tag{2.8}$$

Summation over all the hot and cold streams gives A_i, the total area of heat exchangers in interval i.

$$A_i = \sum_r \sum_s A_{r,s} = \sum_r \sum_s \frac{1}{\Delta T_{LM_i}} * Q_{rs} * (\frac{1}{h_r} + \frac{1}{h_s}) \tag{2.9}$$

Rearranging the summations,

$$A_i = \sum_r \sum_s A_{rs} = \frac{1}{\Delta T_{LM_i}} (\sum_r \sum_s \frac{Q_{rs}}{h_r} + \sum_r \sum_s \frac{Q_{rs}}{h_s}) \tag{2.10}$$

Further simplification gives

$$A_i = \sum_r \sum_s A_{rs} = \frac{1}{\Delta T_{LM_i}} (\sum_r \frac{1}{h_r} \sum_s Q_{rs} + \sum_s \frac{1}{h_s} \sum_r Q_{rs}) \tag{2.11}$$

$\sum_s Q_{rs}$ is the total amount of heat given out by hot stream r to all the cold streams in the temperature interval i. Let this amount be represented as Δq_r. $\sum_r Q_{rs}$ is the total amount of heat given out by cold stream s to all the cold streams in the temperature interval i. Let this amount be represented as Δq_s. Equation 2.11 can now be written as

$$A_i = \frac{1}{\Delta T_{LM_i}} (\sum_r \frac{\Delta q_r}{h_r} + \sum_s \frac{\Delta q_s}{h_s}) \tag{2.12}$$

The first term in equation 2.12 is for the set of hot streams in interval i and, the second term is for the set of cold streams. We can combine the two terms into one by defining a set K which includes all the hot as well as cold streams in the interval i. Equation 2.12 is rewritten as

$$A_i = \frac{1}{\Delta T_{LM_i}} \sum_k \frac{\Delta q_k}{h_k} \tag{2.13}$$

where k is any stream which belongs to the set K of all the process streams in temperature interval i. The total area of all the heat exchangers in the process can now be calculated by summing over all the temperature intervals as given in equation 2.14. This estimate for the total area is the minimum area needed for synthesizing an MER network for the given process.

$$A_{\min} = \sum_i A_i = \sum_i \frac{1}{\Delta T_{LM_i}} \sum_k \frac{\Delta q_k}{h_k} \tag{2.14}$$

where h_k is the film heat transfer coefficient of stream k ; Δq_k is the amount of heat to be given or absorbed by the stream k in temperature interval i and, ΔT_{LM_i} is the log mean temperature difference in interval i.

Essentially, the heat exchanger area needed in each temperature interval is calculated from the heat transfer load in that interval and the film heat transfer coefficients of the process streams. Then, these areas are added to get an estimate of the total area. The film heat transfer coefficients can be obtained in any of the following ways (Smith, 1995):

1. Tabulated experience values
2. By assuming a reasonable fluid velocity, together with fluid physical properties, standard heat transfer correlations can be used.
3. If the pressure drop available for the stream is known, the expressions of Polley et al. (1990) can be used.

Reddy et al.(1998) have suggested the use of a correction factor to account for the partial cross flow in a multi-pass heat exchanger. The design equation for multi-pass heat exchangers is

$$Q = U\ A\ F\ \Delta T_{LM} \tag{2.15}$$

where F is the correction factor. The work of Bowmen et al. (1940) provides the value of F for different shell and tube pass combinations.

D-4. Cost Target (Ahmad, 1985)

The total heat exchanger network cost comprises of the operating cost and the capital cost. The operating cost is the cost of the utilities and is given by

$$CO = C_{hu}\ Q_{hu,min} + C_{cu}\ Q_{cu,min} \tag{2.16}$$

where C_{hu} is the cost of unit hot utility and C_{cu} is the cost of unit cold utility. $Q_{hu,min}$ is the minimum hot utility and $Q_{cu,min}$ is the minimum cold utility required.

The capital cost for a single exchanger is given by

$$C_{Ci} = a + b\ A_i^c \tag{2.17}$$

where A_i is the area and a, b, c are cost coefficients which depend on the type of exchanger and material of construction.

Ahmad et al. (1990) made the assumption that all the heat exchangers have the same area. This assumption gives the following equation

$$A_i = A_{min} / N_{u,mer} \tag{2.18}$$

where A_{min} is the total area of all the heat exchangers in the network. Using equation 2.17 in equation 2.18 gives

$$C_{Ci} = a + b\ (A / N_{u,\ mer})^c \tag{2.19}$$

Thus, the total capital cost of all the heat exchangers in a MER network is given by

$$CC = N_{u,mer} * C_{Ci} = N_{u,mer} * (\ a + b\ (\ A_{min} / N_{u,mer}\ )^c) \tag{2.20}$$

where A_{min} is the area target described earlier. The total cost target can be calculated as

$$CT = CO + CC \tag{2.21}$$

By substituting the expressions for CO and CC in the equation 2.20, we get

$$CT = C_{hu}\, Q_{hu,min} + C_{cu}\, Q_{cu,min} + N_{u,mer} * (a + b (A_{min} / N_{u,mer})^{c}) \qquad (2.22)$$

The only assumption involved in the above method is that all the heat exchangers have the same area and this assumption appears to give good predictions according to Ahmad et al. (1990).

We have discussed the targeting methods for utilities, number of units, area and cost. Having all these targets available ahead of design is of great value during the design process. It also gives the engineer the confidence that his design is close to the optimum.

E. Design

The heat recovery pinch is the most important consideration in the design procedure. As explained earlier, the pinch corresponds to a particular temperature level in the process, and it divides the process into two thermodynamically separate regions such that the heat flow at the pinch is zero.

For minimum use of external utilities (MER, in other words), the following criteria have to be satisfied while determining the stream matches.

1. No heat transfer must occur across the pinch.
2. No cold utility must be used above the pinch.
3. No hot utility must be used below the pinch.

These are the three pinch design rules, which are simply the consequences of the second law of thermodynamics.

Based on this, Linnhoff and Hindmarsh (1983) proposed the basic Pinch Design Method (PDM) for synthesis of MER networks. It uses the all of the above criteria and

develops the design for two separate problems (namely, one above the pinch and another below it). An important difference between this and the other methods is that it identifies the matches between streams, which are essential for the MER. This greatly reduces the number of possible design solutions. It also identifies situations where stream splitting is necessary. All of this identification is done based on the following feasibility criteria.

1. The Number Criteria: This criterion concerns the number of process streams at the pinch. To obtain a MER design, no utility cooling can be provided above the pinch. This implies that every hot stream must be brought to its pinch temperature by a cold stream. In other words, the number of hot streams can not exceed the number of cold streams. The reverse is true below the pinch.

   $N_{hp} \leq N_{cp}$ above the pinch

   $N_{hp} \geq N_{cp}$ below the pinch

   where N_{hp} and N_{cp} are the number of hot and cold streams at the pinch.

2. The MC_p Criteria: This criterion concerns the approach temperature at the pinch. The driving force at the pinch is the smallest. This leads to the following condition.

   $MC_{p,hp} \leq MC_{p,cp}$ above the pinch

   $MC_{p,hp} \geq MC_{p,cp}$ below the pinch

   $MC_{p,hp}$ = heat capacity flowrate of hot stream at the pinch

   $MC_{p,cp}$ = heat capacity flowrate of cold stream at the pinch.

If any of these criteria are not satisfied, then one or more streams will have to be split. These criteria are applicable only at the pinch point and not away from it because pinch is the most constrained region in the process.

A network synthesized with these criteria will meet the utility targets, but it may not meet the target for the minimum number of units. It may have more than the theoretically minimum number of heat exchangers due to the existence of loops. Identification of these loops by mere inspection is not an easy task. Pethe et al. (1989) have proposed a technique based on the incidence matrix to identify loops. Other methods based on graph theory have been proposed, also.

Once the loops have been identified, they can be eliminated to reduce the number of exchangers. Linnhoff et al. (1982) have given simple design heuristics to break the loops. These are as follows:

1. Break the loop with the exchanger having the smallest heat load.
2. Remove the smallest heat load from the loop.
3. Restore the minimum approach temperature if necessary.

Loop breaking can often lead to violation of the minimum approach temperature condition and consequently to higher heat exchanger areas. To avoid this, the approach temperature should be restored by shifting the heat loads along a path. The path is identified from a heater to a cooler such that it involves the exchanger for whom the minimum approach temperature condition is violated. This technique is called as Energy Relaxation. However, this results in an increase in utility consumption if one of the broken loops is crossing the pinch. In that case, the resulting network will satisfy the target for the least number of units but will not be a MER network.

Ahmad (1985) extended the Pinch Design Method to incorporate total cost optimization during network design. This extended method used newer concepts like

Driving Force Plot (Linnhoff and Vredeveld, 1984) and the Remaining Problem Analysis (Ahmad and Smith, 1989).

The previously mentioned techniques for targeting of utilities, area, number of units and cost can be used only for a specified fixed value of the approach temperature. The choice of this parameter has been traditionally based on experience, and a poor choice can lead to non-optimal solutions. Therefore, Linnhoff and Ahmad (1989) introduced the concept of 'Supertargetting'. This involves optimization of the minimum approach temperature and heat recovery level in the pre-design stage by trading off capital cost and operating cost.

Linnhoff and Tjoe (1985) presented a complete methodology for applying pinch analysis to already existing non-optimal networks. This is called the Retrofit problem. Tjoe (1986) gives an in-depth treatment of this topic.

In summary, Pinch analysis is a very powerful tool that is based on thermodynamic principles, which can be used to generate energy efficient networks with minimum investment cost. In the recent years, pinch analysis has been extended to heat and power cycles and total process and plant integration (Linnhoff, 1993). In this section, we have discussed heuristic methods for pinch analysis and in the next section, the mathematical approach and methods will be reviewed.

F. Mathematical Programming Methods

Following the development of computer software and hardware, other methods based on mathematical programming were developed. An important study was done by Papoulias and Grossmann (1983) where they formulated the MER problem as a linear programming (LP) model. This LP model was based on the transshipment model, which

is widely used in the field of operations research. The process was divided into a number of intervals based on the stream and utility temperatures. Heat was considered as a commodity that can flow from higher to lower temperatures and the temperature intervals were considered as warehouses for this heat. The hot streams were sources of heat to these warehouses and the cold streams were the receivers. Each warehouse received heat from hotter streams, transferred heat to colder streams and passed the remaining heat to the warehouse below. This formulation is shown in the Figure 2.3.

The advantage of this formulation is that it leads to a linear problem of a small size. The model can be used to minimize the total utility cost for the process. It includes multiple hot and cold utilities. Also, it is possible to put constraints on the heat load for a particular utility if only a limited amount of it is available. The solution of the model gives the optimum amount for each utility. In addition, a zero residual heat flow from an interval indicates the existence of a pinch point.

One drawback with the above formulation was that it assumed that any hot stream could be matched with any cold stream, which is not true in reality. So, Papoulias and Grossmann (1983) expanded the above model to include restricted matches. The expanded model was conceptually similar to the previous one except that the streams with restricted matches were treated separately.

The above models are useful in determining the minimum operating cost (utility cost), but they do not say anything about the network structure. Generally, for any process, there exist a number of minimum utility cost designs, and the one with the minimum number of units is to be determined because it is the near-optimal solution.

For the above purpose, Papoulias and Grossmann (1983) developed a Mixed Integer Linear Programming (MILP) formulation. This model used the results of the linear transshipment model described above. So, the utility streams were added to the set of process streams to obtain an augmented set of process streams. The existence of a match between two streams was represented by a binary variable (A binary variable can take only a zero or one value). The total number of stream matches was then minimized to obtain the optimum design. Also, it is possible to attach weights to certain matches to increase or decrease their preference.

The results from the LP transshipment problem show the existence of any pinch points in the process. These pinch points divide the problem into a number of sub-networks. The above MILP formulation should be applied to each of the above sub-networks separately. If the MILP model is solved for the whole process together, it will not satisfy the minimum utility cost solution.

The information about the stream matches, which is obtained after solving the MILP problem, can be used to derive the network configuration. However, this is a very tedious trial and error task when done manually. Also, there are many possible network configurations, which will feature the minimum utility cost and also the minimum number of units. Therefore, Floudas et al (1986) developed a procedure for automatic synthesis of optimum heat exchanger networks. This method was a significant improvement over the other methods found in the literature (Ponton et al, 1974, Nishida et al, 1977). These older methods could only work with a limited number of configurations, which excluded stream splitting. The automatic synthesis procedure by Floudas et al, (1986) incorporated splitting and mixing as well as bypassing of streams.

The basis of the above method is an independent superstructure for each of the process units. These process units correspond to the stream matches predicted by the MILP formulation of Papoulias and Grossmann. Each of these superstructures is derived in such a way so as to include alternatives on stream splits, bypasses, matches in series, matches in parallel, matches in series-parallel and so on. When all these individual superstructures are combined into one, the overall superstructure has all the possible configurations embedded inside it. The unknown parameters are the stream interconnections. This is the MILP part of the procedure. The procedure also includes a non-linear programming (NLP) part that ensures that the mass and heat balances are satisfied at every unit. The objective function to be minimized is the total heat exchanger network cost. Thus, the automatic synthesis procedure is a combination of MILP and NLP problems whose solution gives a network configuration having minimum utility cost, fewest number of units and the lowest investment cost.

The optimization strategy used so far to determine the final network was sequential in nature. The entire task was decomposed into smaller problems. The utilities were minimized first, then the number of units and then the cost. This made the problem more manageable and also provided insight into the process. However, the solution obtained in this manner was not necessarily the optimum solution because of the trade-offs involved. The actual optimization problem is stated below:

Minimize Total Cost = Utility Cost + Fixed Cost of units + Area Cost

This was being approximated by the following strategy:

Minimize Area Cost

such that: Minimize Fixed Cost of units

such that: Minimize Utility Cost

This approximation often led to sub-optimal networks. Consequently, procedures with a more simultaneous approach began to appear at the end of 80's.

Floudas and Ciric (1989) developed a Mixed Integer Nonlinear (MINLP) formulation, which simultaneously optimized the selection of process stream matches and derivation of the network structure subject to a given minimum utility cost. This method was based on the stream superstructure model proposed earlier by Floudas et al. (1986). It effectively combined the second and third steps of the above optimization strategy and thus provided an improvement over the earlier one.

The above model still had the drawback that it was based on the definition of the pinch point. So, it eliminated from consideration any truly minimum cost network, which might have a heat exchanger across the pinch. Ciric and Floudas (1991) therefore implemented a MINLP model to simultaneously solve utility consumption, stream matches and network topology, thus combining all the three steps into one. This model was again based on the stream superstructure, and it also used a modified version of the transshipment model.

An alternative model for completely simultaneous optimization came from Yee et al. (1990). This was based on a stage-wise superstructure representation shown in Figure 2.4. The process is divided into a number of stages. Within each stage, potential exchanges occur between every pair of hot and cold streams. At every stage, a process stream is split and sent to an exchanger for a potential match. A potential match is represented by a binary variable. This network also embeds all the possible configurations such as splitting, mixing, series matches except bypassing of streams.

A major advantage of this model is that constraints on stream matching and splits are incorporated very easily. Minimization of the total cost of this network leads to an MINLP problem. The solution identifies the exchangers needed for optimality and the corresponding stream flow configuration. An important point in the above model is the selection of number of stages. Setting the number of stages equal to maximum of the number of hot or cold streams is often adequate. However, a more rigorous choice is to set it equal to the number of temperature intervals based on the minimum approach temperature.

Zamora and Grossmann (1998) presented a global optimization algorithm to rigorously solve the stagewise superstructure model. The simplifying assumptions made were linear area cost, arithmetic mean temperature difference driving forces and no stream splitting.

F-1. Simultaneous Optimization and Heat Integration

The interactions between a process model and the heat exchanger networks are very complex. So, for maximum heat integration, the optimization should also include the process design stage. Duran and Grossmann (1986) presented a mathematical programming approach for simultaneous optimization and heat integration of chemical processes. The hot and cold stream temperatures were variable parameters in the optimization problem. A new pinch location method was proposed to cope with the situation of not having pre-established temperature intervals. The method was found to handle trade-offs between capital cost, utility cost and raw material cost in a very efficient manner.

G. New Methods

Kravanja and Glavic (1997) described the simultaneous optimization of process flowsheets and heat exchanger networks using a combination of pinch technology and mathematical programming techniques. A Discrete Complex Algorithm (DCA) is proposed to carry out the optimization task.

Athier et. al. (1997) proposed a new procedure based on simulated annealing to solve the HENS problem in terms of investment and operating cost. The simulated annealing techniques are derived from the principles of statistical mechanics, which govern the phenomenon of physical annealing of solids.

Methods have also been proposed which use knowledge-based systems or expert systems. Viswanthan and Evans (1987) used a combination of transshipment and transportation models to solve the HENS problem. An expert system was used to generate the various modules and control the interaction between them.

This concludes the review of the developments in heat exchanger network design methods. We discussed techniques based on pinch analysis as well as the mathematical programming approach. The following section gives a brief description of the WAR algorithm for pollution prevention.

H. Pollution Prevention

Cost minimization has traditionally been the objective of chemical process design. However, growing environmental awareness now demands process technologies that minimize or prevent production of wastes. The most important issue in development of such technologies is a method to provide a quantitative measure of

waste production in a process. There is no sound organizing principle that can serve as a basis for measuring pollution in a process.

Many different approaches have been suggested to deal with this problem. One of these is the Waste Reduction Algorithm (WAR) (Hilaly, 1994). The WAR algorithm is based on the generic pollution balance of a process flow diagram.

Pollution Accumulation = Pollution Inputs + Pollution Generation - Pollution Output (2.23)

It defines a quantity called as the 'Pollution Index' to measure the waste generation in the process. This pollution index is defined as:

$$I = \text{wastes/products} = -(\Sigma Out + \Sigma Fugitive) / \Sigma P_n \quad (2.24)$$

This index is used to identify streams and parts of processes to be modified. Also, it allows comparison of pollution production of different processes. The WAR algorithm can be used to minimize waste in the design of new processes as well as modification of existing processes.

H-1. The Environmental Impact Theory

The Environmental Impact Theory (Cabezas et. al., 1997) is a generalization of the WAR algorithm. It describes the methodology for evaluating potential environmental impacts, and it can be used in the design and modification of chemical processes. The environmental impacts of a chemical process are generally caused by the energy and material that the process takes from and emits to the environment. The potential environmental impact is a conceptual quantity that can not be measured. But it can be calculated from related measurable quantities.

The generic pollution balance equation of the WAR algorithm is now applied to the conservation of the Potential Environmental Impact in a process. The flow of impact $\dot{I}$, in and out of the process is related to mass and energy flows but is not equivalent to them. The conservation equation can be written as

$$\frac{dI_{sys}}{dt} = \dot{I}_{in} - \dot{I}_{out} + \dot{I}_{gen} \tag{2.25}$$

where I_{sys} is the potential environmental impact content inside the process, $\dot{I}_{in}$ is the input rate of impact, $\dot{I}_{out}$ is the output rate of impact and $\dot{I}_{gen}$ is the rate of impact generation inside the process by chemical reactions or other means. At steady state, equation 2.23 reduces to

$$0 = \dot{I}_{in} - \dot{I}_{out} + \dot{I}_{gen} \tag{2.26}$$

Application of this equation to chemical processes requires an expression that relates the conceptual impact quantity $\dot{I}$ to measurable quantities. The input rate of impact can be written as

$$\dot{I}_{in} = \sum_{j} \dot{I}_j = \sum_{j} \dot{M}_j^{in} \sum_{k} x_{kj} \Psi_k \tag{2.27}$$

where the subscript ‘in’ stands for input streams. The sum over j is taken over all the input streams. For each input stream j, a sum is taken over all the chemical species present in that stream. M_j is the mass flow rate of the stream j and the x_{kj} is the mass fraction of chemical k in that stream. Ψ_k is the characteristic potential impact of chemical k.

The output streams are further divided into two different types: Product and Non-product. All non-product streams are considered as pollutants with positive potential impact and all product streams are considered to have zero potential impact.

The output rate of impact can be written as

$$\dot{I}_{out} = \sum_j \dot{I}_j = \sum_j \dot{M}_j^{out} \sum_k x_{kj} \Psi_k \tag{2.28}$$

where the subscript 'out' stands for non-product streams. The sum over j is taken over all the non-product streams. For each stream j, a sum is taken over all the chemical species.

Knowing the input and output rate of impact from the equations 2.25 and 2.26, the generation rate can be calculated using equation 2.24. Equations 2.25 and 2.26 need values of potential environmental impacts of chemical species. The potential environmental impact of a chemical species (Ψ_k) is calculated using the following expression

$$\Psi_k = \sum_l \alpha_l \Psi^s_{k,l} \tag{2.29}$$

where the sum is taken over the categories of environmental impact. α_l is the relative weighting factor for impact of type l independent of chemical k. $\Psi^s_{k,l}$ is the potential environmental impact of chemical k for impact of type l. Values of $\Psi^s_{k,l}$ for a number of chemical species can be obtained from the report on environmental life cycle assessment of products (Heijungs, 1992).

There are nine different categories of impact. These can be subdivided into four physical potential impacts (acidification, greenhouse enhancement, ozone depletion and photochemical oxidant formation), three human toxicity effects (air, water and soil) and

two ecotoxicity effects (aquatic and terrestrial). The relative weighting factor α_l allows the above expression for the impact to be customized to specific or local conditions. The suggested procedure is to initially set values of all relative weighting factors to one and then allow the user to vary them according to local needs. More information on impact types and choice of weighting factors can be obtained from the report on environmental life cycle assessment of products (Heijungs, 1992).

To quantitatively describe the pollution impact of a process, the conservation equation is used to define two categories of Impact Indexes. The first category is based on generation of potential impact within the process. These are useful in addressing the questions related to the internal environmental efficiency of the process plant, i.e., the ability of the process to produce desired products while creating a minimum of environmental impact. The second category measures the emission of potential impact by the process. This is a measure of the external environmental efficiency of the process i.e. the ability to produce the desired products while inflicting on the environment a minimum of impact.

Within each of these categories, three types of indexes are defined which can be used for comparison of different processes. In the first category (generation), the three indexes are as follows.

1) $\dot{I}_{gen}^{NP}$ This measures the the total rate at which the process generates potential environmental impact due to nonproducts. This can be calculated by subtracting the input rate of impact ($\dot{I}_{in}$) from the output rate of impact ($\dot{I}_{out}$).

2) $\hat{I}_{gen}^{NP}$ This measures the potential impact created by all nonproducts in manufacturing a unit mass of all the products. This can be obtained from dividing $\dot{I}_{gen}^{NP}$ by the rate at which the process outputs products.

3) $\hat{M}_{gen}^{NP}$ This is a measure of the mass efficiency of the process, i.e., the ratio of mass converted to an undesirable form to mass converted to a desirable form. This can be calculated from $\hat{I}_{gen}^{NP}$ by assigning a value of 1 to the potential impacts of all non-products.

The indexes in the second category (emission) are as follows.

4) $\dot{I}_{out}^{NP}$ This measures the the total rate at which the process outputs potential environmental impact due to nonproducts. This is calculated using equation 2.26.

5) $\hat{I}_{out}^{NP}$ This measures the potential impact emitted in manufacturing a unit mass of all the products. This is obtained from dividing $\dot{I}_{out}^{NP}$ by the rate at which the process outputs products.

6) $\hat{M}_{out}^{NP}$ This is the amount of pollutant mass emitted in manufacturing a unit mass of product. This can be calculated from $\hat{I}_{out}^{NP}$ by assigning a value of 1 to the potential impacts of all non-products.

Indices 1 and 4 can be used for comparison of different designs on an absolute basis whereas indices 2, 3, 5 and 6 can be used to compare them independent of the plant size. Higher values of indices mean higher pollution impact and suggest that the plant design is inefficient from environmental safety point of view.

I. Summary

This chapter presented an analysis of the important concepts in energy conservation and pollution prevention. Software tools are available which can be used to individually apply these concepts to a chemical process. However, to be able to efficiently use these techniques in process design and optimization of large-scale chemical and refinery industries, a more sophisticated tool such as the Advanced Process Analysis System is needed. It will combine programs for heat exchanger network design, online optimization, reactor design and pollution index calculations into one powerful package and will offer an advanced approach to process analysis for energy conservation, cost minimization and waste reduction. The next chapter explains the methodology of application of these concepts in the Advanced Process Analysis System.

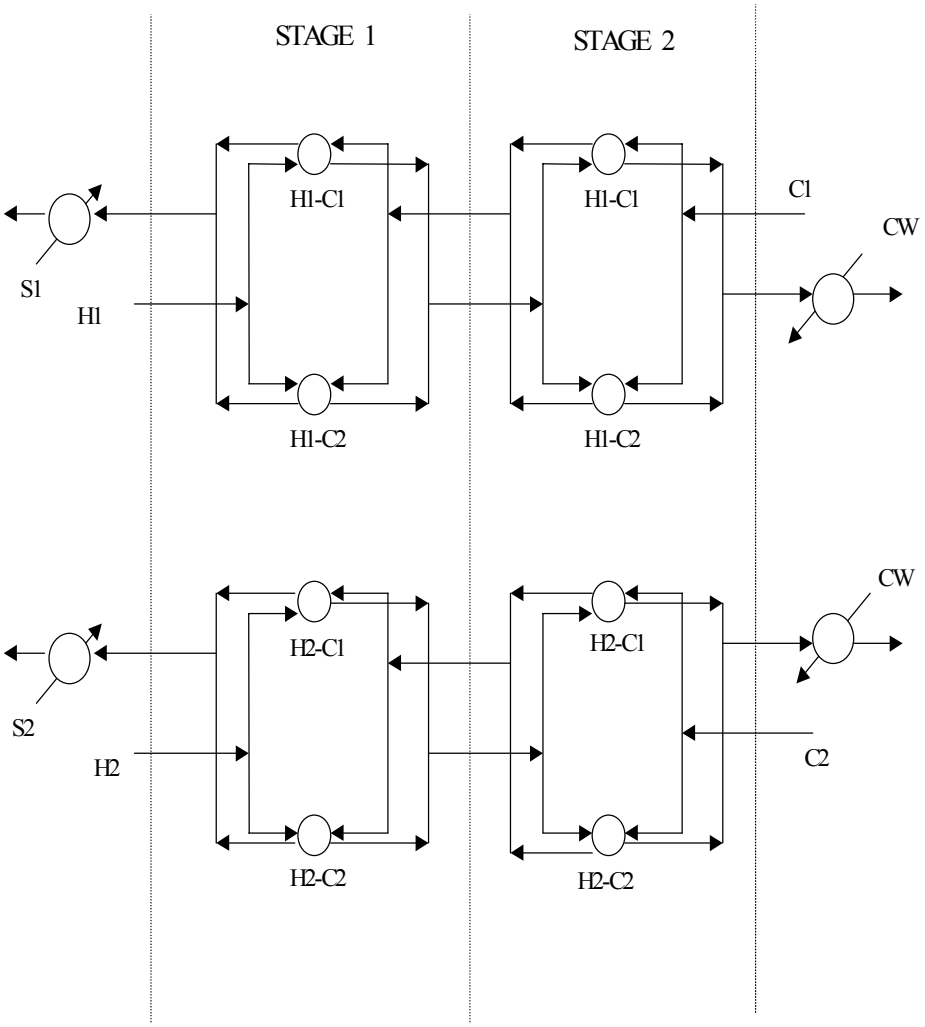

Figure 2.4 The Superstructure Model (Yee, 1990)

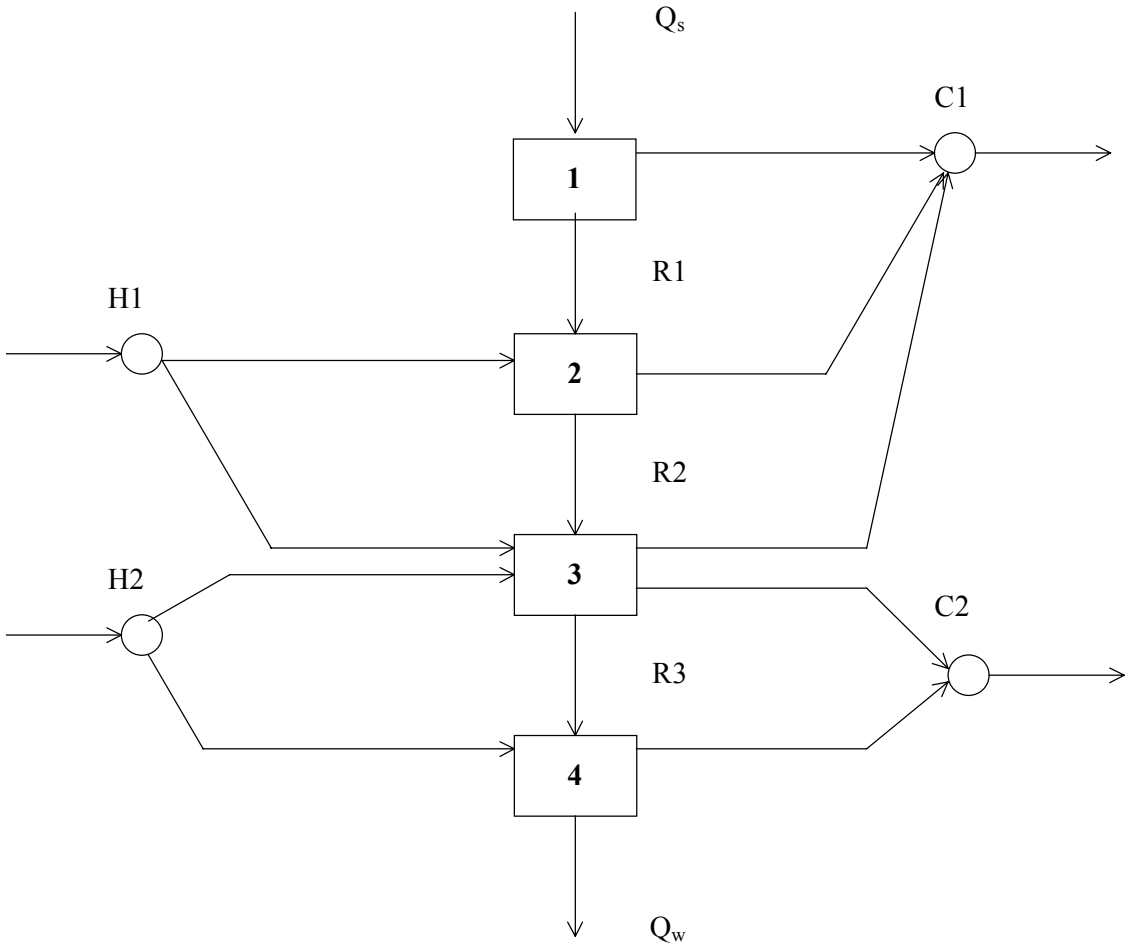

Figure 2.3 The Transshipment Model (Papoulias and Grossmann, 1983)

CHAPTER 3 THE METHODOLOGY

This chapter explains the methodology of the Advanced Process Analysis System. The framework for the Advanced Process Analysis System is shown in Figure 1.1. The main components of this system are a flowsheeting program for process material and energy balances, an on-line optimization program, a chemical reactor analysis program, a heat exchanger network design program and a pollution assessment module. An overview of each of these programs was given in Chapter 1.

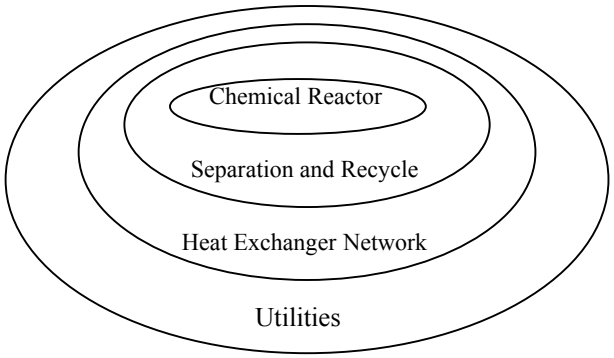

Figure 3.1: The 'Onion Skin' Diagram for Organization of a Chemical Process and Hierarchy of Analysis.

The Advanced Process Analysis System methodology to identify and eliminate the causes of energy inefficiency and pollutant generation is based on the onion skin diagram shown in Figure 3.1. Having an accurate description of the process from on-line optimization, an evaluation of the best types of chemical reactors is done first to modify and improve the process. Then the separation units are evaluated. This is followed by the pinch analysis to determine the best configuration for the heat exchanger network and determine the utilities needed for the process. Not shown in the diagram is the pollution index evaluation, which is used to identify and minimize

emissions. The following gives a detailed description of the components of the Advanced Process Analysis System and how they are used together to control and modify the process to maximize the profit and minimize the wastes and emissions.

A. The Flowsheeting Program

The first step towards implementing the Advanced Process Analysis System is the development of the process model, which is also known as flowsheeting. The process model is a set of constraint equations, which represent a mathematical model of relationships between the various plant units and process streams. Formulation of the process model can be divided into two important steps.

A-1. Formulation of Constraints for Process Units

The formulation of constraints can be classified into empirical and mechanistic methods. The process models used in Advanced Process Analysis System belong to the type of mechanistic models because they are based on conservation laws as well as the physical and chemical attributes of its constituents.

A typical chemical plant includes hundreds of process units such as heat exchangers, reactors, distillation columns, absorption towers and others. The constraints for these units are either based on conservation laws (mass and energy balances) or they are based on some other laws of nature which include models for chemical phase equilibrium, kinetic models etc. Mathematically, the constraints fall into two types: equality constraints and inequality constraints. Equality constraints deal with the exact relationships in the model where as inequality constraints recognize the various bounds involved. Examples of inequality constraints are upper limits on the temperature of certain streams or upper limits on the capacity of certain units.

A-2. Classification of Variables and Determination of Parameters

After the constraints are formulated, the variables in the process are divided into two groups, measured variables and unmeasured variables. The measured variables are the variables which are directly measured from the distributed control systems (DCS) and the plant control laboratory. The remaining variables are the unmeasured variables. For redundancy, there must be more measured variables than the degree of freedom.

The parameters in the model can also be divided into two types. The first type of parameters is the constant parameters, which do not change with time. Examples of these are reaction activation energy, heat exchanger areas etc. The other type of parameters is the time-varying parameters such as reactor efficiencies and heat transfer coefficients. These are treated as parameters because they change very slowly with time. They are related to the equipment conditions and not the operating conditions.

A-3. Flowsim

The program used for flowsheeting in the Advanced Process Analysis System is called 'Flowsim'. Flowsim provides a graphical user interface with interactive capabilities. This Flowsim interface for a sample process is shown in Figure 3.2. Process units are represented as rectangular shapes whereas the process streams are represented as lines with arrows between these units. Each process unit and stream included in the flowsheet must have a name and a description. Process information is divided into the following six categories; equality constraints, inequality constraints, unmeasured variables, measured variables, parameters and constants.

The information in the first five categories is further classified by associating it with either a unit or a stream in the flowsheet. For example, for a unit that is a heat

exchanger, the relevant information includes the mass balance and heat transfer equations, limitations on the flowrates and temperatures if any, the heat transfer coefficient parameter and all the intermediate variables defined for that exchanger.

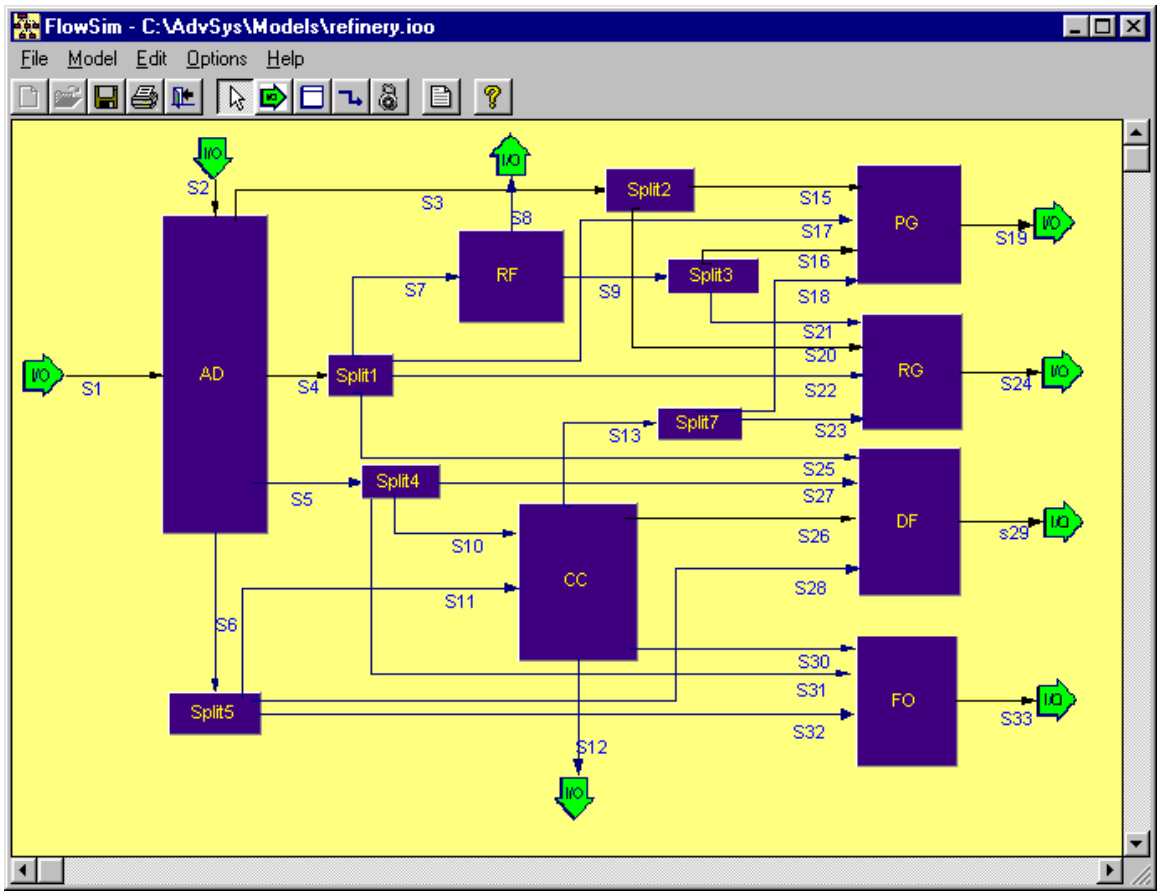

Figure 3.2 The Flowsim Screen for a Sample Process

For a stream, the information includes its temperature, pressure, total flowrate, molar flowrates of individual components etc. Information not linked to any one unit or stream is called the 'Global Data'. For example, the overall daily profit of the process is a global unmeasured variable because it is not related to any particular process unit or stream.

The sixth category of constants can be grouped into different sets based on their physical significance. For example, constants related to heat exchangers can be placed in one group and those related to reactors into another group.

Flowsim also has a seventh category of information called as the 'enthalpy coefficients'. This stores the list of all the chemical components in the process and their enthalpy coefficients for multiple temperature ranges. All of this process information is entered with the help of the interactive, user-customized graphic screens of Flowsim.

The use of Flowsim is illustrated for an actual process in the user's manual in Appendix C. This concludes the description of the flowsheeting part of the Advanced Process Analysis System.

B. The On-Line Optimization Program

Once the process model has been developed using Flowsim, the next step is to conduct on-line optimization. On-line optimization is the use of an automated system which adjusts the operation of a plant based on product scheduling and production control to maximize profit and minimize emissions by providing setpoints to the distributed control system. As shown in Figure 1.5, it includes three important steps: combined gross error detection and data reconciliation, simultaneous data reconciliation and parameter estimation and plant economic optimization. In combined gross error detection and data reconciliation, a set of accurate plant measurements is generated from plant's Distributed Control System (DCS). This set of data is used for estimating the parameters in plant models. Parameter estimation is necessary to have the plant model match the current performance of the plant. Then the economic optimization is conducted to optimize the economic model using this current plant model as constraints.

Each of the above three-optimization problems in on-line optimization has a similar mathematical statement as following:

Optimize: *Objective function*

Subject to: *Constraints from plant model.*

where the objective function is a joint distribution function for data validation or parameter estimation and a profit function (economic model) for plant economic optimization. The constraint equations describe the relationship among variables and parameters in the process, and they are material and energy balances, chemical reaction rates, thermodynamic equilibrium relations, and others.

To perform data reconciliation, there has to be redundancy in the measurements, i.e. there should be more measurements than the degrees of freedom in the process model. For redundancy, the number of measurements to determine the minimum number of measured variables is given by the degree of freedom, which is calculated using the following equation (Felder and Rousseau, 1986).

Degree of freedom = Total number of variables – Total number of equality constraints + Number of independent chemical reactions.

Also, the unmeasured variables have to be determined by the measured variables, called observability. If an unmeasured variable can not be determined by a measured variable, it is unobservable. This is called the 'observability and redundancy criterion', which needs to be satisfied (Chen, 1998).

B-1. Combined Gross Error Detection and Data Reconciliation

The process data from distributed control system is subject to two types of errors, random error and gross error, and the gross error must be detected and rectified before the data is used to estimate plant parameters. Combined gross error detection and

data reconciliation algorithms can be used to detect and rectify the gross errors in measurements for on-line optimization. These algorithms are measurement test method using a normal distribution, Tjoa-Biegler's method using a contaminated Gaussian distribution, and robust statistical method using robust functions. The theoretical performance of these algorithms has been evaluated by Chen, 1998.

Based on Chen's study, the Tjao-Biegler's method or robust method is used to perform combined gross error detection and data reconciliation. It detects and rectifies gross errors in plant data sampled from distributed control system. This step generates a set of measurements containing only random errors for parameter estimation. Then, this set of measurements is used for simultaneous parameter estimation and data reconciliation using the least squares method. This step provides the updated parameter values in the plant model for economic optimization. Finally, optimal set points are generated for the distributed control system from the economic optimization using the updated plant and economic models. This optimal procedure can be used for any process to conduct on-line optimization.

B-2. Simultaneous Data Reconciliation and Parameter Estimation

The general methodology for this is similar to the methodology of combined gross error detection and data reconciliation. The difference is that the parameters in plant model are considered as variables along with process variables in simultaneous data reconciliation and parameter estimation rather than being constants in data reconciliation. Both process variables and parameters are simultaneously estimated. Based on Chen's study, the least squares algorithm is used to carry out the combined gross error detection and data reconciliation. The data set produced by the parameter

estimation is free of any gross errors, and the updated values of parameters represent the current state of the process. These parameter values are now used in the economic optimization step.

B-3. Plant Economic Optimization

The objective of plant economic optimization is to generate a set of optimal operating setpoints for the distributed control system. This set of optimal setpoints will maximize the plant profit, satisfy the current constraints in plant model, meet the requirements for the demand of the product and availability of raw materials, and meet the restriction on pollutant emission. This optimization can be achieved by maximizing the economic model (objective function) subject to the process constraints. The objective function can be different depending on the goals of the optimization. The objectives can be to maximize plant profit, optimize plant configuration for energy conservation, minimize undesired by-products, minimize the waste/pollutant emission, or a combination of these objectives. The result of the economic optimization is a set of optimal values for all the measured and unmeasured variables in the process. These are then sent to the distributed control system (DCS) to provide setpoints for the controllers.

The on-line optimization program of the Advanced Process Analysis System retrieves the process model and the flowsheet diagram from Flowsim. Additional information needed to run online optimization includes plant data and standard deviation for measured variables; initial guess values, bounds and scaling factors for both measured and unmeasured variables; and the economic objective function. The program then constructs the three optimization problems shown in Figure 1.5 and uses GAMS (General Algebraic Modeling System) to solve them. Results of all three

problems can be viewed using the graphical interface of Flowsim. This is illustrated in the user's manual in Appendix C.

C. The Chemical Reactor Analysis Program

Having optimized the process operating conditions for the most current state of the plant, the next step in the Advanced Process Analysis System is to evaluate modifications to improve the process and reduce emission and energy consumption. First, the chemical reactors in the process are examined. The reactors are the key units of chemical plants. The performance of reactors significantly affects the economic and environmental aspects of the plant operation. The formulation of constraints in these types of units is very important and complicated owing to the various types of reactors and the complex reaction kinetics. Unlike a heat exchanger whose constraints are similar regardless of types of equipment, there is a great variation in deriving the constraints for reactors.

The chemical reactor design program of the Advanced Process Analysis System is a comprehensive, interactive computer simulation that can be used for modeling various types of reactors such as Plug Flow, CSTR and Batch reactors. This is shown in Figure 1.2. Reaction phases included are homogeneous gas, homogeneous liquid, catalytic liquid, gas-liquid etc. The options for energy model include isothermal, adiabatic and non-adiabatic.

The kinetic data needed for the reactor system includes the number of reactions taking place in the reactor and the number of chemical species involved. For each reaction, the stoichiometry and reaction rate expressions also need to be supplied. The physical properties for the chemical species can be retrieved from Flowsim.

The feed stream for the reactor is obtained from Flowsim and its temperature, pressure and flowrate are retrieved using the results from on-line optimization. Finally, the dimensions of the reactor and heat transfer coefficients are supplied. All of this data is used to simulate the reactor conditions and predict its performance. The reactant concentration, conversion, temperature and pressure are calculated as function of reactor length or space-time. The results can be viewed in both tabular and graphical form. The details of using the program are described in Appendix C along with an example.

As the operating process conditions change, the performance of the reactors also can vary to a significant extent. The reactor design program provides a tool to develop an understanding of these relationships. It provides a wide range of different types of reactors, which can be examined and compared to decide the best reactor configuration for economic benefits and waste reduction.

D. The Heat Exchanger Network Program

The optimization of the chemical reactors is followed by the heat exchanger network optimization as shown in the onion skin diagram in Figure 3.1. Most chemical processes require the heating and cooling of certain process streams before they enter another process unit or are released into the environment. This heating or cooling requirement can be satisfied by matching of these streams with one another and by supplying external source of heating or cooling. These external sources are called as utilities, and they add to the operating cost of the plant. The Heat Exchanger Network program aims at minimizing the use of these external utilities by increasing energy

recovery within the process. It also synthesizes a heat exchanger network that is feasible and has a low investment cost.

There are several ways of carrying out the above optimization problem. Two of the most important ones are the pinch analysis and the mathematical programming methods. Pinch analysis is based on thermodynamic principles whereas the mathematical methods are based on mass and energy balance constraints. The Heat Exchanger Network Program (abbreviated as THEN) is based on the method of pinch analysis.

The first step in implementation of THEN is the identification of all the process streams, which are important for energy integration. These important streams usually include streams entering or leaving heat exchangers, heaters and coolers. The flowsheeting diagram of Flowsim can be an important aid in selection of these streams.

The next step in this optimization task involves retrieval of the necessary information related to these streams. Data necessary to perform heat exchanger network optimization includes the temperature, the flowrate, the film heat transfer coefficient and the enthalpy data. The enthalpy data can be in the form of constant heat capacities for streams with small temperature variations. For streams with large variations, it can be entered as temperature-dependent enthalpy coefficients. The film heat transfer coefficients are needed only to calculate the areas of heat exchangers in the new network proposed by THEN.

The temperature and flowrates of the various process streams are automatically retrieved from the results of online optimization. The setpoints obtained after the plant economic optimization are used as the source data. The physical properties such as the

heat capacities, enthalpy coefficients and film heat transfer coefficients are retrieved from the Flowsim.

The third step in the heat exchanger network optimization is classification of streams into hot streams and cold streams. A hot stream is a stream that needs to be cooled to a lower temperature whereas a cold stream is a stream that needs to be heated to a higher temperature. Usually, streams entering a cooler or the hot side of a heat exchanger are the hot streams whereas streams entering through a heater or the cold side of a heat exchanger are the cold streams. The final step in this problem requires the specification of the minimum approach temperature. This value is usually based on experience.

Having completed all of the above four steps, the heat exchanger network optimization is now performed using THEN. Thermodynamic principles are applied to determine the minimum amount of external supply of hot and cold utilities. The Grand Composite Curve is constructed for the process, which shows the heat flows at various temperature levels. A new network of heat exchangers, heaters and coolers is proposed, which features the minimum amount of external utilities. This network drawn in a graphical format is called the Network Grid Diagram. An example of a network grid diagram is given in Figure 1.4. Detailed information about the network can be viewed using the interactive features of the user interface.

The amount for minimum hot and cold utilities calculated by the Heat Exchanger Network Program is compared with the existing amount of utilities being used in the process. If the existing amounts are greater than the minimum amounts, the process has potential for reduction in operating cost. The network grid diagram

synthesized by THEN can be used to construct a heat exchanger network that achieves the target of minimum utilities. The savings in operating costs are compared with the cost of modification of the existing network, and a decision is made about the implementation of the solution proposed by THEN.

E. The Pollution Index Program

The final step in the Advanced Process Analysis System is the assessment of the pollution impact of the process on the environment. This has become an important issue in the design and optimization of chemical processes because of growing environmental awareness.

The pollution assessment module of the Advanced Process Analysis System is called 'The Pollution Index Program'. It is based on the Waste Reduction Algorithm and the Environmental Impact Theory as described in Chapter 2. It defines a quantity called as the pollution index to provide a basis for measuring the pollution caused by a process.

Environmental impact of a chemical process is caused by the streams that the process takes from and emits to the environment. Only these input and output streams are considered in performing the pollution index analysis. Other streams, which are completely internal to the process, are excluded. In the Pollution Index Program, this selection of input-output streams is automatically done based on the plant information entered in Flowsim.

The next step in the pollution index analysis is the classification of the output streams into product and non-product streams. All streams which are either sold as product or which are used up in a subsequent process in the production facility are

considered as product streams. All other output streams, which are released into the environment, are considered as non-product streams. All non-product streams are considered as pollutant streams whereas all product streams are considered to have zero environmental impact.

Pollution index of a stream is a function of its composition. The composition data for the streams is retrieved from the results of on-line optimization performed earlier. This can be either in terms of the molar flowrates or fractions. Additional data needed for the pollution analysis is the specific environmental impact potential values of the individual chemical species present in a stream. These values for various chemical species are available in the report on environmental life cycle assessment of products.

The last piece of information required is the relative weighting factors for the process plant. According to the Waste Reduction Algorithm, the environmental impact of chemical processes can be broadly classified into nine categories e.g. acidification, photochemical oxidation etc. The relative weighting factors allow the customization of the analysis to local conditions. Their values depend on the location of the plant and its surrounding conditions. For example, the weighting factor for photochemical oxidation is higher in areas which suffer from smog.

Having finished all of the above prerequisite steps, the pollution index program is now called to perform the analysis. Mass balance constraints are solved for the process streams involved, and the equations of the Environmental Impact Theory are used to calculate the pollution index values. Six types of pollution indices are reported for the process. Three of these are based on internal environmental efficiency whereas

the other three are based on external environmental efficiency. Higher the values of these indices, higher is the environmental impact of the process.

The pollution index program also calculates pollution indices for each of the individual process streams. These values help in identification of the streams which contribute more to the overall pollution impact of the process. Suitable process modifications can be done to reduce the pollutant content of these streams.

Every run of on-line optimization for the process is followed by the pollution index calculations. The new pollution index values are compared with the older values. The comparison shows how the change in process conditions affects the environmental impact. Thus, the pollution index program can be used in continuous on-line monitoring of the process.

F. Summary

To summarize, the Flowsim program is used first to develop the process model. The On-Line Optimization program is used to control the process to maximize the profit, and in doing this it has to continually update the process model to match the current state of the plant. This is followed by the process modification analysis. The Chemical Reactor Design program is used to determine the best type of chemical reactors for the process and to optimize their performance. The Heat Exchanger Network Program then optimizes the heat recovery in the system and minimizes the amount of external utilities. Finally, the Pollution Index Program is called to carry out the pollution analysis to measure the environmental impact of the process and to direct changes to reduce waste generation.

This concludes the methodology of the Advanced Process Analysis System. The subsequent chapters show the results of application of the Advanced Process Analysis System to an actual chemical process plant, the contact process for sulfuric acid.

CHAPTER 4 PROCESS MODELS

The Advanced Process Analysis System was applied to an actual plant to ensure that the program meets the needs and requirements of the process and design engineers. The contact process for sulfuric acid at IMC Agrico's plant in Convent, Louisiana was chosen for this demonstration. This process incorporates nearly all of the process units found in chemical plant and refineries including packed bed catalytic chemical reactors, absorption towers and heat exchangers among others. The company has two plants producing sulfuric acid by the contact process, called the D-train and the E-train. Detailed description of both of these processes is given below.

A. D-Train Contact Sulfuric Acid Process Description

IMC Agrico's "D" train is a 4800 TPD 93% sulfuric acid plant built by Chemical Construction Company in 1966. The overall yield of elemental sulfur to sulfuric acid is 97.5%.

The contact process is a three-step process that produces sulfuric acid and steam from air, molten sulfur and water. The process flow diagram is shown in Figure 4.1, and the process consists of three sections, which are the feed preparation section, the reactor section, and the absorber section.

In the feed preparation section, molten sulfur feed is combusted with dry air in the sulfur burner. The reaction is:

$$S + O_2 ==> SO_2 + Heat$$

The reaction is exothermic and goes to completion. The gas leaving the burner is composed of sulfur dioxide, nitrogen, and unreacted oxygen at approximately 1800 ^{o}F.

The equipment used in this section includes an air filter, drying tower, a blower and a sulfur burner. The blower is five-stage, polytropic steam driven turbine with an efficiency of about 65%. The pump takes in approximately 130,000 cfm of ambient air at -10 inches of water and discharges it at about 170 inches of water and 165 ^{o}F under normal operation. The blower turbine speed is adjusted to change the production rate for each train. The drying tower removes ambient moisture from the intake air with 98 wt. % sulfuric acid flowing at a rate of about 4-5000 gpm. The tower is 25 feet in diameter and contains 17 ft 2 inches of packing.

In the sulfur burner, the dry compressed air discharged from the turbine reacts with molten sulfur to produce sulfur dioxide. A cold air bypass is used to maintain the burner exit temperature at 1800 ^{o}F. This temperature is setpoint controlled because it is the inlet temperature for the waste heat boiler (WB). The setpoint is dictated by equipment limitations and design considerations.

The sulfur dioxide, along with nitrogen and unreacted oxygen enters the waste heat boiler. The waste heat boiler is equipped with a hot gas bypass so that the temperature of the gases entering the first catalyst bed can be controlled at 800 ^{o}F. This boiler is a shell and tube type supplied with water from the steam drum. The boiler produces saturated steam at about 500^{o}F and 670 psig and utilizes about 10% blowdown.

The second section of the contact process plant is the reactor section. The reactor consists of four beds packed with two different types of Vanadium Pentoxide catalyst. The first two beds are packed with Monsanto's type LP-120 catalyst whereas the third and forth beds are packed with type LP-110. The purpose of using two different catalysts is to have higher catalyst activity in the low temperature zones of the third and fourth beds.

In the reactor section, the gas mixture from the feed preparation section is further reacted in the fixed catalyst beds to produce sulfur trioxide and heat according to the reaction:

$$2SO_2 + O_2 \rightleftharpoons 2SO_3 + \text{Heat}$$

The reaction is exothermic and the equilibrium conversion decreases with the increase in reaction temperature. For this reason, the process uses four packed beds, and heat exchangers between each bed remove the produced energy to reduce the temperature.

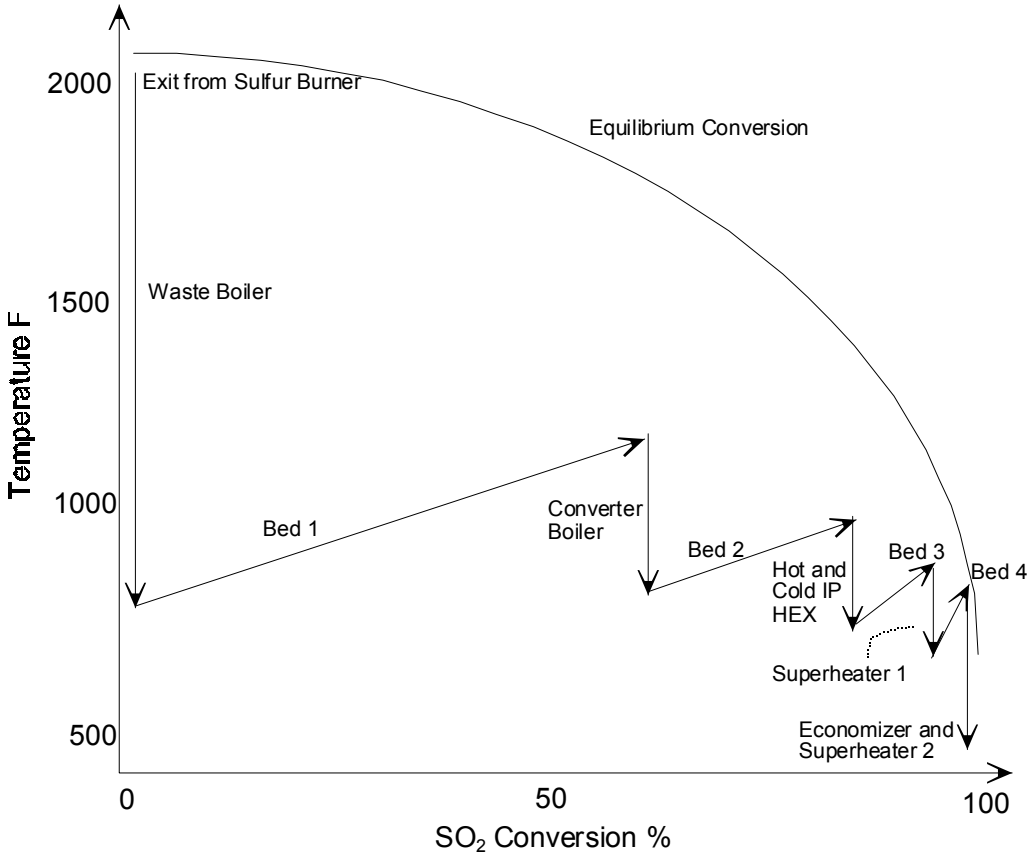

Figure 4.2 Temperature-Conversion of SO_2 Plot for D-train Sulfuric Acid Process

As shown in Figure 4.2, the equilibrium conversion of sulfur dioxide decreases with the increase in operating temperature. Removing reaction heat from each reactor increases the conversion of sulfur dioxide to sulfur trioxide and this removed heat is used to produce steam. Also, the equilibrium conversion increases by decreasing the concentration of sulfur trioxide and an inter-pass tower is used to absorb and remove sulfur trioxide from the gas stream between the second and the third catalyst beds. This design ensures higher conversion in the reactor beds.

As shown in Figure 4.1, the exit gases from the first bed are cooled in the converter boiler (CB). This boiler has the same configuration as the waste heat boiler. It is supplied with water from the steam drum. It produces saturated steam at 500^{o}F and 670 psig and utilizes about 10% blowdown. The hot and cold inter-pass heat exchangers (H and C) are used to cool the gases from the second catalyst bed before these gases are passed to the inter-pass tower. The gases from the third catalyst bed are cooled by superheater-1, which is a finned tube heat exchanger. This superheater produces superheated steam from the saturated steam produced by the boilers. The gases from the fourth bed consist of sulfur trioxide, nitrogen, oxygen and a small amount of sulfur dioxide. They are first cooled by superheater-2 followed by the economizer (E). In the superheater-2, cooling is done by the saturated steam coming from the steam drum whereas in the economizer, it is done by the boiler feed water. The cooled gases are then passed to the final tower for absorption of sulfur trioxide.

The final section of the contact process plant is the absorber section. In this section the SO_3 is absorbed from the reaction gas mixture into 98 wt. % sulfuric acid to produce a more concentrated acid. Also, heat is produced according to the equation:

$$SO_3 + H_2O \Rightarrow H_2SO_4 + \text{Heat}$$

As shown in Figure 4.1, the equipment in this section includes the final acid absorption tower, an inter-pass absorption tower, two acid absorption tanks and a drying tower acid tank. The two absorption towers use 98 wt. % acid to produce more concentrated acid. Water is added to the tanks to keep the sulfuric acid strength at 93 wt. % in drying tower acid tank and 98 wt. % in absorption tower tanks. The 93 wt. % acid from the drying tower acid tank is sold as the product acid. The exit gases from the final absorption tower containing unreacted air and small amount of sulfur dioxide are discharged to the air.

In the steam system, the boiler feed water is pre-heated to 380^{o}F at 740 psig by the economizer and is then sent to the steam drum. It then passes to the waste heat boiler and the converter boiler to produce saturated steam at 675 psig. This saturated steam is circulated back to the steam drum. It then goes to superheater-1 and superheater-2 to generate superheated steam at 626 psig. The superheated steam is used to drive the turbine and the excess steam is one of the products, which is used in an adjacent plant.

This concludes the description of the D-train sulfuric acid process. The following section describes the E-train process of the Uncle Sam Sulfuric Acid plant.

B. E-Train Contact Sulfuric Acid Process Description

Uncle Sam plant's “E” train is a 3200 TPD 93 mole % sulfuric acid plant designed by the Monsanto Enviro-Chem System, Inc. which began to operate in March, 1992. The overall conversion of elemental sulfur to sulfuric acid is about 99.7%. It represents the state-of-art technology of the contact process. The contact process is a three-step process that produces sulfuric acid and steam from air, molten sulfur and water. The process flow

diagram is shown in Figure 4.3, and the process consists of three sections, which are the feed preparation section, the reactor section, and the absorber section.

In the feed preparation section, molten sulfur feed is combusted with dry air in the sulfur burner. The reaction is:

$S + O_2 ==> SO_2 + Heat$

The reaction is exothermic and goes to completion. The gas leaving the burner is composed of sulfur dioxide, nitrogen, and unreacted oxygen at approximately 1400 ^oF. The equipment used in this section include an air filter, drying tower, a main compressor and a sulfur burner. The compressor is steam driven turbine with an efficiency of about 65%. It is a five stage, polytropic turbine on steam side and a centrifugal blower on the gas side. The pump takes in approximately 150,000 cfm of ambient air at -3 inches of water and discharges it at about 160 inches of water and 230^oF under normal operation. The compressor turbine speed is adjusted to change the production rate for each train. The drying tower removes ambient moisture from the intake air with 98 wt. % sulfuric acid flowing at a rate of about 3600 gpm.

In the sulfur burner, the dry compressed air discharged from the turbine reacts with molten sulfur to produce sulfur dioxide. The sulfur dioxide, along with nitrogen and unreacted oxygen enters waste heat boiler. The waste heat boiler is equipped with a hot gas bypass so that the temperature of the gases entering the first catalyst bed can be controlled to 788^oF. This boiler is a shell and tube type supplied with water from the economizers. The boiler produces saturated steam at about 500^oF and 670 psig and utilizes about 9% blowdown. The rest of the steam is passed to superheater to produce superheated steam at about 750^oF.

The second section of the contact process plant is the reactor or converter section. The reactor consists of four beds packed with two different types of vanadium pentoxide catalyst. In this part the gas mixture from the feed preparation section is further reacted in the fixed catalyst beds to produce sulfur trioxide and heat according to the reaction:

$$2SO_2 + O_2 \rightleftharpoons 2SO_3 + \text{Heat}$$

The reaction is exothermic and the equilibrium conversion decreases with the increase in reaction temperature. For this reason, the process uses four packed beds, and heat exchangers between each bed remove the produced energy to reduce the temperature. The equilibrium conversion of sulfur dioxide decreases with the increase in operating temperature. Removing reaction heat from each reactor increases the conversion of sulfur dioxide to sulfur trioxide and this removed heat is used to produce steam. Also, the equilibrium conversion increases by decreasing the concentration of sulfur trioxide, and an inter-pass tower is used to absorb and remove sulfur trioxide from the gas stream between the third and the fourth catalyst beds. This design ensures the high conversion.

As shown in Figure 4.3, the superheater (SH) is used to cool the exit gas from the first bed by the saturated steam from waste heat boiler (BLR). It produces superheated steam at about 750^{o}F and 630 psig. The hot inter-pass heat exchanger (H) is used to cool the gases from the second catalyst bed. The cold inter-pass heat exchanger (C) and economizer (E) are used to cool the gases from the third catalyst bed before these gases pass to the inter-pass tower. The hot and cold inter-pass heat exchangers are used also to heat the unabsorbed gases from the inter-pass tower while cooling the gases from the second and the third bed respectively. The gases from the fourth bed consist of sulfur trioxide, nitrogen, oxygen and a small amount of sulfur dioxide, and they are cooled by the

superheater (SH') and economizers (E') before passing to the final tower for absorption of sulfur trioxide. The superheated steam is used to drive the compressor turbine, and the excess steam is one of the plant products.

The final section of the contact process plant is the absorber section. In this section the SO_3 is absorbed from the reaction gas mixture into 98 wt. % sulfuric acid to produce a more concentrated acid. Also, heat is produced according to the equation:

$$SO_3 + H_2O \Rightarrow H_2SO_4 + \text{Heat}$$

As shown in Figure 4.3, the equipments in this section include the final acid absorption tower, inter-pass absorption tower, acid pump tank, dilution acid tank and three heat exchangers. These two absorption towers use 98 wt. % acid to produce more concentrated acid. Water is added to the two tanks to keep the sulfuric acid strength at 93 wt. % in acid dilution tank and 98 wt. % in acid tower pump tank. The exit gases from the final absorption tower are discharged to the air with less than 4 lb of SO_2 per ton of sulfuric acid produced.

This concludes the brief description of the contact sulfuric acid process. The next section describes the process model for the D-train sulfuric acid process.

C. Process Model for D-train Sulfuric Acid Process

As described earlier, process model is a set of constraint equations, which are the material and energy balances, rate equations and equilibrium relations that describe the material and energy transport and the chemical reactions of the process. These form a mathematical model of relationships between the various plant units and process streams. Before the constraint equations are formulated, it is important to note that in order to have an accurate model of the process, it is essential to include the key process units such as

reactors, heat exchangers and absorbers. These units affect the economic and pollution performance of the process to a significant extent. Certain other units are not so important and can be excluded from the model without compromising the accuracy of the simulation. For the D-train process, the four converters, sulfur burner, boilers, superheaters, acid absorbers were identified as the important units to be included in the model whereas the acid tanks, acid coolers, air blower, air filter etc. were excluded from the model. The complete list of the process units and process streams included in the model is given in Tables 4.1 and 4.2. The process model diagram with these units and streams is shown in Figure 4.4. The same diagram drawn using the graphical interface of Flowsim is shown in Appendix C.

Having selected the process units and streams, the next step is to develop the constraint equations. The constraint equations are programmed in the GAMS language and are used to reconcile plant measurements, estimate parameters, optimize the profit and minimize emissions from the plant. The constraint formulation techniques are very similar for process units of the same type. Therefore, this section is divided into four sub-sections; heat exchanger network, reactors, absorption towers and overall balance for the plant. Each of these sub-sections explains how constraints are written for that particular type of unit. For each type, detailed constraint equations are shown for a representative unit.

C-1. Heat Exchanger Network

As shown in Figure 4.4, the heat exchanger network in sulfuric acid plant includes two boilers, two gas-to-gas hot and cold inter-pass heat exchangers, two superheaters and a gas-to-compressed-water economizer. In these units, there is no mass transfer or chemical reaction. The inlet component flowrates are equal to the outlet component flow rates for

both sides. The energy balance states that the decrease of the enthalpy (MJ/s) in the hot side is equal to the increase of enthalpy in cold side plus the heat loss, i.e.,

$$(H^{inlet} - H^{outlet})_{hot} = (H^{outlet} - H^{inlet})_{cold} + Q_{loss}. \quad (4.1)$$

Table 4.1 Process Units in the D-train Sulfuric Acid Process Model (Refer to Figure 4.4, the Process Model Diagram for the D-train)

Name of Unit	Description
Burner	Sulfur Burner
Cboiler	Converter Boiler
ColdIP	Cold Interpass Heat Exchanger
Converter1	Reactor Bed 1
Converter2	Reactor Bed 2
Converter3	Reactor Bed 3
Converter4	Reactor Bed 4
Drum	Steam Drum
Economizer	Economizer
Finalab	Secondary Acid Absorber
Furnspl	Splitter after the burner
HotIP	Hot Interpass Heat Exchanger
Interab	Primary Acid Absorber
MixRec	Mixer after the waste heat boiler
Mixsteam	Steam Mixer before the drum
Sh1	Superheater1
Sh2	Superheater2
Splsteam	Steam Splitter after the drum
Splwater	Water Splitter after the economizer
Wboiler	Waste Heat Boiler

Table 4.2 Process Streams in the D-train Sulfuric Acid Process Model (Refer to Figure 4.4, the Process Model Diagram for the D-train)

Name of Stream	Description
s06	Inlet Air Stream
s07	Sulfur Burner Outlet Gas Stream
s08	Gas stream entering the waste heat boiler
s08a	Waste Heat Boiler Bypass
s09	Waste Heat Boiler Outlet
s10	Converter 1 Inlet
s11	Converter 1 Outlet
s12	Converter 2 Inlet
s13	Converter 2 Outlet
s14	Hot gases entering Cold IP exchanger
s15	Gas stream entering secondary absorber
s16	Gas stream leaving secondary absorber
s19	Cold gases entering Hot IP exchanger
s20	Converter 3 Inlet
s21	Converter 3 Outlet
s22	Converter 4 Inlet
s23	Converter 4 Outlet
s235	Gas stream entering economizer
s24	Gas stream leaving economizer
s25	Stack gas stream
s50	Sulfur Stream
sbd	Blowdown stream from the drum
sbfw	Boiler Feed Water
shp1	Superheated steam from superheater1
shp2	Superheated steam from superheater2
ss1	Saturated steam entering the drum
ss1a	Saturated steam from the waste heat boiler
ss1b	Saturated steam from the converter boiler
ss2	Saturated steam leaving the drum
ss4	Saturated steam entering superheater1
ss5	Saturated steam entering superheater1
sw1	Water leaving the economizer
sw1a	Water entering the waste heat boiler
sw1b	Water entering the converter boiler

For the hot inter-pass heat exchanger (HotIP), s13 is the inlet stream on the cold side whereas s14 is the outlet stream on the hot side. s19 is the inlet stream on the cold side and s20 is the outlet stream on cold side. The energy balance can be written as

$$(H^{inlet} - H^{outlet})_{hot} = \Sigma F_{13}^{(i)} h_{13}^{(i)} - \Sigma F_{14}^{(i)} h_{14}^{(i)} \quad \text{and} \tag{4.2}$$

$$(H^{inlet} - H^{outlet})_{cold} = \Sigma F_{19}^{(i)} h_{19}^{(i)} - \Sigma F_{20}^{(i)} h_{20}^{(i)}$$

where $F_{13}^{(i)}$ is the molar flowrate (kmol/s) of species i in stream s13 and $h_{13}^{(i)}$ is the enthalpy (MJ/kmol) of species i in stream s13. The total molar flowrate of stream s13 and the total enthalpy of stream s13 are given by the equations

$$F_{13} = \Sigma F_{13}^{(i)} \quad \text{and} \tag{4.3}$$

$$H_{13} = \Sigma F_{13}^{(i)} h_{13}^{(i)}$$

where the summation is done over all the species i present in stream s13. This naming convention is used for all the flowrates and enthalpies. The number in the subscript of the variable can be used to identify the stream to which it belongs. H^{inlet}_{hot} is the enthalpy of the inlet stream on hot side, and it has units of MJ/s.

The heat transferred in an exchanger is proportional to heat transfer area A, overall heat transfer coefficient U, and the logarithm mean temperature difference between the two sides ΔT_{lm}, i.e., $Q = UA\,\Delta T_{lm}$, where Q is the enthalpy change on cold side, i.e.,

$$Q = (H^{inlet} - H^{outlet})_{cold} = \Sigma F_{19}^{(i)} h_{19}^{(i)} - \Sigma F_{20}^{(i)} h_{20}^{(i)} \tag{4.4}$$

The material and energy balances as well as heat transfer equations are similar for all units in heat exchanger network. Table 4.3 gives the constraint equations for the hot inter-pass heat exchanger as an example of process constraint equations for all heat exchanger units. The first two rows of the Table 4.3 under material balance give the overall mass balance and all of the species mass balances. The overall mass balance is the

summation of all species mass balances. Therefore, if all of the species mass balances are used to describe the process, then the overall mass balance does not need to be included since it is redundant. The species mass balances are used to describe the relationship of the input and output flow rate variables.

Table 4.3 The Constraint Equations for Hot Inter-Pass Heat Exchanger

Material Balances	
Overall	$(F_{14}^{(SO_3)} + F_{14}^{(SO_2)} + F_{14}^{(O_2)} + F_{14}^{(N_2)}) - (F_{13}^{(SO_3)} + F_{13}^{(SO_2)} + F_{13}^{(O_2)} + F_{13}^{(N_2)}) = 0$ $(F_{20}^{(SO_3)} + F_{20}^{(SO_2)} + F_{20}^{(O_2)} + F_{20}^{(N_2)}) - (F_{19}^{(SO_3)} + F_{19}^{(SO_2)} + F_{19}^{(O_2)} + F_{19}^{(N_2)}) = 0$
Species	O_2: $F_{14}^{(O_2)} - F_{13}^{(O_2)} = 0$, $F_{20}^{(O_2)} - F_{19}^{(O_2)} = 0$ N_2: $F_{14}^{(N_2)} - F_{13}^{(N_2)} = 0$, $F_{20}^{(N_2)} - F_{19}^{(N_2)} = 0$ SO_2: $F_{14}^{(SO_2)} - F_{13}^{(SO_2)} = 0$, $F_{20}^{(SO_2)} - F_{19}^{(SO_2)} = 0$ SO_3: $F_{14}^{(SO_3)} - F_{13}^{(SO_3)} = 0$, $F_{20}^{(SO_3)} - F_{19}^{(SO_3)} = 0$
Energy Balances	
Overall	$\left(\sum_i F_{14}^{(i)} h_{14}^{(i)} - \sum_i F_{13}^{(i)} h_{13}^{(i)}\right) - \left(\sum_i F_{19}^{(i)} h_{19}^{(i)} - \sum_i F_{20}^{(i)} h_{20}^{(i)}\right) + Q_{loss} = 0$ where $h^i{}_k(T) = R(a_1^i T + \frac{1}{2} a_2^i T^2 + \frac{1}{3} a_3^i T^3 + \frac{1}{4} a_4^i T^4 + \frac{1}{5} a_5^i T^5 + b_1^i - H_{298}^i)$ $i = SO_2, SO_3, O_2, N_2;\ k = 13, 14, 19, 20$
Heat Transfer	$\left(\sum_i F_{20}^{(i)} h_{20}^{(i)} - \sum_i F_{19}^{(i)} h_{19}^{(i)}\right) - (U_{ex66} A_{ex66} \Delta T_{lm}) = 0$

In the constraints of Table 4.3, F denotes the component molar flow rate, kmol/sec, and its superscript i and subscript k denote the component names and stream numbers respectively. h's in the equations represent the species enthalpies of streams (MJ/kmol), and Q_{loss} is the heat loss from the exchanger (MJ/kmol). T is the stream temperature (K), and ΔT_{lm} is the logarithm mean temperature difference (K) between hot and cold sides of the exchanger. In the heat transfer equation, U and A are the overall heat transfer coefficient and heat transfer area respectively.

The two rows in Table 4.3 under energy balances give the overall energy balance and heat transfer equation. In addition, the enthalpy for each species, h(T), expressed as a polynomial function of the stream temperature is also given in the table. The enthalpy equations for gases, compressed water, and superheated steam are developed in the Appendix A.

In these equations, the total flow rates, species flow rates (or composition), and temperatures of streams are the measurable variables. Species enthalpies and the mean temperature difference are the unmeasured variables. The heat transfer coefficients are the process parameters to be estimated. The heat transfer area and coefficients in enthalpy equations and the heat losses are constants. The heat loss from the exchanger was estimated to be 2% of the amount of heat exchanged from the plant design data for the E-train.

C-2. Reactor System

The reactor system in this plant includes a sulfur burner and four catalytic converters. The following describes the constraint equations for sulfur burner and the first converter.

When a chemical reaction is involved in the process, it is convenient to use the mole balance to describe relationship of input and output flow rates of a unit for a component. Also, the overall mole balance is obtained from the component mole balances, i.e., the summation of component mole balance gives the overall mole balance. The sulfuric acid process involves three reactions, i.e., reaction of sulfur to sulfur dioxide, reaction of sulfur dioxide to sulfur trioxide, and absorption reaction of sulfur trioxide to sulfuric acid. Mole balances are used to describe the material balances of the units in the process, i.e., all material balance equations for the sulfuric acid process are written with mole balance relations. Moles are conserved when there is no reaction, and the change in the number of moles for a component is determined by the reaction rate and stoichiometric coefficients when there are reactions.

As shown in Figure 4.4, the inputs of sulfur burner are dry air stream (S06) from main compressor, and liquid sulfur stream (S50). The dry air reacts with molten sulfur to produce sulfur dioxide and heat in the burner. The sulfur dioxide, along with nitrogen and unreacted oxygen enters the waste heat boiler. At the design operating temperature of the sulfur burner, all of the sulfur is converted to sulfur dioxide, and some sulfur trioxide is formed from sulfur dioxide. The plant measurements have shown that 2 % (mol) of the SO_2 is converted into SO_3 in this unit, and this value is incorporated in the mass and energy balances of this unit.

The mole and energy balance equations for the sulfur burner are given in Table 4.4. The two rows of this table under mole balance give the overall mole balance and component mole balances. The mole balance for each component is established based on the conservation law. The steady state mole balance for a component is written as:

$$F_{in}(i) - F_{out}(i) + F_{gen}(i) = 0 \quad (4.5)$$

where i represents the names of components. For the sulfur burner, $F_{in}(i)$, $F_{out}(i)$, and $F_{gen}(i)$ are input air flow rate F06(i), output flow rate F07(i), and generation rates of components from reaction, r(i). The overall mole balance is the summation of all component mole balance equations.

Table 4.4 The Process Constraint Equations for Sulfur Burner

Mole Balances	
Overall	$F_{06} - F_{07} - 0.01F_{50} = 0$ $where\ F_{06} = F_{06}^{O2} + F_{06}^{N2}$ $F_{07} = F_{07}^{O2} + F_{07}^{N2} + F_{07}^{SO2} + F_{07}^{SO3}$
Species	$O_2: \quad F_{06}^{(O_2)} - F_{07}^{(O_2)} - 1.01F_{50} = 0$ $N_2: \quad F_{06}^{(N_2)} - F_{07}^{(N_2)} = 0$ $SO_2: \quad F_{06}^{(SO_2)} - F_{07}^{(SO_2)} + 0.98F_{50} = 0$ $SO_3: \quad F_{06}^{(SO_3)} - F_{07}^{(SO_3)} + 0.02F_{50} = 0$ $S: \quad F_{50} - F_{07}^{(S)} - F_{07}^{(SO2)} - F_{07}^{(SO3)} = 0$ $where \quad F_{06}^{(SO_2)} = 0,\ F_{06}^{(SO_3)} = 0,\ F_{07}^{(S)} = 0$
Energy Balances	
Overall	$F_{50}h^{(sulfur)} + \sum_i F_{06}^{(i)}h_{06}^{(i)} + F_{50}\Delta h_{rxn}^{SO_2} + 0.02F_{50}\Delta h_{rxn}^{SO_3} - \sum_i F_{07}^{(i)}h_{07}^{(i)} - Q_{loss} = 0$ *where* $\Delta h_{rxn}^{SO_2} = h(T)^{S} + h(T)^{O_2} - h(T)^{SO_2},$ $\Delta h_{rxn}^{SO_3} = 1.827 \times (-24{,}097 - 0.26T + 1.69 \times 10^{-3}T^2 + 1.5 \times 10^5/T),\ BTU/lb-mol$
Enthalpy Function	$h^i{}_k(T) = R(a_1^i T + \frac{1}{2}a_2^i T^2 + \frac{1}{3}a_3^i T^3 + \frac{1}{4}a_4^i T^4 + \frac{1}{5}a_5^i T^5 + b_1^i - H_{298}^i) \quad MJ/kmol$ $i = SO_2, SO_3, O_2, N_2, sulfur(L);\ k = 06, 07$

Two reactions take place in this unit, i.e., reaction one of sulfur to sulfur dioxide and reaction two of sulfur dioxide to sulfur trioxide. All of the sulfur is completely converted to sulfur dioxide, and 2% (mole) of the produced sulfur dioxide is further converted to sulfur trioxide in this unit. Therefore, the reaction (generation) rate for each component is related to the input flow rate of sulfur F_{50} and the stoichiometric coefficient of a component in the reaction. Also, the reaction rate of a product component has a positive value and the reaction rate of a reactant component has a negative value. For example, the component mole balance for sulfur dioxide is:

$$SO_2: \quad F_{06}^{SO2} - F_{07}^{SO2} + 0.98 * F_{50} = 0 \tag{4.6}$$

where F_{06}^{SO2} and F_{07}^{SO2} are the input and output flow rates of sulfur dioxide, and $0.98*F_{50}$ is the generation rate of sulfur dioxide. For reaction one (complete conversion of sulfur to sulfur dioxide), sulfur dioxide is a product with stoichiometric coefficient of one. In reaction two, sulfur dioxide is a reactant with stoichiometric coefficient of one. Therefore, the total reaction rate for sulfur dioxide in the two reactions is

$$F_{50} - 0.02*F_{50} = 0.98*F_{50}. \tag{4.7}$$

The steady state overall energy balance is based on the first law of thermodynamics. Neglecting changes in kinetic and potential energy, this equation is (Felder and Rousseau, 1986):

$$-\Delta H + Q - W = 0 \tag{4.8}$$

where ΔH is the change in enthalpy between input and output streams, i.e.,

$\Delta H = H_{out} - H_{in}$ and

$$\Delta H = \sum_{output} F^{(i)} h^{(i)} - \sum_{input} F^{(i)} h^{(i)} + \frac{n_{AR}}{v_A} \Delta h^0{}_{rxn} \tag{4.9}$$

Here n_{AR} is the number of moles of reactant A that is reacted, v_A is the stoichiometric coefficient of reactant A in the reaction and Δh^0_{rxn} is the standard heat of reaction. Here, the reference conditions are that the reactant and product species are at 298°K and 1.0 atmosphere as described in Appendix B. Q is the heat added to the system and W is the work done by the system on the surroundings. The energy equation for sulfur burner unit is written as:

$$F_{50}\, h^{sulfur} + \Sigma\, F_{06}^{(i)}\, h_{06}^{(i)} + F_{50}\, \Delta h^{SO2}{}_{rxn} + 0.02{*}F_{50}\, \Delta h^{SO3}{}_{rxn} - \Sigma\, F_{07}^{(i)}\, h_{07}^{(i)} - Q_{loss} = 0 \quad (4.10)$$

where the first and second terms represent the energy for input streams S50 and S06. The third and fourth terms in this equation denote the generated rates of heat for reaction one and two. The fifth and sixth terms are the energy for output stream S07 and heat loss from this unit.

In Table 4.4, F denotes stream species flow rate, kmol/sec, and h represents species enthalpy, MJ/kmol. $\Delta h_{rxn}{}^{SO2}$ and $\Delta h_{rxn}{}^{SO3}$ are the heats of reaction of sulfur oxidation and SO_2 oxidation at the temperature of the burner. Q_{loss} in energy equation denotes the heat loss from sulfur burner.

The heat of reaction for sulfur oxidation is calculated from the enthalpies of components at reaction temperature:

$$\Delta h_{rxn}SO_2 = h(T)_S + h(T)_{O2} - h(T)_{SO2} \quad (4.11)$$

where the enthalpies are calculated by the regression equations from NASA Technical Manual 4513C (McBride et al., 1993). The detail enthalpy regression functions for all components are given in Appendix A. The enthalpy function used in Eq. 4.11 is slightly different from enthalpy functions for determining the sensible heat. In the process model,

all enthalpy functions for gas streams use sensible enthalpy function except the enthalpy function in Eq. 4.11. The reference state for sensible enthalpy function is 298.15 K and 1Bar for species or elements, and enthalpies for O_2, N_2, SO_2, SO_3 at the reference state (298.15 K and 1 Bar) is zero. In Eq. 4.11, the enthalpy functions are not subtracted by the enthalpies of the species or elements at 298.15 K. Therefore, the enthalpy for species (e.g., SO_2) at reference state is the heat of formation for the species, and the enthalpy for elements (e.g., O_2, S) at reference state is zero. The heat of reaction for sulfur dioxide oxidation to sulfur trioxide is calculated from an empirical formula, a function of reaction temperature, which is given in the kinetic model section of Appendix B.

The four catalytic reactors are adiabatic, plug flow reactors. In these converters, sulfur dioxide is converted to sulfur trioxide in an exothermic chemical reaction. The kinetic model for this catalytic reaction was given by Harris and Norman (1972). Harris and Norman developed an empirical function to determine the intrinsic rate for the oxidation reaction of sulfur dioxide, which is discussed in Appendix B. The intrinsic reaction rate equation is given in Figure 4.5. The real reaction rate of SO_2 (r_{SO3}) is calculated from the intrinsic rate by multiplying by the reaction effectiveness factor E_f, i.e., $r_{SO3} = r_{SO2}E_f$. This reaction effectiveness factor is a lump parameter that combines all of the mismatches in the kinetic model, and this includes current bulk density and current activity of the catalyst, variation of real wet surface of catalyst. Also, the heat of SO_2 oxidation reaction is determined from an empirical function discussed in Appendix B (Harris and Norman, 1972), which is given with the function (Eq. B-6) to determine the temperature difference between bulk gas and catalyst pellet (in Bulk Gas to Pellet Temperature Gradient section of Appendix B.

Reaction: $SO_2 + \frac{1}{2}O_2 \leftrightharpoons SO_3$

SO_2 *conversion rate equation* (*instrinstic reaction rate*):

$$r_{SO_2} = \frac{P^0_{SO_2} P^{0\,1/2}_{O_2}}{(A + BP^{0\,1/2}_{O_2} + CP^0_{SO_2} + DP_{SO_3})^2} \left[1 - \frac{P_{SO_3}}{K_p P_{SO_2} P_{O_2}^{1/2}} \right]$$

r_{SO_2} = *rate of reaction*, $\frac{lb\ mole\ of\ SO_2\ converted}{hr - lb\ catalyst}$

$P_{O_2}, P_{SO_2}, P_{SO_3}$ = *interfacial partial pressures of* O_2, SO_2, SO_3, atm

$P^0_{O_2}, P^0_{SO_2}$ = *interfacial partial pressures of* O_2 *and* SO_2 *at zero conversion under the total pressure at the point in the reator, atm*

K_p = *thermodynamic equilibrium constant*, $atm^{-\frac{1}{2}}$

$$Log_{10} K_P = 5129/T - 4.869, \qquad T \text{ in } {}^oK$$

A, B, C, D are function of temperature T:

Catalyst Type LP-110:

$$A = e^{-6.80 + 4960/T},\quad B = 0,\quad C = e^{10.32 - 7350/T},\quad D = e^{-7.38 + 6370/T}$$

Catalyst Type LP-120:

$$A = e^{-5.69 + 4060/T},\quad B = 0,\quad C = e^{6.45 - 4610/T},\quad D = e^{-8.59 + 7020/T}$$

Figure 4.5 Rate Equation for the Catalytic Oxidation of SO_2 to SO_3 Using Type LP-110 and LP-120 Vanadium Pentoxide Catalyst

The empirical function for heat of SO_2 oxidation reaction is:

$$\Delta h_{rxn}SO_3 = 1.827\times(-24{,}097-0.26T+1.69\times10\text{-}3T2+1.5\times105/T),\ \text{Btu/lb-mole} \qquad (4.12)$$

The four reactors are assumed to be perfect plug flow reactors. Therefore, the material and energy balance equations are differential equations for these four packed bed reactors, and they are established based on the conservation laws. The following gives a discussion on the formulation of constraint equations for Converter I, and the material and energy balance equations for this reactor are given in Table 4.5.

In Figure 4.4, the input to Converter I is the gas (S10) from the waste heat boiler and the output (S11) goes to converter boiler. In Table 4.5, the two rows under material balances give overall and species material balances. The two rows under energy balances give the overall energy balance and the enthalpy function for each species. In these equations, r^I_{so2} and r^I_{so3} are the intrinsic reaction rate and the actual reaction rate for Converter I. The intrinsic reaction rate, r^I_{so2}, is determined by an empirical equation given in Figure 4.5, and the actual reaction rate of SO_2 oxidation, r^I_{so3}, is the product of intrinsic reaction rate and the reaction effectiveness factor E_f^I for Converter I. In Table 4.5, ρ^I_B is the bulk density of catalyst in lb/ft^3, and A is the cross section area of converters. $\Delta h_{rxn}{}^{SO3}$ is the heat of the reaction, and it is determined by an empirical function of temperature given in Eq. 4.12. F_I and H_I are the molar flow rate in kmol/sec and enthalpy in MJ/sec for Converter I. Also, the boundary conditions for these differential equations are required to connect the variables in these equations to the variables in the input and output streams. These boundary conditions are given with the equations as shown in Table 4.5.

Table 4.5 The Process Constraint Equations for Converter I

Material Balances	
Overall	$\frac{dF_I}{dL} = -\frac{1}{2} r_{SO_3} A$ $F_I = F10$, *at* $L=0$; $F_I = F11$, *at* $L=l_I$ *where* $r_{SO_3} = r^I_{SO_2} E^I_f \rho^I_B$; $F_I = \sum_i F_I^{(i)}$ $F_I = F_I^{SO2} + F_I^{SO3} + F_I^{O2} + F_I^{N2}$
Species	SO_3: $\frac{dF_I^{(SO_3)}}{dL} = r_{SO_3} A$ SO_2: $\frac{dF_I^{(SO_2)}}{dL} = -r_{SO_3} A$ O_2: $\frac{dF_I^{(O_2)}}{dL} = -\frac{1}{2} r_{SO_3} A$ N_2: $F_{11}^{(N_2)} - F_{10}^{(N_2)} = 0$ *B. C.*: $F_I^{(i)} = F10^{(i)}$, *at* $L=0$; $F_I^{(i)} = F11^{(i)}$, *at* $L=l_I$ *where* $i = SO_3, SO_2, O_2$
Energy Balances	
Overall	$\frac{dH_I}{dL} = r_{SO_3} \Delta h_{rxn}^{SO_3} A$ $H_I = H10$, *at* $L=0$; $H_I = H11$, *at* $L=l_I$ *where* $H_I = \sum_i F_I^{(i)} h_I^{(i)}$
Enthalpy Function	$h^i_I(T) = R(a_1^i T + \frac{1}{2} a_2^i T^2 + \frac{1}{3} a_3^i T^3 + \frac{1}{4} a_4^i T^4 + \frac{1}{5} a_5^i T^5 + b_1^i - H^i_{298})$ *MJ/kmol* $i = SO_2, SO_3, O_2, N_2$

In the constraint equations for this unit, total flow rates, composition (or species flow rates), and temperatures are measurable variables. The reaction rates and species enthalpies are unmeasurable variables. E_f^I is the process parameter to be estimated. The others, such as cross section area of converter, bulk density of catalyst, and coefficients in enthalpy equations are constants.

The ordinary differential equations for material and energy balances in this unit are discretized into the algebraic difference equations using improved Euler's method (Carnahan, et al., 1969). These algebraic difference equations are written in GAMS program and solved with the other constraints in the plant model. The boundary conditions of the algebraic difference equations are the input and output conditions of the packed beds.

C-3. Absorption Tower Section

This section includes an inter-pass absorption tower and a final absorption tower. These units involve mass transfer of SO_3 from gas phase to liquid phase, i.e., the absorption reaction of sulfur trioxide. For both towers, it is assumed that SO_3 in gas stream is completely absorbed by sulfuric acid solution, and all other gases are considered as inert gases. Also, the total molar flow rate for sulfuric acid stream is counted as the sum of molar flow rates of SO_3 and water in the acid stream. Based on these assumptions, the mole flow rate of water in acid stream should remain unchanged between input and output at the absorption tower. The difference between output and input for both SO_3 and total molar flow rates in acid stream is equal to the molar flow rate of SO_3 in gas stream. In Table 4.6, the material balance equations for interpass absorption tower and final absorption tower are given where SO_3 is completely absorbed from the gas stream S20 and

S24 respectively.

Table 4.6 The Process Constraint Equations for the Interpass Absorption Tower and Final Absorption Tower

Material Balances for Interpass Absorption Tower	
Overall	$F_{15} - F_{15}^{(SO_3)} = F_{16}$
Species	$O_2: \quad F_{16}^{(O_2)} - F_{15}^{(O_2)} = 0$ $N_2: \quad F_{16}^{(N_2)} - F_{15}^{(N_2)} = 0$ $SO_2: \quad F_{16}^{(SO_2)} - F_{15}^{(SO_2)} = 0$ $SO_3: \quad F_{16}^{(SO_3)} = 0$
Material Balances for Final Absorption Tower	
Overall	$F_{24} - F_{24}^{(SO_3)} = F_{25}$
Species	$O_2: \quad F_{25}^{(O_2)} - F_{24}^{(O_2)} = 0$ $N_2: \quad F_{25}^{(N_2)} - F_{24}^{(N_2)} = 0$ $SO_2: \quad F_{25}^{(SO_2)} - F_{24}^{(SO_2)} = 0$ $SO_3: \quad F_{25}^{(SO_3)} = 0$
Stack Gas	$F_{25}C_{O_2} = F_{25}^{(O_2)}$ $F_{25}C_{SO_2} = F_{25}^{(SO_2)}$

The material balance equations in Table 4.6 are only written for the gas streams. They do not include the sulfuric acid streams because they are excluded from the process

model. This was necessary because there are very few measurements available for the acid streams. Also, the rates of absorption of SO_3 in the absorption towers are sufficient to calculate the sulfuric acid product flowrate, which means that exclusion of acid streams does not affect the accuracy of the plant model.

In Table 4.6, the first tow rows give the total and component mole balances for the Interpass absorption tower whereas the next two rows give the same information for final absorption tower. The gas stream leaving the final absorber, S25 is the stack gas stream. The last row in the table relates the component flowrates in the absorber with the stack gas concentrations of SO_2 and O_2.

C-4. Overall Material Balance

The overall material balance relates the flow rates of raw materials to the production of products and wastes. For the sulfuric acid process, the production rate of sulfuric acid, f_{prod} can be determined by the SO_3 absorption rates in inter-pass and final towers.

$$(F_{15,SO3} + F_{24,SO3}) / F_{prod} = X_{prod} \quad (4.13)$$

where X_{prod} is the molar fraction of SO_3 in the acid product stream. The unit of all the flowrates (F_{prod}, $F_{15,SO3}$, $F_{24,SO3}$) is kmol/sec.

The dilution water is used for both the inter-pass and final acid tower dilution tanks. It is used to adjust the acid strength. The amount of dilution water flow rate, F_{dw} (kmol/sec) is determined by the production rate of sulfuric acid (F_{prod}) and the product concentration (X_{prod}), i.e.,

$$F_{dw} = F_{prod}*(1-X_{prod}) \quad (4.14)$$

The constraint for the ratio of oxygen to nitrogen in the air is:

$$F_{06,O2} / F_{06,N2} = 0.21 / 0.79 \quad (4.15)$$

The average molecular weight of the sulfuric acid product stream can be calculated as

$$mwprod = X_{prod}*mw\_SO_3 + (1-X_{prod})*mw\_H_2O \quad (4.16)$$

where mw_SO_3 and mw_H_2O are molecular weights of SO_3 and H_2O respectively. The SO_2 emission from the plant, which is defined as the pounds of SO_2 released to the environment per ton of acid produced is calculated as

$$emiss = (F_{25,so2}*64.0*2.204)/(F_{prod}*(X_{prod}*mw\_SO_3+(1-X_{prod})*mw\_H_2O) /1000) \quad (4.17)$$

The factor of 1000 converts kgs of acid flowrate to tons whereas the factor of 2.204 converts SO_2 flowrate from kgs to pounds.

This concludes the discussion of formulation of process model for the D-train of the sulfuric acid process. The next section will explain the validation of this process model.

D. Process Model Validation

Based on the method proposed in Chapter 3, the process variables are classified as measured variables and unmeasured variables according to the availability of measurements from plant distributed control system. The process variables that are classified as measured variables are given in Table 4.7. The table also gives the brief descriptions of these variables, their values obtained from the plant data measurements and their standard deviations. The plant data used is from February 3, 1997. The heat transfer coefficients and reactor effectiveness factors are considered as parameters since they change very slowly with time. The complete list of parameters is given in Table 4.8. The table also shows the initial values of these parameters, which are based on the work of Richard (1987).

The design data for the D-train process is not available to us. So, the current operating data from distributed control system is used to conduct model validation. Combined gross error detection and data reconciliation method will be used to simulate the

Table 4.7 Measured Variables for the Sulfuric Acid Process Model

Measurement	Description	Plant Data	Standard Deviation
F06	Total Flowrate of inlet air stream - kmol/s	1.741	0.1
F50	Total Flowrate of burner outlet gas - kmol/s	0.245	0.025
Fsbfw	Total Flowrate of boiler feed water - kmol/s	1.93	0.17
O2percent	O_2 % in stack gas	6.0	0.21
Pshp1	Pressure of superheated steam coming out of superheater1 - psia	614.7	5.0
Pshp2	Pressure of superheated steam coming out of superheater2 - psia	614.7	5.0
Pss2	Pressure of saturated steam leaving the drum	709.7	10
SO2ppm	SO_2 ppm in stack gas	355.0	10
T06	Temperature of inlet air - K	359.8	2.9
T07	Temperature of burner outlet gas - K	1321.5	3.2
T09	Temperature of waste heat boiler outlet - K	646.5	2.7
T10	Temperature of converter1 inlet gas - K	708.0	3.3
T11	Temperature of converter1 outlet gas - K	893.7	3.5
T12	Temperature of converter2 inlet gas - K	689.3	2.7
T13	Temperature of converter2 outlet gas - K	785.9	2.6
T15	Temperature of gas entering secondary absorber	501.5	3.0
T16	Temperature of gas leaving secondary absorber	349.8	3.0
T19	Temperature of gas entering hot IP exchanger K	549.3	2.6
T20	Temperature of converter3 inlet gas - K	690.9	3.1
T21	Temperature of converter3 outlet gas - K	737.0	3.3
T22	Temperature of converter4 inlet gas - K	683.5	3.5
T23	Temperature of converter4 outlet gas - K	692.6	2.7
T235	Temperature of gas entering economizer - K	673.2	2.9
T24	Temperature of gas leaving economizer - K	504.8	2.8
T25	Temperature of stack gas - K	350.4	3.0
TSBFW	Temperature of boiler feed water - K	225.0	2.4

TSHP1	Temperature of superheated steam coming out of superheater1- K	665.0	3.1
TSHP2	Temperature of superheated steam coming out of superheater2- K	650.0	3.1
TSW1	Temperature of water leaving the economizer- K	340.0	2.6

process model. The simulation results will be compared with the operating data to examine the accuracy. Before doing combined gross error detection and data reconciliation, the observability and redundancy condition needs to be checked. This condition is given below.

Number of measured variables > Degree of freedom

where Degree of freedom = Number of variables – Number of equality constraints + Number of independent chemical reactions

Table 4.8 Parameters in the Sulfuric Acid Process Model

Parameter	Description	Initial Point
blrU	Heat Transfer Coefficient in waste heat boiler	0.364
clrU	Heat Transfer Coefficient in converter boiler	0.239
effi	Efficiency in converter 1	0.245
effii	Efficiency in converter 2	0.233
effiii	Efficiency in converter 3	0.0925
effiv	Efficiency in converter 4	0.0533
ex65U	Heat Transfer Coefficient in cold IP exchanger	0.257
ex66U	Heat Transfer Coefficient in hot IP exchanger	0.273
ex67U	Heat Transfer Coefficient in superheater-1	0.582

ex68U	Heat Transfer Coefficient in superheater-2	0.169
ex71U	Heat Transfer Coefficient in economizer	0.143
Unit of all heat transfer coefficients in Table 4.8 is 10e-1 KJ/s-K-sqft.		

For the D-train sulfuric acid model, there are 779 variables and 765 equations. The number of independent chemical reactions taking place in the process is six (two in the sulfur burner and four in the reactors). The degree of freedom for this problem is 779– 765 + 6 = 20. The number of measured variables is 29, which is larger than the degree of freedom. Therefore, the plant model satisfies the redundancy criterion.

For the combined gross error detection and data reconciliation step, in addition to the plant operating data, the standard deviation values are needed. These are shown in the Table 4.7. The plant data used is from February 3, 1997. The set of reconciled data obtained after combined gross error detection and data reconciliation is shown in Table 4.9. The table also shows the relative difference between plant data and the reconciled values.

As can be seen from Table 4.9, the relative difference for most of the variables is less than 1%. For three variables, the difference was found to be greater than 10%. These are listed below.

1) F06 Input Air flowrate

2) SO2ppm SO_2 ppm level in stack gas

3) O2percent Molar percentage of O_2 in stack gas

The large difference in these variables was attributed to the errors in the measuring instruments. These three variables are therefore identified as gross errors. The average difference between the plant data and reconciled values for all the temperature variables is

0.56% whereas the average difference for all the variables excluding the gross errors is 0.47 %. Thus, the results of combined gross error detection and data reconciliation agree with the plant operating data within the accuracy of the data.

Table 4.9 Comparison of Reconciled Data and Plant Data for Measured Variables

Measurement		Plant Data	Reconciled Data	Relative Difference
F06	Kmol/s	1.741	2.2	20.83
F50	Kmol/s	0.245	0.244	0.409
Fsbfw	Kmol/s	1.93	1.943	0.681
O2percent		6	5.237	14.56
Pshp1	Psia	614.7	614.7	0
Pshp2	Psia	614.7	614.7	0
Pss2	Psia	709.7	710.2	0.0791
T06	K	359.81	355	1.355
T07	K	1321.48	1325	0.266
T09	K	646.48	642.6	0.599
T10	K	708	713.2	0.734
T11	K	893.70	890	0.4157
T12	K	689.26	689.8	0.085
T13	K	785.92	780.5	0.687
T15	K	501.48	505	0.697
T16	K	349.81	350.5	0.197
T19	K	549.26	545	0.782
T20	K	690.92	694.5	0.513
T21	K	737.03	739.8	0.371
T22	K	683.45	677.9	0.819
T23	K	692.59	689.3	0.475
T235	K	673.15	677.1	0.59
T24	K	504.81	500	0.962
T25	K	350.37	350.4	0.000634
TSBFW	K	225	225	0.00452
TSHP1	K	665	665.2	0.0307
TSHP2	K	650	649.9	0.00611
TSW1	K	340	344.9	1.429
SO2ppm		355	219.6	38.1

This concludes the validation of the D-train process model. The next chapter describes the results of application of the Advanced Process Analysis System to the D-train and the E-train sulfuric acid processes.

CHAPTER 4 PROCESS MODELS

The Advanced Process Analysis System was applied to an actual plant to ensure that the program meets the needs and requirements of the process and design engineers. The contact process for sulfuric acid at IMC Agrico's plant in Convent, Louisiana was chosen for this demonstration. This process incorporates nearly all of the process units found in chemical plant and refineries including packed bed catalytic chemical reactors, absorption towers and heat exchangers among others. The company has two plants producing sulfuric acid by the contact process, called the D-train and the E-train. Detailed description of both of these processes is given below.

A. D-Train Contact Sulfuric Acid Process Description

IMC Agrico's "D" train is a 4800 TPD 93% sulfuric acid plant built by Chemical Construction Company in 1966. The overall yield of elemental sulfur to sulfuric acid is 97.5%.

The contact process is a three-step process that produces sulfuric acid and steam from air, molten sulfur and water. The process flow diagram is shown in Figure 4.1, and the process consists of three sections, which are the feed preparation section, the reactor section, and the absorber section.

In the feed preparation section, molten sulfur feed is combusted with dry air in the sulfur burner. The reaction is:

$$S + O_2 ==> SO_2 + Heat$$

The reaction is exothermic and goes to completion. The gas leaving the burner is composed of sulfur dioxide, nitrogen, and unreacted oxygen at approximately 1800 ^{o}F.

The equipment used in this section includes an air filter, drying tower, a blower and a sulfur burner. The blower is five-stage, polytropic steam driven turbine with an efficiency of about 65%. The pump takes in approximately 130,000 cfm of ambient air at -10 inches of water and discharges it at about 170 inches of water and 165 ^{o}F under normal operation. The blower turbine speed is adjusted to change the production rate for each train. The drying tower removes ambient moisture from the intake air with 98 wt. % sulfuric acid flowing at a rate of about 4-5000 gpm. The tower is 25 feet in diameter and contains 17 ft 2 inches of packing.

In the sulfur burner, the dry compressed air discharged from the turbine reacts with molten sulfur to produce sulfur dioxide. A cold air bypass is used to maintain the burner exit temperature at 1800 ^{o}F. This temperature is setpoint controlled because it is the inlet temperature for the waste heat boiler (WB). The setpoint is dictated by equipment limitations and design considerations.

The sulfur dioxide, along with nitrogen and unreacted oxygen enters the waste heat boiler. The waste heat boiler is equipped with a hot gas bypass so that the temperature of the gases entering the first catalyst bed can be controlled at 800 ^{o}F. This boiler is a shell and tube type supplied with water from the steam drum. The boiler produces saturated steam at about 500^{o}F and 670 psig and utilizes about 10% blowdown.

The second section of the contact process plant is the reactor section. The reactor consists of four beds packed with two different types of Vanadium Pentoxide catalyst. The first two beds are packed with Monsanto's type LP-120 catalyst whereas the third and forth beds are packed with type LP-110. The purpose of using two different catalysts is to have higher catalyst activity in the low temperature zones of the third and fourth beds.

In the reactor section, the gas mixture from the feed preparation section is further reacted in the fixed catalyst beds to produce sulfur trioxide and heat according to the reaction:

$$2SO_2 + O_2 \rightleftharpoons 2SO_3 + \text{Heat}$$

The reaction is exothermic and the equilibrium conversion decreases with the increase in reaction temperature. For this reason, the process uses four packed beds, and heat exchangers between each bed remove the produced energy to reduce the temperature.

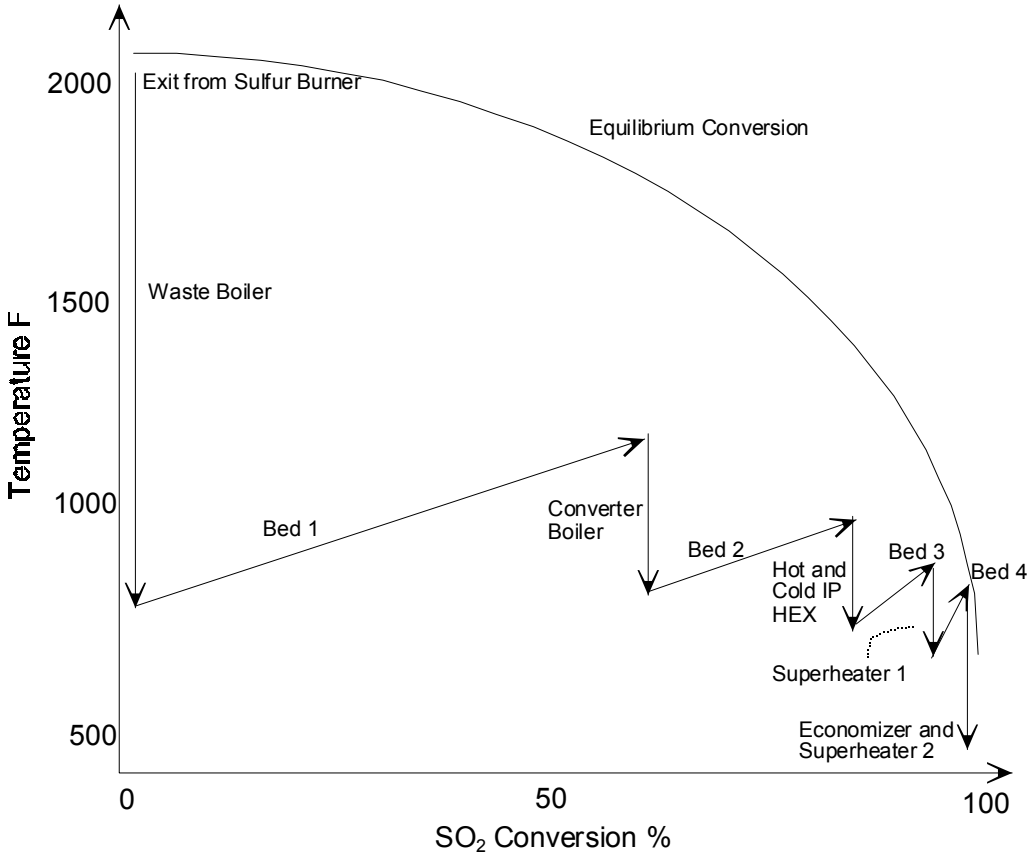

Figure 4.2 Temperature-Conversion of SO_2 Plot for D-train Sulfuric Acid Process

As shown in Figure 4.2, the equilibrium conversion of sulfur dioxide decreases with the increase in operating temperature. Removing reaction heat from each reactor increases the conversion of sulfur dioxide to sulfur trioxide and this removed heat is used to produce steam. Also, the equilibrium conversion increases by decreasing the concentration of sulfur trioxide and an inter-pass tower is used to absorb and remove sulfur trioxide from the gas stream between the second and the third catalyst beds. This design ensures higher conversion in the reactor beds.

As shown in Figure 4.1, the exit gases from the first bed are cooled in the converter boiler (CB). This boiler has the same configuration as the waste heat boiler. It is supplied with water from the steam drum. It produces saturated steam at 500^{o}F and 670 psig and utilizes about 10% blowdown. The hot and cold inter-pass heat exchangers (H and C) are used to cool the gases from the second catalyst bed before these gases are passed to the inter-pass tower. The gases from the third catalyst bed are cooled by superheater-1, which is a finned tube heat exchanger. This superheater produces superheated steam from the saturated steam produced by the boilers. The gases from the fourth bed consist of sulfur trioxide, nitrogen, oxygen and a small amount of sulfur dioxide. They are first cooled by superheater-2 followed by the economizer (E). In the superheater-2, cooling is done by the saturated steam coming from the steam drum whereas in the economizer, it is done by the boiler feed water. The cooled gases are then passed to the final tower for absorption of sulfur trioxide.

The final section of the contact process plant is the absorber section. In this section the SO_3 is absorbed from the reaction gas mixture into 98 wt. % sulfuric acid to produce a more concentrated acid. Also, heat is produced according to the equation:

$$SO_3 + H_2O \Rightarrow H_2SO_4 + \text{Heat}$$

As shown in Figure 4.1, the equipment in this section includes the final acid absorption tower, an inter-pass absorption tower, two acid absorption tanks and a drying tower acid tank. The two absorption towers use 98 wt. % acid to produce more concentrated acid. Water is added to the tanks to keep the sulfuric acid strength at 93 wt. % in drying tower acid tank and 98 wt. % in absorption tower tanks. The 93 wt. % acid from the drying tower acid tank is sold as the product acid. The exit gases from the final absorption tower containing unreacted air and small amount of sulfur dioxide are discharged to the air.

In the steam system, the boiler feed water is pre-heated to 380^{o}F at 740 psig by the economizer and is then sent to the steam drum. It then passes to the waste heat boiler and the converter boiler to produce saturated steam at 675 psig. This saturated steam is circulated back to the steam drum. It then goes to superheater-1 and superheater-2 to generate superheated steam at 626 psig. The superheated steam is used to drive the turbine and the excess steam is one of the products, which is used in an adjacent plant.

This concludes the description of the D-train sulfuric acid process. The following section describes the E-train process of the Uncle Sam Sulfuric Acid plant.

B. E-Train Contact Sulfuric Acid Process Description

Uncle Sam plant's “E” train is a 3200 TPD 93 mole % sulfuric acid plant designed by the Monsanto Enviro-Chem System, Inc. which began to operate in March, 1992. The overall conversion of elemental sulfur to sulfuric acid is about 99.7%. It represents the state-of-art technology of the contact process. The contact process is a three-step process that produces sulfuric acid and steam from air, molten sulfur and water. The process flow

diagram is shown in Figure 4.3, and the process consists of three sections, which are the feed preparation section, the reactor section, and the absorber section.

In the feed preparation section, molten sulfur feed is combusted with dry air in the sulfur burner. The reaction is:

$S + O_2 ==> SO_2 + Heat$

The reaction is exothermic and goes to completion. The gas leaving the burner is composed of sulfur dioxide, nitrogen, and unreacted oxygen at approximately 1400 ^oF. The equipment used in this section include an air filter, drying tower, a main compressor and a sulfur burner. The compressor is steam driven turbine with an efficiency of about 65%. It is a five stage, polytropic turbine on steam side and a centrifugal blower on the gas side. The pump takes in approximately 150,000 cfm of ambient air at -3 inches of water and discharges it at about 160 inches of water and 230^oF under normal operation. The compressor turbine speed is adjusted to change the production rate for each train. The drying tower removes ambient moisture from the intake air with 98 wt. % sulfuric acid flowing at a rate of about 3600 gpm.

In the sulfur burner, the dry compressed air discharged from the turbine reacts with molten sulfur to produce sulfur dioxide. The sulfur dioxide, along with nitrogen and unreacted oxygen enters waste heat boiler. The waste heat boiler is equipped with a hot gas bypass so that the temperature of the gases entering the first catalyst bed can be controlled to 788^oF. This boiler is a shell and tube type supplied with water from the economizers. The boiler produces saturated steam at about 500^oF and 670 psig and utilizes about 9% blowdown. The rest of the steam is passed to superheater to produce superheated steam at about 750^oF.

The second section of the contact process plant is the reactor or converter section. The reactor consists of four beds packed with two different types of vanadium pentoxide catalyst. In this part the gas mixture from the feed preparation section is further reacted in the fixed catalyst beds to produce sulfur trioxide and heat according to the reaction:

$$2SO_2 + O_2 \rightleftharpoons 2SO_3 + \text{Heat}$$

The reaction is exothermic and the equilibrium conversion decreases with the increase in reaction temperature. For this reason, the process uses four packed beds, and heat exchangers between each bed remove the produced energy to reduce the temperature. The equilibrium conversion of sulfur dioxide decreases with the increase in operating temperature. Removing reaction heat from each reactor increases the conversion of sulfur dioxide to sulfur trioxide and this removed heat is used to produce steam. Also, the equilibrium conversion increases by decreasing the concentration of sulfur trioxide, and an inter-pass tower is used to absorb and remove sulfur trioxide from the gas stream between the third and the fourth catalyst beds. This design ensures the high conversion.

As shown in Figure 4.3, the superheater (SH) is used to cool the exit gas from the first bed by the saturated steam from waste heat boiler (BLR). It produces superheated steam at about 750^{o}F and 630 psig. The hot inter-pass heat exchanger (H) is used to cool the gases from the second catalyst bed. The cold inter-pass heat exchanger (C) and economizer (E) are used to cool the gases from the third catalyst bed before these gases pass to the inter-pass tower. The hot and cold inter-pass heat exchangers are used also to heat the unabsorbed gases from the inter-pass tower while cooling the gases from the second and the third bed respectively. The gases from the fourth bed consist of sulfur trioxide, nitrogen, oxygen and a small amount of sulfur dioxide, and they are cooled by the

superheater (SH') and economizers (E') before passing to the final tower for absorption of sulfur trioxide. The superheated steam is used to drive the compressor turbine, and the excess steam is one of the plant products.

The final section of the contact process plant is the absorber section. In this section the SO_3 is absorbed from the reaction gas mixture into 98 wt. % sulfuric acid to produce a more concentrated acid. Also, heat is produced according to the equation:

$$SO_3 + H_2O \Rightarrow H_2SO_4 + \text{Heat}$$

As shown in Figure 4.3, the equipments in this section include the final acid absorption tower, inter-pass absorption tower, acid pump tank, dilution acid tank and three heat exchangers. These two absorption towers use 98 wt. % acid to produce more concentrated acid. Water is added to the two tanks to keep the sulfuric acid strength at 93 wt. % in acid dilution tank and 98 wt. % in acid tower pump tank. The exit gases from the final absorption tower are discharged to the air with less than 4 lb of SO_2 per ton of sulfuric acid produced.

This concludes the brief description of the contact sulfuric acid process. The next section describes the process model for the D-train sulfuric acid process.

C. Process Model for D-train Sulfuric Acid Process

As described earlier, process model is a set of constraint equations, which are the material and energy balances, rate equations and equilibrium relations that describe the material and energy transport and the chemical reactions of the process. These form a mathematical model of relationships between the various plant units and process streams. Before the constraint equations are formulated, it is important to note that in order to have an accurate model of the process, it is essential to include the key process units such as

reactors, heat exchangers and absorbers. These units affect the economic and pollution performance of the process to a significant extent. Certain other units are not so important and can be excluded from the model without compromising the accuracy of the simulation. For the D-train process, the four converters, sulfur burner, boilers, superheaters, acid absorbers were identified as the important units to be included in the model whereas the acid tanks, acid coolers, air blower, air filter etc. were excluded from the model. The complete list of the process units and process streams included in the model is given in Tables 4.1 and 4.2. The process model diagram with these units and streams is shown in Figure 4.4. The same diagram drawn using the graphical interface of Flowsim is shown in Appendix C.

Having selected the process units and streams, the next step is to develop the constraint equations. The constraint equations are programmed in the GAMS language and are used to reconcile plant measurements, estimate parameters, optimize the profit and minimize emissions from the plant. The constraint formulation techniques are very similar for process units of the same type. Therefore, this section is divided into four sub-sections; heat exchanger network, reactors, absorption towers and overall balance for the plant. Each of these sub-sections explains how constraints are written for that particular type of unit. For each type, detailed constraint equations are shown for a representative unit.

C-1. Heat Exchanger Network

As shown in Figure 4.4, the heat exchanger network in sulfuric acid plant includes two boilers, two gas-to-gas hot and cold inter-pass heat exchangers, two superheaters and a gas-to-compressed-water economizer. In these units, there is no mass transfer or chemical reaction. The inlet component flowrates are equal to the outlet component flow rates for

both sides. The energy balance states that the decrease of the enthalpy (MJ/s) in the hot side is equal to the increase of enthalpy in cold side plus the heat loss, i.e.,

$$(H^{inlet} - H^{outlet})_{hot} = (H^{outlet} - H^{inlet})_{cold} + Q_{loss}. \quad (4.1)$$

Table 4.1 Process Units in the D-train Sulfuric Acid Process Model (Refer to Figure 4.4, the Process Model Diagram for the D-train)

Name of Unit	Description
Burner	Sulfur Burner
Cboiler	Converter Boiler
ColdIP	Cold Interpass Heat Exchanger
Converter1	Reactor Bed 1
Converter2	Reactor Bed 2
Converter3	Reactor Bed 3
Converter4	Reactor Bed 4
Drum	Steam Drum
Economizer	Economizer
Finalab	Secondary Acid Absorber
Furnspl	Splitter after the burner
HotIP	Hot Interpass Heat Exchanger
Interab	Primary Acid Absorber
MixRec	Mixer after the waste heat boiler
Mixsteam	Steam Mixer before the drum
Sh1	Superheater1
Sh2	Superheater2
Splsteam	Steam Splitter after the drum
Splwater	Water Splitter after the economizer
Wboiler	Waste Heat Boiler

Table 4.2 Process Streams in the D-train Sulfuric Acid Process Model (Refer to Figure 4.4, the Process Model Diagram for the D-train)

Name of Stream	Description
s06	Inlet Air Stream
s07	Sulfur Burner Outlet Gas Stream
s08	Gas stream entering the waste heat boiler
s08a	Waste Heat Boiler Bypass
s09	Waste Heat Boiler Outlet
s10	Converter 1 Inlet
s11	Converter 1 Outlet
s12	Converter 2 Inlet
s13	Converter 2 Outlet
s14	Hot gases entering Cold IP exchanger
s15	Gas stream entering secondary absorber
s16	Gas stream leaving secondary absorber
s19	Cold gases entering Hot IP exchanger
s20	Converter 3 Inlet
s21	Converter 3 Outlet
s22	Converter 4 Inlet
s23	Converter 4 Outlet
s235	Gas stream entering economizer
s24	Gas stream leaving economizer
s25	Stack gas stream
s50	Sulfur Stream
sbd	Blowdown stream from the drum
sbfw	Boiler Feed Water
shp1	Superheated steam from superheater1
shp2	Superheated steam from superheater2
ss1	Saturated steam entering the drum
ss1a	Saturated steam from the waste heat boiler
ss1b	Saturated steam from the converter boiler
ss2	Saturated steam leaving the drum
ss4	Saturated steam entering superheater1
ss5	Saturated steam entering superheater1
sw1	Water leaving the economizer
sw1a	Water entering the waste heat boiler
sw1b	Water entering the converter boiler

For the hot inter-pass heat exchanger (HotIP), s13 is the inlet stream on the cold side whereas s14 is the outlet stream on the hot side. s19 is the inlet stream on the cold side and s20 is the outlet stream on cold side. The energy balance can be written as

$$(H^{inlet} - H^{outlet})_{hot} = \Sigma F_{13}^{(i)} h_{13}^{(i)} - \Sigma F_{14}^{(i)} h_{14}^{(i)} \quad \text{and} \tag{4.2}$$

$$(H^{inlet} - H^{outlet})_{cold} = \Sigma F_{19}^{(i)} h_{19}^{(i)} - \Sigma F_{20}^{(i)} h_{20}^{(i)}$$

where $F_{13}^{(i)}$ is the molar flowrate (kmol/s) of species i in stream s13 and $h_{13}^{(i)}$ is the enthalpy (MJ/kmol) of species i in stream s13. The total molar flowrate of stream s13 and the total enthalpy of stream s13 are given by the equations

$$F_{13} = \Sigma F_{13}^{(i)} \quad \text{and} \tag{4.3}$$

$$H_{13} = \Sigma F_{13}^{(i)} h_{13}^{(i)}$$

where the summation is done over all the species i present in stream s13. This naming convention is used for all the flowrates and enthalpies. The number in the subscript of the variable can be used to identify the stream to which it belongs. H^{inlet}_{hot} is the enthalpy of the inlet stream on hot side, and it has units of MJ/s.

The heat transferred in an exchanger is proportional to heat transfer area A, overall heat transfer coefficient U, and the logarithm mean temperature difference between the two sides ΔT_{lm}, i.e., $Q = UA\,\Delta T_{lm}$, where Q is the enthalpy change on cold side, i.e.,

$$Q = (H^{inlet} - H^{outlet})_{cold} = \Sigma F_{19}^{(i)} h_{19}^{(i)} - \Sigma F_{20}^{(i)} h_{20}^{(i)} \tag{4.4}$$

The material and energy balances as well as heat transfer equations are similar for all units in heat exchanger network. Table 4.3 gives the constraint equations for the hot inter-pass heat exchanger as an example of process constraint equations for all heat exchanger units. The first two rows of the Table 4.3 under material balance give the overall mass balance and all of the species mass balances. The overall mass balance is the

summation of all species mass balances. Therefore, if all of the species mass balances are used to describe the process, then the overall mass balance does not need to be included since it is redundant. The species mass balances are used to describe the relationship of the input and output flow rate variables.

Table 4.3 The Constraint Equations for Hot Inter-Pass Heat Exchanger

Material Balances	
Overall	$(F_{14}^{(SO_3)} + F_{14}^{(SO_2)} + F_{14}^{(O_2)} + F_{14}^{(N_2)}) - (F_{13}^{(SO_3)} + F_{13}^{(SO_2)} + F_{13}^{(O_2)} + F_{13}^{(N_2)}) = 0$ $(F_{20}^{(SO_3)} + F_{20}^{(SO_2)} + F_{20}^{(O_2)} + F_{20}^{(N_2)}) - (F_{19}^{(SO_3)} + F_{19}^{(SO_2)} + F_{19}^{(O_2)} + F_{19}^{(N_2)}) = 0$
Species	O_2: $F_{14}^{(O_2)} - F_{13}^{(O_2)} = 0$, $F_{20}^{(O_2)} - F_{19}^{(O_2)} = 0$ N_2: $F_{14}^{(N_2)} - F_{13}^{(N_2)} = 0$, $F_{20}^{(N_2)} - F_{19}^{(N_2)} = 0$ SO_2: $F_{14}^{(SO_2)} - F_{13}^{(SO_2)} = 0$, $F_{20}^{(SO_2)} - F_{19}^{(SO_2)} = 0$ SO_3: $F_{14}^{(SO_3)} - F_{13}^{(SO_3)} = 0$, $F_{20}^{(SO_3)} - F_{19}^{(SO_3)} = 0$
Energy Balances	
Overall	$\left(\sum_i F_{14}^{(i)} h_{14}^{(i)} - \sum_i F_{13}^{(i)} h_{13}^{(i)}\right) - \left(\sum_i F_{19}^{(i)} h_{19}^{(i)} - \sum_i F_{20}^{(i)} h_{20}^{(i)}\right) + Q_{loss} = 0$ where $h^i{}_k(T) = R(a_1^i T + \frac{1}{2} a_2^i T^2 + \frac{1}{3} a_3^i T^3 + \frac{1}{4} a_4^i T^4 + \frac{1}{5} a_5^i T^5 + b_1^i - H_{298}^i)$ $i = SO_2, SO_3, O_2, N_2;\ k = 13, 14, 19, 20$
Heat Transfer	$\left(\sum_i F_{20}^{(i)} h_{20}^{(i)} - \sum_i F_{19}^{(i)} h_{19}^{(i)}\right) - (U_{ex66} A_{ex66} \Delta T_{lm}) = 0$

In the constraints of Table 4.3, F denotes the component molar flow rate, kmol/sec, and its superscript i and subscript k denote the component names and stream numbers respectively. h's in the equations represent the species enthalpies of streams (MJ/kmol), and Q_{loss} is the heat loss from the exchanger (MJ/kmol). T is the stream temperature (K), and ΔT_{lm} is the logarithm mean temperature difference (K) between hot and cold sides of the exchanger. In the heat transfer equation, U and A are the overall heat transfer coefficient and heat transfer area respectively.

The two rows in Table 4.3 under energy balances give the overall energy balance and heat transfer equation. In addition, the enthalpy for each species, h(T), expressed as a polynomial function of the stream temperature is also given in the table. The enthalpy equations for gases, compressed water, and superheated steam are developed in the Appendix A.

In these equations, the total flow rates, species flow rates (or composition), and temperatures of streams are the measurable variables. Species enthalpies and the mean temperature difference are the unmeasured variables. The heat transfer coefficients are the process parameters to be estimated. The heat transfer area and coefficients in enthalpy equations and the heat losses are constants. The heat loss from the exchanger was estimated to be 2% of the amount of heat exchanged from the plant design data for the E-train.

C-2. Reactor System

The reactor system in this plant includes a sulfur burner and four catalytic converters. The following describes the constraint equations for sulfur burner and the first converter.

When a chemical reaction is involved in the process, it is convenient to use the mole balance to describe relationship of input and output flow rates of a unit for a component. Also, the overall mole balance is obtained from the component mole balances, i.e., the summation of component mole balance gives the overall mole balance. The sulfuric acid process involves three reactions, i.e., reaction of sulfur to sulfur dioxide, reaction of sulfur dioxide to sulfur trioxide, and absorption reaction of sulfur trioxide to sulfuric acid. Mole balances are used to describe the material balances of the units in the process, i.e., all material balance equations for the sulfuric acid process are written with mole balance relations. Moles are conserved when there is no reaction, and the change in the number of moles for a component is determined by the reaction rate and stoichiometric coefficients when there are reactions.

As shown in Figure 4.4, the inputs of sulfur burner are dry air stream (S06) from main compressor, and liquid sulfur stream (S50). The dry air reacts with molten sulfur to produce sulfur dioxide and heat in the burner. The sulfur dioxide, along with nitrogen and unreacted oxygen enters the waste heat boiler. At the design operating temperature of the sulfur burner, all of the sulfur is converted to sulfur dioxide, and some sulfur trioxide is formed from sulfur dioxide. The plant measurements have shown that 2 % (mol) of the SO_2 is converted into SO_3 in this unit, and this value is incorporated in the mass and energy balances of this unit.

The mole and energy balance equations for the sulfur burner are given in Table 4.4. The two rows of this table under mole balance give the overall mole balance and component mole balances. The mole balance for each component is established based on the conservation law. The steady state mole balance for a component is written as:

$$F_{in}(i) - F_{out}(i) + F_{gen}(i) = 0 \quad (4.5)$$

where i represents the names of components. For the sulfur burner, $F_{in}(i)$, $F_{out}(i)$, and $F_{gen}(i)$ are input air flow rate F06(i), output flow rate F07(i), and generation rates of components from reaction, r(i). The overall mole balance is the summation of all component mole balance equations.

Table 4.4 The Process Constraint Equations for Sulfur Burner

Mole Balances	
Overall	$F_{06} - F_{07} - 0.01F_{50} = 0$ $where\ F_{06} = F_{06}^{O2} + F_{06}^{N2}$ $F_{07} = F_{07}^{O2} + F_{07}^{N2} + F_{07}^{SO2} + F_{07}^{SO3}$
Species	$O_2: \quad F_{06}^{(O_2)} - F_{07}^{(O_2)} - 1.01F_{50} = 0$ $N_2: \quad F_{06}^{(N_2)} - F_{07}^{(N_2)} = 0$ $SO_2: \quad F_{06}^{(SO_2)} - F_{07}^{(SO_2)} + 0.98F_{50} = 0$ $SO_3: \quad F_{06}^{(SO_3)} - F_{07}^{(SO_3)} + 0.02F_{50} = 0$ $S: \quad F_{50} - F_{07}^{(S)} - F_{07}^{(SO2)} - F_{07}^{(SO3)} = 0$ $where \quad F_{06}^{(SO_2)} = 0,\ F_{06}^{(SO_3)} = 0,\ F_{07}^{(S)} = 0$
Energy Balances	
Overall	$F_{50}h^{(sulfur)} + \sum_i F_{06}^{(i)}h_{06}^{(i)} + F_{50}\Delta h_{rxn}^{SO_2} + 0.02F_{50}\Delta h_{rxn}^{SO_3} - \sum_i F_{07}^{(i)}h_{07}^{(i)} - Q_{loss} = 0$ *where* $\Delta h_{rxn}^{SO_2} = h(T)^{S} + h(T)^{O_2} - h(T)^{SO_2},$ $\Delta h_{rxn}^{SO_3} = 1.827 \times (-24{,}097 - 0.26T + 1.69 \times 10^{-3}T^2 + 1.5 \times 10^5/T),\ BTU/lb-mol$
Enthalpy Function	$h^i{}_k(T) = R(a_1^i T + \frac{1}{2}a_2^i T^2 + \frac{1}{3}a_3^i T^3 + \frac{1}{4}a_4^i T^4 + \frac{1}{5}a_5^i T^5 + b_1^i - H_{298}^i) \quad MJ/kmol$ $i = SO_2, SO_3, O_2, N_2, sulfur(L);\ k = 06, 07$

Two reactions take place in this unit, i.e., reaction one of sulfur to sulfur dioxide and reaction two of sulfur dioxide to sulfur trioxide. All of the sulfur is completely converted to sulfur dioxide, and 2% (mole) of the produced sulfur dioxide is further converted to sulfur trioxide in this unit. Therefore, the reaction (generation) rate for each component is related to the input flow rate of sulfur F_{50} and the stoichiometric coefficient of a component in the reaction. Also, the reaction rate of a product component has a positive value and the reaction rate of a reactant component has a negative value. For example, the component mole balance for sulfur dioxide is:

$$SO_2: \quad F_{06}^{SO2} - F_{07}^{SO2} + 0.98 * F_{50} = 0 \tag{4.6}$$

where F_{06}^{SO2} and F_{07}^{SO2} are the input and output flow rates of sulfur dioxide, and $0.98*F_{50}$ is the generation rate of sulfur dioxide. For reaction one (complete conversion of sulfur to sulfur dioxide), sulfur dioxide is a product with stoichiometric coefficient of one. In reaction two, sulfur dioxide is a reactant with stoichiometric coefficient of one. Therefore, the total reaction rate for sulfur dioxide in the two reactions is

$$F_{50} - 0.02*F_{50} = 0.98*F_{50}. \tag{4.7}$$

The steady state overall energy balance is based on the first law of thermodynamics. Neglecting changes in kinetic and potential energy, this equation is (Felder and Rousseau, 1986):

$$-\Delta H + Q - W = 0 \tag{4.8}$$

where ΔH is the change in enthalpy between input and output streams, i.e.,

$\Delta H = H_{out} - H_{in}$ and

$$\Delta H = \sum_{output} F^{(i)} h^{(i)} - \sum_{input} F^{(i)} h^{(i)} + \frac{n_{AR}}{v_A} \Delta h^0{}_{rxn} \tag{4.9}$$

Here n_{AR} is the number of moles of reactant A that is reacted, v_A is the stoichiometric coefficient of reactant A in the reaction and Δh^0_{rxn} is the standard heat of reaction. Here, the reference conditions are that the reactant and product species are at 298°K and 1.0 atmosphere as described in Appendix B. Q is the heat added to the system and W is the work done by the system on the surroundings. The energy equation for sulfur burner unit is written as:

$$F_{50}\, h^{sulfur} + \Sigma\, F_{06}^{(i)}\, h_{06}^{(i)} + F_{50}\, \Delta h^{SO2}{}_{rxn} + 0.02{*}F_{50}\, \Delta h^{SO3}{}_{rxn} - \Sigma\, F_{07}^{(i)}\, h_{07}^{(i)} - Q_{loss} = 0 \quad (4.10)$$

where the first and second terms represent the energy for input streams S50 and S06. The third and fourth terms in this equation denote the generated rates of heat for reaction one and two. The fifth and sixth terms are the energy for output stream S07 and heat loss from this unit.

In Table 4.4, F denotes stream species flow rate, kmol/sec, and h represents species enthalpy, MJ/kmol. $\Delta h_{rxn}{}^{SO2}$ and $\Delta h_{rxn}{}^{SO3}$ are the heats of reaction of sulfur oxidation and SO_2 oxidation at the temperature of the burner. Q_{loss} in energy equation denotes the heat loss from sulfur burner.

The heat of reaction for sulfur oxidation is calculated from the enthalpies of components at reaction temperature:

$$\Delta h_{rxn}SO_2 = h(T)_S + h(T)_{O2} - h(T)_{SO2} \quad (4.11)$$

where the enthalpies are calculated by the regression equations from NASA Technical Manual 4513C (McBride et al., 1993). The detail enthalpy regression functions for all components are given in Appendix A. The enthalpy function used in Eq. 4.11 is slightly different from enthalpy functions for determining the sensible heat. In the process model,

all enthalpy functions for gas streams use sensible enthalpy function except the enthalpy function in Eq. 4.11. The reference state for sensible enthalpy function is 298.15 K and 1Bar for species or elements, and enthalpies for O_2, N_2, SO_2, SO_3 at the reference state (298.15 K and 1 Bar) is zero. In Eq. 4.11, the enthalpy functions are not subtracted by the enthalpies of the species or elements at 298.15 K. Therefore, the enthalpy for species (e.g., SO_2) at reference state is the heat of formation for the species, and the enthalpy for elements (e.g., O_2, S) at reference state is zero. The heat of reaction for sulfur dioxide oxidation to sulfur trioxide is calculated from an empirical formula, a function of reaction temperature, which is given in the kinetic model section of Appendix B.

The four catalytic reactors are adiabatic, plug flow reactors. In these converters, sulfur dioxide is converted to sulfur trioxide in an exothermic chemical reaction. The kinetic model for this catalytic reaction was given by Harris and Norman (1972). Harris and Norman developed an empirical function to determine the intrinsic rate for the oxidation reaction of sulfur dioxide, which is discussed in Appendix B. The intrinsic reaction rate equation is given in Figure 4.5. The real reaction rate of SO_2 (r_{SO3}) is calculated from the intrinsic rate by multiplying by the reaction effectiveness factor E_f, i.e., $r_{SO3} = r_{SO2}E_f$. This reaction effectiveness factor is a lump parameter that combines all of the mismatches in the kinetic model, and this includes current bulk density and current activity of the catalyst, variation of real wet surface of catalyst. Also, the heat of SO_2 oxidation reaction is determined from an empirical function discussed in Appendix B (Harris and Norman, 1972), which is given with the function (Eq. B-6) to determine the temperature difference between bulk gas and catalyst pellet (in Bulk Gas to Pellet Temperature Gradient section of Appendix B.

Reaction: $SO_2 + \frac{1}{2}O_2 \leftrightharpoons SO_3$

SO_2 *conversion rate equation* (*instrinstic reaction rate*):

$$r_{SO_2} = \frac{P^0_{SO_2} P^{0\,1/2}_{O_2}}{(A + BP^{0\,1/2}_{O_2} + CP^0_{SO_2} + DP_{SO_3})^2} \left[1 - \frac{P_{SO_3}}{K_p P_{SO_2} P_{O_2}^{1/2}} \right]$$

r_{SO_2} = *rate of reaction*, $\frac{lb\ mole\ of\ SO_2\ converted}{hr - lb\ catalyst}$

$P_{O_2}, P_{SO_2}, P_{SO_3}$ = *interfacial partial pressures of* O_2, SO_2, SO_3, atm

$P^0_{O_2}, P^0_{SO_2}$ = *interfacial partial pressures of* O_2 *and* SO_2 *at zero conversion under the total pressure at the point in the reator, atm*

K_p = *thermodynamic equilibrium constant*, $atm^{-\frac{1}{2}}$

$$Log_{10} K_P = 5129/T - 4.869, \qquad T \text{ in } {}^oK$$

A, B, C, D are function of temperature T:

Catalyst Type LP-110:

$$A = e^{-6.80 + 4960/T},\quad B = 0,\quad C = e^{10.32 - 7350/T},\quad D = e^{-7.38 + 6370/T}$$

Catalyst Type LP-120:

$$A = e^{-5.69 + 4060/T},\quad B = 0,\quad C = e^{6.45 - 4610/T},\quad D = e^{-8.59 + 7020/T}$$

Figure 4.5 Rate Equation for the Catalytic Oxidation of SO_2 to SO_3 Using Type LP-110 and LP-120 Vanadium Pentoxide Catalyst

The empirical function for heat of SO_2 oxidation reaction is:

$$\Delta h_{rxn}SO_3 = 1.827\times(-24{,}097-0.26T+1.69\times10\text{-}3T2+1.5\times105/T),\ \text{Btu/lb-mole} \qquad (4.12)$$

The four reactors are assumed to be perfect plug flow reactors. Therefore, the material and energy balance equations are differential equations for these four packed bed reactors, and they are established based on the conservation laws. The following gives a discussion on the formulation of constraint equations for Converter I, and the material and energy balance equations for this reactor are given in Table 4.5.

In Figure 4.4, the input to Converter I is the gas (S10) from the waste heat boiler and the output (S11) goes to converter boiler. In Table 4.5, the two rows under material balances give overall and species material balances. The two rows under energy balances give the overall energy balance and the enthalpy function for each species. In these equations, r^I_{so2} and r^I_{so3} are the intrinsic reaction rate and the actual reaction rate for Converter I. The intrinsic reaction rate, r^I_{so2}, is determined by an empirical equation given in Figure 4.5, and the actual reaction rate of SO_2 oxidation, r^I_{so3}, is the product of intrinsic reaction rate and the reaction effectiveness factor E_f^I for Converter I. In Table 4.5, ρ^I_B is the bulk density of catalyst in lb/ft^3, and A is the cross section area of converters. $\Delta h_{rxn}{}^{SO3}$ is the heat of the reaction, and it is determined by an empirical function of temperature given in Eq. 4.12. F_I and H_I are the molar flow rate in kmol/sec and enthalpy in MJ/sec for Converter I. Also, the boundary conditions for these differential equations are required to connect the variables in these equations to the variables in the input and output streams. These boundary conditions are given with the equations as shown in Table 4.5.

Table 4.5 The Process Constraint Equations for Converter I

Material Balances	
Overall	$\frac{dF_I}{dL} = -\frac{1}{2} r_{SO_3} A$ $F_I = F10$, *at* $L=0$; $F_I = F11$, *at* $L=l_I$ *where* $r_{SO_3} = r^I_{SO_2} E^I_f \rho^I_B$; $F_I = \sum_i F_I^{(i)}$ $F_I = F_I^{SO2} + F_I^{SO3} + F_I^{O2} + F_I^{N2}$
Species	SO_3: $\frac{dF_I^{(SO_3)}}{dL} = r_{SO_3} A$ SO_2: $\frac{dF_I^{(SO_2)}}{dL} = -r_{SO_3} A$ O_2: $\frac{dF_I^{(O_2)}}{dL} = -\frac{1}{2} r_{SO_3} A$ N_2: $F_{11}^{(N_2)} - F_{10}^{(N_2)} = 0$ *B. C.*: $F_I^{(i)} = F10^{(i)}$, *at* $L=0$; $F_I^{(i)} = F11^{(i)}$, *at* $L=l_I$ *where* $i = SO_3, SO_2, O_2$
Energy Balances	
Overall	$\frac{dH_I}{dL} = r_{SO_3} \Delta h_{rxn}^{SO_3} A$ $H_I = H10$, *at* $L=0$; $H_I = H11$, *at* $L=l_I$ *where* $H_I = \sum_i F_I^{(i)} h_I^{(i)}$
Enthalpy Function	$h^i_I(T) = R(a_1^i T + \frac{1}{2} a_2^i T^2 + \frac{1}{3} a_3^i T^3 + \frac{1}{4} a_4^i T^4 + \frac{1}{5} a_5^i T^5 + b_1^i - H^i_{298})$ *MJ/kmol* $i = SO_2, SO_3, O_2, N_2$

In the constraint equations for this unit, total flow rates, composition (or species flow rates), and temperatures are measurable variables. The reaction rates and species enthalpies are unmeasurable variables. E_f^I is the process parameter to be estimated. The others, such as cross section area of converter, bulk density of catalyst, and coefficients in enthalpy equations are constants.

The ordinary differential equations for material and energy balances in this unit are discretized into the algebraic difference equations using improved Euler's method (Carnahan, et al., 1969). These algebraic difference equations are written in GAMS program and solved with the other constraints in the plant model. The boundary conditions of the algebraic difference equations are the input and output conditions of the packed beds.

C-3. Absorption Tower Section

This section includes an inter-pass absorption tower and a final absorption tower. These units involve mass transfer of SO_3 from gas phase to liquid phase, i.e., the absorption reaction of sulfur trioxide. For both towers, it is assumed that SO_3 in gas stream is completely absorbed by sulfuric acid solution, and all other gases are considered as inert gases. Also, the total molar flow rate for sulfuric acid stream is counted as the sum of molar flow rates of SO_3 and water in the acid stream. Based on these assumptions, the mole flow rate of water in acid stream should remain unchanged between input and output at the absorption tower. The difference between output and input for both SO_3 and total molar flow rates in acid stream is equal to the molar flow rate of SO_3 in gas stream. In Table 4.6, the material balance equations for interpass absorption tower and final absorption tower are given where SO_3 is completely absorbed from the gas stream S20 and

S24 respectively.

Table 4.6 The Process Constraint Equations for the Interpass Absorption Tower and Final Absorption Tower

Material Balances for Interpass Absorption Tower	
Overall	$F_{15} - F_{15}^{(SO_3)} = F_{16}$
Species	$O_2: \quad F_{16}^{(O_2)} - F_{15}^{(O_2)} = 0$ $N_2: \quad F_{16}^{(N_2)} - F_{15}^{(N_2)} = 0$ $SO_2: \quad F_{16}^{(SO_2)} - F_{15}^{(SO_2)} = 0$ $SO_3: \quad F_{16}^{(SO_3)} = 0$
Material Balances for Final Absorption Tower	
Overall	$F_{24} - F_{24}^{(SO_3)} = F_{25}$
Species	$O_2: \quad F_{25}^{(O_2)} - F_{24}^{(O_2)} = 0$ $N_2: \quad F_{25}^{(N_2)} - F_{24}^{(N_2)} = 0$ $SO_2: \quad F_{25}^{(SO_2)} - F_{24}^{(SO_2)} = 0$ $SO_3: \quad F_{25}^{(SO_3)} = 0$
Stack Gas	$F_{25}C_{O_2} = F_{25}^{(O_2)}$ $F_{25}C_{SO_2} = F_{25}^{(SO_2)}$

The material balance equations in Table 4.6 are only written for the gas streams. They do not include the sulfuric acid streams because they are excluded from the process

model. This was necessary because there are very few measurements available for the acid streams. Also, the rates of absorption of SO_3 in the absorption towers are sufficient to calculate the sulfuric acid product flowrate, which means that exclusion of acid streams does not affect the accuracy of the plant model.

In Table 4.6, the first tow rows give the total and component mole balances for the Interpass absorption tower whereas the next two rows give the same information for final absorption tower. The gas stream leaving the final absorber, S25 is the stack gas stream. The last row in the table relates the component flowrates in the absorber with the stack gas concentrations of SO_2 and O_2.

C-4. Overall Material Balance

The overall material balance relates the flow rates of raw materials to the production of products and wastes. For the sulfuric acid process, the production rate of sulfuric acid, f_{prod} can be determined by the SO_3 absorption rates in inter-pass and final towers.

$$(F_{15,SO3} + F_{24,SO3}) / F_{prod} = X_{prod} \quad (4.13)$$

where X_{prod} is the molar fraction of SO_3 in the acid product stream. The unit of all the flowrates (F_{prod}, $F_{15,SO3}$, $F_{24,SO3}$) is kmol/sec.

The dilution water is used for both the inter-pass and final acid tower dilution tanks. It is used to adjust the acid strength. The amount of dilution water flow rate, F_{dw} (kmol/sec) is determined by the production rate of sulfuric acid (F_{prod}) and the product concentration (X_{prod}), i.e.,

$$F_{dw} = F_{prod}*(1-X_{prod}) \quad (4.14)$$

The constraint for the ratio of oxygen to nitrogen in the air is:

$$F_{06,O2} / F_{06,N2} = 0.21 / 0.79 \quad (4.15)$$

The average molecular weight of the sulfuric acid product stream can be calculated as

$$mwprod = X_{prod}*mw\_SO_3 + (1-X_{prod})*mw\_H_2O \quad (4.16)$$

where mw_SO_3 and mw_H_2O are molecular weights of SO_3 and H_2O respectively. The SO_2 emission from the plant, which is defined as the pounds of SO_2 released to the environment per ton of acid produced is calculated as

$$emiss = (F_{25,so2}*64.0*2.204)/(F_{prod}*(X_{prod}*mw\_SO_3+(1-X_{prod})*mw\_H_2O) /1000) \quad (4.17)$$

The factor of 1000 converts kgs of acid flowrate to tons whereas the factor of 2.204 converts SO_2 flowrate from kgs to pounds.

This concludes the discussion of formulation of process model for the D-train of the sulfuric acid process. The next section will explain the validation of this process model.

D. Process Model Validation

Based on the method proposed in Chapter 3, the process variables are classified as measured variables and unmeasured variables according to the availability of measurements from plant distributed control system. The process variables that are classified as measured variables are given in Table 4.7. The table also gives the brief descriptions of these variables, their values obtained from the plant data measurements and their standard deviations. The plant data used is from February 3, 1997. The heat transfer coefficients and reactor effectiveness factors are considered as parameters since they change very slowly with time. The complete list of parameters is given in Table 4.8. The table also shows the initial values of these parameters, which are based on the work of Richard (1987).

The design data for the D-train process is not available to us. So, the current operating data from distributed control system is used to conduct model validation. Combined gross error detection and data reconciliation method will be used to simulate the

Table 4.7 Measured Variables for the Sulfuric Acid Process Model

Measurement	Description	Plant Data	Standard Deviation
F06	Total Flowrate of inlet air stream - kmol/s	1.741	0.1
F50	Total Flowrate of burner outlet gas - kmol/s	0.245	0.025
Fsbfw	Total Flowrate of boiler feed water - kmol/s	1.93	0.17
O2percent	O_2 % in stack gas	6.0	0.21
Pshp1	Pressure of superheated steam coming out of superheater1 - psia	614.7	5.0
Pshp2	Pressure of superheated steam coming out of superheater2 - psia	614.7	5.0
Pss2	Pressure of saturated steam leaving the drum	709.7	10
SO2ppm	SO_2 ppm in stack gas	355.0	10
T06	Temperature of inlet air - K	359.8	2.9
T07	Temperature of burner outlet gas - K	1321.5	3.2
T09	Temperature of waste heat boiler outlet - K	646.5	2.7
T10	Temperature of converter1 inlet gas - K	708.0	3.3
T11	Temperature of converter1 outlet gas - K	893.7	3.5
T12	Temperature of converter2 inlet gas - K	689.3	2.7
T13	Temperature of converter2 outlet gas - K	785.9	2.6
T15	Temperature of gas entering secondary absorber	501.5	3.0
T16	Temperature of gas leaving secondary absorber	349.8	3.0
T19	Temperature of gas entering hot IP exchanger K	549.3	2.6
T20	Temperature of converter3 inlet gas - K	690.9	3.1
T21	Temperature of converter3 outlet gas - K	737.0	3.3
T22	Temperature of converter4 inlet gas - K	683.5	3.5
T23	Temperature of converter4 outlet gas - K	692.6	2.7
T235	Temperature of gas entering economizer - K	673.2	2.9
T24	Temperature of gas leaving economizer - K	504.8	2.8
T25	Temperature of stack gas - K	350.4	3.0
TSBFW	Temperature of boiler feed water - K	225.0	2.4

TSHP1	Temperature of superheated steam coming out of superheater1- K	665.0	3.1
TSHP2	Temperature of superheated steam coming out of superheater2- K	650.0	3.1
TSW1	Temperature of water leaving the economizer- K	340.0	2.6

process model. The simulation results will be compared with the operating data to examine the accuracy. Before doing combined gross error detection and data reconciliation, the observability and redundancy condition needs to be checked. This condition is given below.

Number of measured variables > Degree of freedom

where Degree of freedom = Number of variables – Number of equality constraints + Number of independent chemical reactions

Table 4.8 Parameters in the Sulfuric Acid Process Model

Parameter	Description	Initial Point
blrU	Heat Transfer Coefficient in waste heat boiler	0.364
clrU	Heat Transfer Coefficient in converter boiler	0.239
effi	Efficiency in converter 1	0.245
effii	Efficiency in converter 2	0.233
effiii	Efficiency in converter 3	0.0925
effiv	Efficiency in converter 4	0.0533
ex65U	Heat Transfer Coefficient in cold IP exchanger	0.257
ex66U	Heat Transfer Coefficient in hot IP exchanger	0.273
ex67U	Heat Transfer Coefficient in superheater-1	0.582

ex68U	Heat Transfer Coefficient in superheater-2	0.169
ex71U	Heat Transfer Coefficient in economizer	0.143
Unit of all heat transfer coefficients in Table 4.8 is 10e-1 KJ/s-K-sqft.		

For the D-train sulfuric acid model, there are 779 variables and 765 equations. The number of independent chemical reactions taking place in the process is six (two in the sulfur burner and four in the reactors). The degree of freedom for this problem is 779– 765 + 6 = 20. The number of measured variables is 29, which is larger than the degree of freedom. Therefore, the plant model satisfies the redundancy criterion.

For the combined gross error detection and data reconciliation step, in addition to the plant operating data, the standard deviation values are needed. These are shown in the Table 4.7. The plant data used is from February 3, 1997. The set of reconciled data obtained after combined gross error detection and data reconciliation is shown in Table 4.9. The table also shows the relative difference between plant data and the reconciled values.

As can be seen from Table 4.9, the relative difference for most of the variables is less than 1%. For three variables, the difference was found to be greater than 10%. These are listed below.

1) F06 Input Air flowrate

2) SO2ppm SO_2 ppm level in stack gas

3) O2percent Molar percentage of O_2 in stack gas

The large difference in these variables was attributed to the errors in the measuring instruments. These three variables are therefore identified as gross errors. The average difference between the plant data and reconciled values for all the temperature variables is

0.56% whereas the average difference for all the variables excluding the gross errors is 0.47 %. Thus, the results of combined gross error detection and data reconciliation agree with the plant operating data within the accuracy of the data.

Table 4.9 Comparison of Reconciled Data and Plant Data for Measured Variables

Measurement		Plant Data	Reconciled Data	Relative Difference
F06	Kmol/s	1.741	2.2	20.83
F50	Kmol/s	0.245	0.244	0.409
Fsbfw	Kmol/s	1.93	1.943	0.681
O2percent		6	5.237	14.56
Pshp1	Psia	614.7	614.7	0
Pshp2	Psia	614.7	614.7	0
Pss2	Psia	709.7	710.2	0.0791
T06	K	359.81	355	1.355
T07	K	1321.48	1325	0.266
T09	K	646.48	642.6	0.599
T10	K	708	713.2	0.734
T11	K	893.70	890	0.4157
T12	K	689.26	689.8	0.085
T13	K	785.92	780.5	0.687
T15	K	501.48	505	0.697
T16	K	349.81	350.5	0.197
T19	K	549.26	545	0.782
T20	K	690.92	694.5	0.513
T21	K	737.03	739.8	0.371
T22	K	683.45	677.9	0.819
T23	K	692.59	689.3	0.475
T235	K	673.15	677.1	0.59
T24	K	504.81	500	0.962
T25	K	350.37	350.4	0.000634
TSBFW	K	225	225	0.00452
TSHP1	K	665	665.2	0.0307
TSHP2	K	650	649.9	0.00611
TSW1	K	340	344.9	1.429
SO2ppm		355	219.6	38.1

This concludes the validation of the D-train process model. The next chapter describes the results of application of the Advanced Process Analysis System to the D-train and the E-train sulfuric acid processes.

CHAPTER 5 RESULTS

The Advanced Process Analysis System was used to optimize the contact sulfuric acid process at the IMC Agrico plant. This process incorporates nearly all of the process units found in chemical plant and refineries including packed bed catalytic chemical reactors, absorption towers and heat exchangers among others. The process is thus ideally suited for demonstration of the Advanced Process Analysis System. This chapter presents a discussion of the results obtained for the D-train as well as the E-train process.

A. The D-train Sulfuric Acid Process

As described in Chapter 3, the first step in the implementation of Advanced Process Analysis System is development of the process model. The model formulation for the D-train process was described in Chapter 4. This process model was incorporated in the Advanced Process Analysis System using the Flowsim program. The following section explains how the details of the D-train process model are entered in the Flowsim program.

A-1. Flowsim

Before using Flowsim to enter any process details, a model name and a description has to be selected. The model name ‘contact’ was used for the D-train process as shown in Figure C.V.1 in Appendix C, the User’s Manual. All of the process information for D-train will now be associated with this model name.

The next step of using Flowsim is drawing the flowsheet diagram. The flowsheet diagram gives a convenient visual representation of the entire process model. Flowsim program has an interactive graphical interface to facilitate easy drawing and

editing of the flowsheet diagram. It provides a toolbox with all the necessary buttons to draw units and streams, move them, resize them and change their appearance. The process model diagram for the D-train was shown in Figure 4.4. All of the units and streams in Figure 4.4 are entered into the Flowsim screen using the various commands available. The detailed instructions for this are given in Appendix C, Section V. The flowsheet diagram with the complete process model for D-train is shown in Figure C.V.7.

Each stream and unit in the flowsheet diagram of Flowsim has a unique name and description. The names for the various streams and units appear on the flowsheet diagram as seen in Figure C.V.7. The names and descriptions of the process units and streams for the D-train were shown in Tables 4.1 and Table 4.2 respectively.

The flowsheet diagram drawn in Flowsim is used not only for a convenient visual representation but also to enter the process information in a logical and organized manner. The process information needed to implement Advanced Process Analysis System is of diverse types and is therefore divided into different categories. The following gives more details about how the D-train process information is divided into these different categories.

A-1-1. Measured Variables

The first category of information is the measured variables. As described earlier, a measured variable is a process variable for which measurements are available from the distributed control system. The complete list of measured variables for the D-train was given in Table 4.7. Before entering all these measured variables into Flowsim, they need to be associated with a process unit or process stream in the flowsheet diagram of

Flowsim. This association should be done such that the physical quantity represented by this measured variable is a characteristic of that unit or stream. For example, the measured variable, T06 represents the temperature of stream s06, and it is associated with that stream. This is shown in Figure C.V.11. The measured variable O2percent is associated with stream s25 because it represents the percent of oxygen present in that stream. The D-train model does not have any measured variable that can be associated with a unit. Once, all the measured variables have been associated with a process unit or a stream, they can be now conveniently entered using the interactive features of Flowsim. Details about entering the measured variables are shown in Appendix C, Section V.

For each measured variable, Flowsim stores the all the data needed to carry out the various steps of Advanced Process Analysis System in an Access database. This is shown in Figure C.V.11. This includes a name and a description for the variable. The descriptions for the measured variables of D-train are shown in Table 4.7. It also includes plant data and the standard deviation values, which are needed for on-line optimization. These values for D-train are also given in Table 4.7. The initial point, scaling factor, lower bound and upper bound values are used in on-line optimization to solve the GAMS problems. These values are optional because GAMS provides default values for all of them. However, to obtain a good solution, these have to be chosen judiciously by the user, and this requires a thorough understanding of the process. The last data item in Figure C.V.11 is the units used for that variable. For example, the unit of measured variable T06 is K.

A-1-2. Unmeasured Variables

The second category of information is the unmeasured variables. An unmeasured variable is a variable for which plant measurement is not available. All of process variables except those in the Table 4.7 are unmeasured variables in D-train model. Similar to the measured variables, the unmeasured variables need to be associated with a process unit or process stream in the flowsheet diagram of Flowsim based on their physical significance. For example, variable F20, which represents the flowrate of stream s20, is associated with that stream. Unmeasured variable, ex66dt, is associated with heat exchanger HotIP because it represents the temperature difference inside that unit. There are some variables, which can not be logically linked to any one particular unit or a stream. These are called as global data. Example of a global unmeasured variable is the emissions from the D-train plant. The emissions function depends on many different streams and units. So, it is a global variable. Details on entering global variables are given in Appendix C, Section V.

The data stored for unmeasured variables is similar to the data for measured variables except that they do not have plant data and standard deviation values. The data entry screen for an unmeasured variable is shown in Figure C.V.12.

A-1-3. Parameters

The third category of information is the parameters. As described in Chapter 3, a parameter is a quantity in the process model, which changes slowly over time. Typical examples of these are heat transfer coefficients in heat exchangers. The complete list of process parameters for the D-train process is given in Table 4.8. Unlike the measured and unmeasured variables, the parameters can only be associated to a process unit. For

example, the parameter blru is tied to the unit Wboiler because it represents the heat transfer coefficient in that unit. This is shown in Figure C.V.14. Each of the parameters is thus tied to one unit in the flowsheet diagram. It is also possible to have global parameters but the D-train model does not have any. Data stored for a parameter includes its name, description, initial value, lower bound, upper bound and the units. The descriptions and initial values for all the parameters in D-train are given in Table 4.8.

A-1-4. Equality Constraints

The fourth category of information is the equality constraints. These are the mass and energy balance equations and also empirical equations, which are written during process model formulation. The various equality constraints for the D-train process have been described in Chapter 4. The equality constraints also have to be linked to a process unit or a stream in the flowsheet diagram based on the physical significance of that constraint. For example, the constraint equations in Table 4.4 represent the mole and energy balances for the sulfur burner, and are therefore linked to that unit. The equality constraint that specifies the ratio of moles of oxygen to moles of nitrogen in the inlet air stream, s06 is linked to that stream. Equality constraints can also be global if they involve more than one unit or stream. For example, the equality constraint that specifies the emissions from the plant is a global equality because it depends on the flowrates of many different input and output streams. Data entry screen for this equality constraint is shown in Figure C.V.15a. There is an optional scaling factor that can be specified for each constraint for use in the GAMS program.

A-1-5. Inequality Constraints

The fifth category of information is the inequality constraints. These are normally used to recognize the various limitations such as the maximum permissible temperature in a unit or minimum permissible flowrate of a stream. All of the details for the inequality constraints are the same as for the equality constraints. In the D-Train process, there are upper and lower limits for temperature of the reactor inlet streams. These have been included in the form of bounds on the temperature variables.

Thus, the information in the above five categories is associated with either a unit or a stream. It is entered into the Flowsim program or accessed from the program by clicking on the corresponding unit or stream in the flowsheet diagram. For example, the unmeasured variables, measured variables, parameters, equality constraints and inequality constraints for the waste heat boiler can be changed by clicking on the unit 'Wboiler' in the flowsheet diagram.

A-1-6. Constants

The sixth category of information is the constants. Constants are numeric quantities in the process model whose values do not change. For example, area of a heat exchanger and molecular weight of a component are constants. In Flowsim, the constants are stored in logical groups called as 'constant property'. For example, areas of the seven heat exchangers in D-train process are stored together in a constant property called as 'scalar4'. The detailed instructions for creating a constant property are given in Appendix C, Section V. Every constant property is also given a suitable description. For example, the constant property 'scalar4' has the description 'Heat

Exchanger Areas'. This is shown in Figure C.V.19. The constants stored in 'scalar4' are shown in Figure C.V.20. Each constant has a name, a description and a value.

A-1-7. Tables

The seventh category of information is Tables. Process models often have numeric data in a tabular form. For example, in the D-train process, there are four chemical components in the reacting gases. These are O_2, N_2, SO_2, and SO_3. Each of these components has five heat capacity coefficients ranging from a1 to a5. All of this data for the four components can be stored in one table with four rows and five columns. The rows correspond to the components and the columns correspond to the coefficients.

Detailed instructions for creating and modifying a table are given in Appendix C, Section V. Every table has a name and a description. The data for the heat capacity coefficients for the above four components in D-train is stored in table 'Coe_Cp' with description 'Heat capacity coefficients'. This is shown in Figure C.V.16. The number of columns has to be entered before creating the table, and it can not be changed once the table is created. Rows can however be added or deleted. Since there are five heat capacity coefficients for the table 'Coe_Cp', the number of columns is five. Once the table is created, data can be entered in it in a tabular form. The table 'Coe_Cp' with all the heat capacity coefficient values is shown in Figure C.V.17.

A-1-8. Enthalpies

The eighth and final category of information is called 'Enthalpies'. An enthalpy table is a special type of table, which can store only the enthalpy coefficients of chemical components in a process model. These enthalpy tables are used in the

Advanced Process Analysis System to carry out heat exchanger network optimization. The enthalpy formula used here is:

$$\text{Enthalpy} = A0 + A1*T + A2*T^2 + A3*T + A4*T^4 + A5*T^5$$

where A0 to A5 are the enthalpy coefficients and T is the temperature. Any consistent set of units can be used here.

For the D-train process, enthalpy coefficients of O_2, N_2, SO_2, and SO_3 are stored in an enthalpy table called 'Enthalpy1'. Detailed instructions for creating an enthalpy table are shown in Appendix C, Section V. The data in enthalpy table 'Enthalpy1' is shown in Figure C.V.18.

Each row in an enthalpy table stores the enthalpy coefficients for a component in a given temperature range. The temperature range is specified by entering a lower temperature (Tlow) and an upper temperature (Tup). These two temperature limits are also stored in the table as seen in Figure C.V.18. It is possible to have more than one temperature range for a component provided the ranges do not overlap.

This concludes the description of how the information for D-train process model is categorized and entered into the Flowsim program. In the next step of Advanced Process Analysis System, this process model will be used to carry out on-line optimization.

A-2. Online Optimization

The current operating data for the D-train sulfuric acid plant is used to conduct on-line optimization. This includes rectifying gross errors of plant data sampled from distributed control system using combined gross error detection and data reconciliation method, estimating process parameters and reconciling plant data using simultaneous

data reconciliation and parameter estimation method, and optimizing plant operating set points using the updated process and economic models. These three steps are shown in Figure 1.5.

The first step of on-line optimization is combined gross error detection and data validation. This was done in Chapter 4 to validate the D-train process model. The set of reconciled values for measured variables was shown in Table 4.9. Three gross errors were reported as shown in Figure C.VI.14. These are F06-input air flowrate; SO2ppm-SO_2 ppm level in stack gas; and O2percent-molar percentage of O_2 in stack gas. These were attributed to errors in the measuring instruments. Excluding the three errors, the average difference between plant data and reconciled values was 0.47%.

The next step in the online optimization program is the simultaneous data reconciliation and parameter estimation. For the variables with gross errors, the values obtained from plant data are replaced by the reconciled values. The parameter values are assumed to be unmeasured variables. Data reconciliation is now carried out simultaneously for variables and parameters. The updated parameter values are given in Table 5.1 along with their initial values. The updated values represent the most current state of the process and are shown in Figure C.VI.17. In the next step of economic optimization, the parameters are considered as constants.

For the economic optimization problem, two different cases are carried out. Case 1 is to maximize the profit of the sulfuric acid plant. Case 2 is to minimize the emissions from the plant.

For case 1, the profit function used is given in Table 5.2. It lists the various factors that contribute to the net profit of the plant. As shown in Table 5.2, the profit

function is equal to the total value of products (sulfuric acid and steam) subtracted by the cost of raw materials (sulfur feed rate, boiler feed water and dilution water). The sales and cost coefficients were obtained from Chen (1998).

For case 2, the objective is to investigate the limitation of reducing SO_2 discharge (in lbs) per ton of sulfuric acid. EPA requires that this discharge be less that 4 pounds per ton of acid. The objective function is now to minimize the discharge, emiss, which is calculated as shown in Equation 4.17.

Table 5.1 Estimated Parameter Values for the Sulfuric Acid Plant

Parameter	Description	Estimated Value	Initial Point
blrU	Heat Transfer Coefficient in waste heat boiler	0.36	0.364
clrU	Heat Transfer Coefficient in converter boiler	0.236	0.239
effi	Efficiency in converter 1	0.254	0.245
effii	Efficiency in converter 2	0.239	0.233
effiii	Efficiency in converter 3	0.08519	0.0925
Effiv	Efficiency in converter 4	0.0335	0.0533
ex65U	Heat Transfer Coefficient in cold IP exchanger	0.261	0.257
ex66U	Heat Transfer Coefficient in hot IP exchanger	0.26	0.273
ex67U	Heat Transfer Coefficient in superheater-1	0.475	0.582
ex68U	Heat Transfer Coefficient in superheater-2	0.262	0.169
ex71U	Heat Transfer Coefficient in economizer	0.133	0.143

Unit of all heat transfer coefficients in Table 5.1 is 10e-1 KJ/s-K-sqft.

Table 5.2 Profit Function for the Sulfuric Acid Process

Profit Function:

$$Profit = S_{prod}f_{prod} + S_{hp}(f_{shp1}+f_{shp2}) - C_{50}f_{50} - C_{sbfw}f_{sbfw} - C_{dw}f_{dw}$$

Variable	Description	Sale and Cost Coefficients
f_{prod}	Acid Product flow rate	$\$21.34*10^{-3}$/kg
$(f_{shp1}+f_{shp2})$	Superheated steam flow rate	$\$2.34/10^3$ lb
f_{50}	Raw sulfur flow rate	\$54/ton
f_{sbfw}	Boiler feed water flow rate	$\$0.17/10^3$ lb
f_{dw}	Dilution water flow rate	$\$0.05/10^3$ lb

Table 5.3 Comparison of Case I and Case II for Economic Optimization

Key variable		Base Case	Case I- maximize profit	Case II- minimize emissions
Air flowrate	Kmol/s	2.17	2.208	2.215
Sulfur flowrate	Kmol/s	0.24	0.244	0.243
Boiler feed water	Kmol/s	1.91	1.95	1.91
Dilution water	Kmol/s	0.33	0.365	.363
High-pressure steam	Kmol/s	1.71	1.755	1.72
Acid product	Kg/s	25.1	26.04	25.92
SO_2 ppm in stack	ppm	355	380	210.86
Emissions	Lb/ton	3.98	3.79	2.125
Overall profit	\$/sec	0.292	0.308	0.304

Table 5.3 summarizes the results obtained from the above two cases with the base case. The base case is the current operating condition of the plant. In case I, the maximum profit from the plant was \$0.3076 /s, which is an improvement of 4.8% over the base case. The case I profit is shown in Figure C.VI.14. Case II results showed that the SO_2 level in stack gas can be reduced to 210.8 ppm, a 44% reduction. Going from profit maximization in case I to emissions minimization in case II, the air flowrate increased slightly and the sulfur flowrate decreased. The boiler feed water intake was reduced resulting in lower quantity of high-pressure steam production. Sulfur intake also decreased in turn reducing the rate of sulfuric acid production. Lower acid production and lower steam production caused the decrease in overall profit from \$0.308 /sec to \$0.304 /sec, a 1.3% decrease.

Table 5.4 SO_2 Conversions in the Reactor Beds

Conversion %	Case I- maximize profit	Case II- minimize emissions
Converter 1	58.93	59.37
Converter 2	87.49	87.97
Converter 3	97.58	97.94
Converter 4	99.71	99.84

Table 5.4 gives the SO_2 conversions for the converters in the process for both the cases of economic optimization. Conversion in converter 4 is also the overall sulfur conversion in the process. It can be seen that conversion increased for all of the converters to reduce the stack gas emissions.

This concludes the on-line optimization of the D-train sulfuric acid process. The results of case 1 (profit maximization) will be now used to perform heat exchanger network optimization in the next step of Advanced Process Analysis System.

A-3. Heat Exchanger Network Optimization

The Heat Exchanger Network (THEN) program integrates networks of heat exchangers, boilers, condensers and furnaces. It uses pinch analysis as the basis for designing an optimum solution. As a part of the Advanced Process Analysis System, it is used to optimize the heat exchange occurring in the process by a more efficient matching between the process streams.

The sulfuric acid manufacturing process is highly exothermic. The heat released during the reaction is utilized to produce steam from water. This steam is a valuable product of this process. So, the heat exchange is an important consideration in the optimization of the D-train plant. Therefore, this process is an ideal choice for illustration of THEN methodology.

As discussed in Chapter 3, the first step in the implementation of THEN is the identification of streams important for heat integration. These streams are usually input and output streams of the heat exchanging units. This can be used as a criterion for preliminary selection of streams. The screen for selection of streams is shown in Figure C.VII.3. The D-train process has seven heat exchanging units which are listed in Table 5.5, along with their areas.

Table 5.5 Heat Exchanging Units in D-Train Process.

Unit name	Description	Area (10000 sqft)
Wboiler	Waste heat boiler	0.2571
Cboiler	Converter boiler	0.2
Cold IP	Cold interpass heat exchanger	0.32
Hot IP	Hot interpass heat exchanger	0.32
SH1	Superheater1	0.04284
SH2	Superheater2	0.0338
Economizer	Economizer for boiler feed water	0.4005

The input and output streams of these units are s08, s09, s10, s11, s13, s14, s15, s16, s19, s20, s21, s22, s23, s235, and s24. The descriptions for these streams are given in Table 4.2. From the above set of streams, those streams, which are intermediate streams in the process, are omitted. Intermediate streams are those which lie between two heat exchanger units. For example, stream s14 is an intermediate stream between HotIP and ColdIP. Other intermediate streams in the process are s19 and s235. These three streams can be excluded from the analysis.

In the second step of THEN implementation, the necessary stream data is retrieved from the results for case 1 (profit maximization) of on-line optimization. The screen for data retrieval is shown in Figure C.VII.5. The temperature, flowrate and compositions data for the selected process streams is shown in Table 5.6.

Table 5.6 Stream Data for THEN Optimization for D-Train Process

Stream	Temperature	Flowrate (kmol/s)				
	(K)	Total	O_2	N_2	SO_2	SO_3
s08	1321.85183	2.01164	0.19806	1.59096	0.21817	0.00445
s09	650	2.01164	0.19806	1.59096	0.21817	0.00445
s11	892.21573	2.13582	0.14766	1.74411	0.10023	0.14382
s12	692.21117	2.13582	0.14766	1.74411	0.10023	0.14382
s13	784.06513	2.10097	0.11281	1.74411	0.03053	0.21352
s15	505	2.10097	0.11281	1.74411	0.03053	0.21352
s16	345	1.88744	0.11281	1.74411	0.03053	0
s20	695	1.88744	0.11281	1.74411	0.03053	0
s21	736.02923	1.87513	0.1005	1.74411	0.00591	0.02462
s22	684.66023	1.87513	0.1005	1.74411	0.00591	0.02462
s23	693.40773	1.87253	0.0979	1.74411	0.0007	0.02983
s24	506.74692	1.87253	0.0979	1.74411	0.0007	0.02983

Since the temperature changes of the process streams involved are fairly large, temperature-dependent enthalpy coefficients are used instead of constant heat capacities. The temperature-dependent enthalpy equation used is as follows:

$$H = A_0 + A_1 T + A_2 T^2 + A_3 T^3 + A_4 T^4 + A_5 T^5 \qquad KJ/s \qquad (5.1)$$

Values of the coefficients in the above equation for O_2, N_2, SO_2, SO_3 are given in Table 5.7.

The enthalpy coefficients for the streams are calculated based on the enthalpy coefficient data in Table 5.7 and the composition data in Table 5.6. The average enthalpy coefficient for a stream is given by the equation

$$A_{avg} = \Sigma A_i x_i \qquad i = O_2, N_2, SO_2, SO_3 \qquad (5.2)$$

where A_i and x_i are the enthalpy coefficient and mole fraction values for the species i. The screen for calculation of enthalpy coefficients is shown in Figure C.VII.11.

Table 5.7 Enthalpy Coefficients for Individual Chemical Species

Component	A_0	A_1	A_2	A_3	A_4	A_5
O_2	-8846	31.4	-0.0124	2.72E-05	-2E-08	5.39E-12
N_2	-8705	29.3	-0.00051	-1.4E-06	5.06E-09	-2.3E-12
SO_2	-10038	27.1	0.0221	1.89E-06	-1.1E-08	4.26E-12
SO_3	-11091	21.4	0.0605	-2.5E-05	-1.6E-09	3.28E-12

The film heat-transfer coefficient values are needed to calculate heat exchanger areas in the solution network. An average value of 0.05675 KJ/sqft-K-sec is used for all the streams. This is calculated based on the updated values of overall heat transfer coefficients obtained from parameter estimation. The overall heat transfer coefficient of

a heat exchanger is related to the film heat transfer coefficients of the streams by Equation 2.7. Assuming that the film heat transfer coefficients are equal for all the process streams, this equation gives

$$\frac{1}{U_{avg}} = \frac{1}{h_{avg}} + \frac{1}{h_{avg}} = \frac{2}{h_{avg}} \tag{5.3}$$

where U_{avg} is the average of the overall heat transfer coefficients of the heat exchangers. Therefore,

$$h_{avg} = 2 * U_{avg} \tag{5.4}$$

Here, U_{avg} is the average of the updated values of heat transfer coefficients given in Table 5.1.

In the third step of THEN optimization, the process streams are divided into hot streams and cold streams. As described in Chapter 3, a hot stream is a stream that needs to be cooled, and a cold stream is a stream that needs to be heated. Gas stream s11, which comes out of converter 1 needs to be cooled to stream s12 before it enters converter 2. Therefore, s11 is a hot stream with s12 as the target. Similarly, s16, the gas stream that comes out of interpass absorber, needs to be heated to stream s20 before it enters converter 3. Therefore, s16 is a cold stream with s20 as the target. The complete classification of streams into these two categories is given in Table 5.8. This is also shown in Figure C.VII.15.

Finally, the minimum approach temperature is chosen to be 15 K. This allows sufficient driving force between the streams in the heat exchangers. The Heat Exchanger Network program uses all of the above information to apply pinch analysis to the D-train process. The results are described next.

Table 5.8 Hot and Cold Streams for D-Train

Stream type	Source stream	Target stream
Hot	s08	s09
Hot	s11	s12
Hot	s13	s14
Hot	s21	s22
Hot	s23	s24
Cold	s16	s20

The D-train is found to be a 'below the pinch' process as seen in the Grand Composite Curve shown in Figure C.VII.18. The minimum hot utility amount is zero whereas the minimum cold utility amount is 85073.8 KJ/s or 85.07 MJ/s. The heat exchanger network diagram proposed by the program is shown in Figure C.VII.19. This network has 3 heat exchangers and 3 coolers. Detailed information about these heat exchangers and coolers is given in Table 5.9 and Table 5.10 respectively.

Table 5.9 Heat Exchanger Details for D-Train

Heat Exchanger	Hot side stream	Cold side stream	Heat load (KJ/s)	Area (Sqft)
1	s21	s16	0.328e4	2627.3
2	s23	s16	0.113e5	6763.0
3	s13	s16	0.568e4	567.4

Table 5.10 Cooler Details for D-Train

Cooler	stream	Heat load KJ/s
1	s08	0.328e4
2	s11	0.113e5
3	s13	0.568e4

The performance of the new network suggested by the program is compared with performance of the existing network at the optimal operating conditions obtained from case 1 (profit maximization) of the on-line optimization. The existing process does not use any external hot utilities. The cold utility being used is the boiler feed water. The heat absorbed from the process by the boiler feed water is calculated below.

Heat absorbed = enthalpy content of superheated steam + enthalpy content of steam blowdown - enthalpy content of boiler feed water.

= 67.826 + 29.538 + 3.45 - 16.03 = 84.79 MJ/s

This value is comparable to the minimum cold utility amount of 85.07 MJ/s calculated by the program. Hence, it can be concluded that the D-train process is already using the minimum amounts of hot and cold utilities in the existing heat exchanger network and is therefore running at optimum conditions. The existing network has seven heat exchanger units whereas the new network has only six. The initial construction cost of a network is approximately proportional to the number of units. Thus, the network suggested by THEN is an improvement over the existing one because it requires lesser initial investment. However, for the D-train process, implementing this solution is not justified because it does not offer any savings in the operating cost.

Table C.VII.1 shows the complete output file for the above results. This completes the heat exchanger network optimization part of the D-train sulfuric acid process. The final step in the Advanced Process Analysis System is the pollution index calculations, which is described next.

A-4. Pollution Index Program

The pollution index program is used to assess the pollution impact of the process on the environment. It calculates a quantity called as the 'pollution index' to provide a basis for comparison of different processes. In the first step in this program, the input and output streams are identified from the process.

The D-train process has a total of 7 input-output streams as can be seen from Figure 4.4. These streams are shown in Table 5.11. The output streams are further divided into product and non-product streams. The drum blowdown (sbd), and stack gas stream (s25) are non-product streams whereas the acid product stream (sprod) and superheated steams (shp1 and shp2) are product streams.

Table 5.11 Input-Output Streams for D-Train Process

Stream	Description	Total flowrate kmol/s	Type
s06	air	2.20773	input
s25	stack gas	1.84271	non-product
s50	sulfur	0.24405	input
sbd	steam blowdown	0.195	non-product
sbfw	boiler feed water	1.95	input
shp1	superheated steam	1.21995	product
shp2	superheated steam	0.53505	product
sprod	Acid product	0.34834	product

The flowrates and compositions of these streams are obtained from the results of case 1 (profit maximization) of on-line optimization. This is shown in Figure C.VIII.3.

Total flowrates of the streams are shown in Table 5.11. The chemical components present in these streams are S, O_2, N_2, SO_2, H_2O and H_2SO_4. The specific environmental impact potentials of these chemicals are obtained from the report on environmental life cycle assessment of products (1992) published by EPA.

There are nine categories of pollution impact as discussed in Chapter 3. The specific environmental impact potentials for O_2, N_2, S, H_2O and H_2SO_4 are zero for all nine categories of impact. The impact potentials of SO_2 are 1 for acidification and 1.2 for human toxicity effect on air. For the other seven categories, SO_2 impact potentials are zero.

Finally, the relative weighting factors for the nine categories of impact are all assumed to be one. This information is shown in Figure C.VIII.4. The pollution index program calculates the six types of pollution indices for the process, which are shown in Table 5.12 and in Figure C.VIII.5.

Table 5.12 Pollution Index Values for D-train Process (Profit Maximization)

Index type	Value	
Total rate of impact generation	0.00154	impact/time
Specific impact generation	7.322e-4	impact/product
Pollutant generation per unit product	-1.124	mass of pollutant/mass of product
Total rate of impact emission	0.00154	impact/time
Specific impact emission	7.322e-4	impact/product
Pollutant emission per unit product	0.9688	mass of pollutant/mass of product

The program also calculates pollution indices for individual streams. The pollution index value for stream s25, the stack gas is 0.00154. The indices for the other six streams in Table 5.11 are zero. This is shown in Figure C.VIII.6. Thus, the stack gas stream is the only stream that emits pollutants into the environment and needs special attention.

Pollution index calculations are also performed for the case 2 (emissions minimization) of on-line optimization. The results are given in Table 5.13.

Table 5.13 Pollution Index Values for D-Train Process (Emissions Minimization)

Index type	Value	
Total rate of impact generation	0.000858	impact/time
Specific impact generation	4.154e-4	impact/product
Pollutant generation per unit product	-1.1255	mass of pollutant/mass of product
Total rate of impact emission	0.000858	impact/time
Specific impact emission	4.154e-4	impact/product
Pollutant emission per unit product	0.9889	mass of pollutant/mass of product

A comparison of the indices for impact generations and emissions for the two cases clearly show that pollution impacts significantly decreased from case 1 to case 2. However, the emission of pollutants per unit product increased. This is because the reduction in steam production outweighed the decrease in SO_2 content in stack gas. This is also reflected in the decrease in overall profit as shown in Table 5.3. Thus, the pollution index program can be used to compare different process designs and process operating conditions. Appendix C, Section VIII gives detailed instructions about how the pollution index program is used.

This concludes the implementation of Advanced Process Analysis System for the D-train Sulfuric Acid process. The next section describes the results obtained for the E-train sulfuric acid process using the Advanced Process Analysis System.

B. The E-train Sulfuric Acid process

The description for the E-train sulfuric acid process was given in the previous chapter. The flowsheeting and on-line optimization of this process was done by Chen, 1998. The results are briefly summarized here.

In the flowsheet development part, constraint equations were written for the sulfur burner, converters, heat exchangers, absorption towers and for the overall process. From the complete set of process variables, the measured variables and parameters were identified. Measurements for the plant data were obtained from the distributed control system. Gross error detection identified six variables as containing gross errors. These were attributed to instrument errors. Parameter estimation was performed to calculate the updated parameter values, which were then used in economic optimization. The economic optimization was run with several different objective functions. Two of the important ones are case 1, profit maximization and case 2, emissions minimization. The optimal setpoint values of key variables for these two cases are given in Table 5.14.

B-1. Heat Exchanger Network Optimization

The results of case 1 of on-line optimization are used to implement the heat exchanger network optimization. The current heat exchanger network in the E-train process has seven heat exchangers. The important streams for heat integration are given

in Table 5.15 along with their temperatures and flowrates. The chemical components present in these streams are O_2, N_2, SO_2, and SO3. Their individual flowrates are also obtained from Chen, 1998. These flowrates and the enthalpy coefficients in Table 5.7 are used in Equations 5.1 and 5.2 to calculate the enthalpy changes.

Table 5.14 Plant Optimization Results for the E-Train Sulfuric Acid Process (Chen, 1998)

Key variable		Case I- maximize profit	Case II- minimize emissions
Air flowrate	Kmol/s	xxx	xxx
Sulfur flowrate	Kmol/s	0.3456	0.342
Boiler feed water	Kmol/s	xxx	xxx
Dilution water	Kmol/s	0.487	0.483
High-pressure	Kmol/s	xxx	xxx
Acid product	kg/s	36.38	36.09
SO_2 ppm in stack	ppm	xxx	xxx
Emissions	lb/ton	4.00	0.742
Overall profit	$/sec	0.4032	0.3791

(xxx - Monsanto Proprietary Information)

An average value of 0.0748 KJ/sqft-K is used as the film heat transfer coefficient for all the process streams. This value is calculated in the same way as explained for the D-Train process. The overall heat transfer coefficients are obtained from the work of Chen (1998).

The streams in Table 5.15 are divided into hot and cold streams. This classification is given in Table 5.16. Finally, the minimum approach temperature is chosen to be 15 K to ensure sufficient driving force. The results obtained from the heat exchanger network program are described next.

Table 5.15 Stream Data for THEN Optimization for E-train Process

Stream	Description	Temperature (K)	Total Flowrate (kmol/s)
s05	Gas stream exiting from sulfur burner to water boiler	1417.4	2.94
s06	Gas stream from boiler to converter 1	700.03	2.94
s07	Gas stream exiting from convertor1 to superheater 1B(HEX067)	895	2.84
s08	Gas stream exiting from super heater 1B to Convertor2	717.7	2.84
s09	Gas stream exiting from Convertor2 to hot inter-pass heat exchanger (HEX066)	800.9	2.80
s10	Gas stream exiting from hot inter-pass heat exchanger to Convertor3	727.1	2.80
s11	Gas stream exiting from Convertor3 to cold inter-pass heat exchanger (HEX065)	753.8	2.79
s13	Gas stream exiting from economizer 3B to inter-pass absorption tower	433.9	2.79
s14	Gas stream exiting from inter-pass absorption tower to cold inter-pass heat exchanger	397.1	2.47
s16	Gas stream exiting from hot inter-pass heat exchanger to the fourth converter	715.9	2.47
s17	Gas stream exiting from the fourth converter to economizer 4CD	742.1	2.45
s20	Gas stream exiting from economizer 4A to final absorption tower	396.2	2.45

Table 5.16 Hot and Cold streams for E-Train

Stream type	Source stream	Target stream
Hot	s05	s06
Hot	s07	s08
Hot	s09	s10
Hot	s11	s13
Hot	s17	s20
Cold	s14	s17

The E-train is found to be a 'below the pinch' process. The minimum hot utility amount is zero whereas the minimum cold utility amount is 149602.6 KJ/s or 149.6 MJ/s. The new heat exchanger network has 2 heat exchangers and 5 coolers. Detailed information about these heat exchangers and coolers is given in Table 5.17 and Table 5.18 respectively.

Table 5.17 Heat Exchanger Details for E-Train

Heat Exchanger	Hot side stream	Cold side stream	Heat load (KJ/s)	Area (Sqft)
1	s17	s14	0.237e5	23377
2	s17	s14	0.668e3	635

Table 5.18 Cooler Details for E-Train

Cooler	stream	Heat load KJ/s
1	s05	8.7048e4
2	s07	1.9217e4
3	s09	7.8915e3
4	s11	3.1558e4
5	s17	2.237e3

As can be seen in Table 5.17, the two heat exchangers have the same pair of hot and cold streams. The two exchangers are in series and therefore, can be combined into one heat exchanger thus reducing the cost. Thus, the solution found by THEN was not the optimum. This can be attributed to the low approach temperature of 15 K. Lower approach temperature result in lower driving forces for heat exchange, which in turn result in higher areas and more number of units. Therefore, approach temperatures greater than 15 K were tried. At approach temperature equal to 27 K, THEN found an optimum solution with one heat exchanger and five coolers. The heat exchanger had an area of 9673.8 sqft, which is less than 50% of the combined area of the two heat exchangers in Table 5.17. The cooler details are the same as in Table 5.18.

The performance of the new network suggested by the program is compared with that of the existing network at the optimal operating conditions. E-train sulfuric acid process does not use any external hot utility. Also, the amount of cold utility (boiler feed water) currently being used was calculated and was found to be comparable to the minimum requirement of 149.6 MJ/s predicted by THEN.

Hence, it can be concluded that the E-train process is already using the minimum amounts of hot and cold utilities and is running at optimum conditions. The energy efficiency of the process can not be improved further. Nevertheless, THEN was successful in designing a network that used the minimum amount of utilities and had less number of units than the existing network, thus indicating savings in initial construction cost. This completes the heat exchanger network optimization part of the E-train sulfuric acid process. The results of pollution index calculations are discussed next.

B-2. Pollution Index Calculations

The input and output streams of the E-train process are identified from the flowsheet diagram. The sulfur, boiler feed water, dilution water and air are input streams. The superheated steam and sulfuric acid are products whereas steam blowdown and stack gas are non-product streams. The flowrates and compositions of these streams are obtained from Chen (1998).

The chemical components in these streams and their specific environmental impact potentials are the same as for the D-train. The relative weighting factors are assumed to equal to one. The pollution index values obtained for the profit maximization case are given in Table 5.19. This concludes the implementation of the Advanced Process Analysis System for the E-train sulfuric acid process.

Table 5.19 Pollution Index Values for E-Train Process (Profit Maximization)

Index type	Value	
Total rate of impact generation	0.002244	impact/time
Specific impact generation	7.58e-4	impact/product
Pollutant generation per unit product	-7.5885	mass of pollutant/mass of product
Total rate of impact emission	0.002244	impact/time
Specific impact emission	7.58e-4	impact/product
Pollutant emission per unit product	0.9058	mass of pollutant/mass of product

C. Comparison of D-Train and E-Train Processes

The following gives a comparison of the results obtained for the D-train and the E-train process. D-train is a plant that was constructed in 1966 by Chemical Construction Company, and E-train has the latest technology being designed by Monsanto Enviro-Chem Systems and was built in 1992. A summary of the comparison

is given in Table 5.20. On-line optimization was run for both the processes to maximize profit and minimize emissions. The results are given in Tables 5.3 and 5.14. For the D-train, the minimum emissions level was 2.12 lb/ton. This is much lower than the EPA standard of 4 lb/ton but is higher than the value of 0.742 lb/ton obtained by Chen, 1998 for E-train. The reason for this is that the efficiency of the fourth converter bed in E-Train is about 25% higher than the efficiency of the fourth converter bed in D-Train. Higher efficiency leads to higher SO_2 conversion. This results in lesser amount of SO_2 in the stack gas stream and subsequently in lesser emissions level. For the profit maximization case, the overall profit for D-train was $0.308 /sec and it was $0.4032 /sec for the E-train. However, the overall profit is not the proper criterion for comparison because the E-train has a higher production capacity, which can be seen by comparing the input sulfur flowrates and the acid production rates. A better criterion for comparison is the profit per acid production. For profit maximization case, the profit per unit acid production was $0.0118 /kg of acid for the D-train and $0.0110 /kg for the E-train process. Under reduced emissions case, the profit per unit production was $0.0117 /kg for the D-train and it was $0.0105 /kg for the E-train. Thus, it can be seen that on-line optimization gave better profitability for the D-train but better emission control for the E-train process.

The results of pinch analysis for the two processes are very similar. These are shown in Figure 5.9, 5.10, 5.17, and 5.18. Both the processes were found to be using minimum amount of external utilities. For both the processes, the network designed by THEN had 6 units, one less than the existing number of units. The minimum approach temperature was 27 K for the E-train and 15 K for the D-train process. Higher approach

temperature indicates larger temperature differences, which in turn lead to more efficient heat transfer and smaller areas in the exchangers. Thus, the heat exchanger network proposed for the E-train is more efficient than the network for the D-train.

Table 5.20 Comparison of the D-Train and E-Train Processes

	D-Train Process	E-Train Process
Minimum Emissions Level	2.12 lb SO_2 /ton acid	0.742 lb SO_2 /ton acid
Overall Profit (Profit Maximization)	$0.308 /sec	$0.432 /sec
Overall Profit (Emissions Minimization)	$0.304 /sec	$0.3791 /sec
Profit per unit acid production (Profit Maximization Case)	$0.0118 /kg of acid	$0.0110 /kg of acid
Profit per unit acid production (Emissions Minimization Case)	$0.0117 /kg of acid	$0.0105 /kg of acid
Number of Units in the Optimum Heat Exchanger Network	6	6
Minimum Approach Temperature	15 K	27 K
Total Pollutant Impact Generation	0.00154 impact/time	0.002244 impact/time
Pollutant Emission Per Unit Product	0.9688	0.9058

Pollution index values were calculated for both the processes. These are given in Tables 5.12 and 5.19 respectively. A comparison shows that the total impact generation of D-train is 0.00154 impact/time, which is much smaller than the value of 0.002244 impact/time for the E-train process. This suggests that the overall pollution impact of the E-train is larger than that of the D-train. However, to account for the difference in production capacity, the sixth type of index called the ‘pollutant emission per unit product’ needs to be examined. This value of 0.9688 for the D-train is larger than the

value of 0.9058 for the E-train. Thus, a comparison independent of size shows that the E-train is environmentally more efficient than the D-train.

D. Summary

In this chapter, the sulfuric acid process at IMC Agrico was used to demonstrate the Advanced Process Analysis System methodology. Two different processes, the 'D-train' and the 'E-train', were studied to facilitate a comparison. Process models were developed using the process flow diagrams available from IMC Agrico. Plant data was obtained from the distributed control systems with the help of the engineers. Gross errors were identified and replaced with reconciled values. Process parameters were updated to ensure that the model represented the current state of the plant equipment. Plant optimization was performed to maximize profit as well as minimize emissions. The optimum values obtained were used with pinch analysis to reduce external use of utilities. Finally, the pollution indices were calculated to provide a quantitative estimate for the environmental impact of the process. The next chapter presents the conclusions and recommendations.

CHAPTER 6 CONCLUSIONS AND RECOMMENDATIONS

A. Conclusions

An Advanced Process Analysis System was developed that combines flowsheeting, on-line optimization, reactor analysis, pinch analysis and a pollution assessment module into one powerful process analysis tool. This is a new methodology proposed for application to chemical and refinery processes for pollution prevention. Process, economic and environmental data is stored together in a database. For implementation of the individual component programs, the relevant information is automatically retrieved and presented to the engineer. Also, the procedures to carry out each of the individual optimization tasks are incorporated in the program. This lessens the burden on the process engineer and allows him to focus on the process. This methodology was successfully tested on the contact sulfuric acid process at IMC Agrico.

Process model formulation using Flowsim provided valuable insights into the contact process. Flowsim's built-in methodology of associating model information with process units and streams was found to be a very convenient feature.

Combined gross error detection and data reconciliation was used to validate the process model. The results obtained were satisfactory proving that this method is a good alternative when the design data is not available.

On-line optimization was used to maximize profit as well as minimize emissions in the D-train contact process. The SO_2 emissions level could be reduced to 2.12 lb/ton of acid, which is significantly lower than the limit of 4lb/ton set by EPA regulations. Profit maximization case increased the overall profit but resulted in higher emissions

level of 3.79 lb/ton. Thus, a clear trade-off was seen between increase in profit and reduction in emissions. This observation is in agreement with the results for the E-train process (Chen, 1998) given in Table 5.14.

The Heat Exchanger Network Program was successfully used to apply pinch analysis to the contact process. Both versions of this process (D-train and E-train) were found to be using the theoretically minimum amount of external utilities. The heat exchanger networks proposed by THEN were compared with the existing networks and were found to be lesser in area and consequently cheaper in cost.

The WAR Algorithm and the Environmental Impact Theory were used to estimate the pollution impact of the process. The pollution index values provided a good quantitative basis for comparison of different operating conditions as well as comparison of different process designs.

The Advanced Process Analysis System was developed using Visual Basic and MS Access. Visual Basic proved to be a powerful language for integration of different component programs and for providing a user-friendly interface. Storing of information in the form of tables in the MS Access database system offered many advantages. It allowed classification of data based on their logical relationships, facilitated easy exchange of information between the component programs and made the software development very efficient.

B. Recommendations

The reactor analysis program could not be used to describe the packed bed converters of contact process. The program should be improved to incorporate user-supplied rate expressions in the reactor model.

The Heat Exchanger Network program should be expanded to include a subroutine for calculation of the heat network cost using Equation 2.17. This subroutine will accept the values of cost coefficients for the heat exchangers from the user, and use them to calculate the capital cost of the network excluding the piping cost. Also, better graphical software tools can be used to enhance the appearance of the grand composite curve and the network grid diagram in the Heat Exchanger Network program.

The pollution index program can be made more useful by linking it to a library of environmental impact potential values for commonly found chemical species. These values are available in the report by Heijungs (1992).

Optimization of a real chemical or refinery process using GAMS involves hundreds of equations, and it invariably results in many unsuccessful attempts before a good solution is obtained. The on-line optimization program can be improved to provide a better reporting of the errors found in the GAMS output. This will alleviate some effort on part of the engineer to analyze the output files.

APPENDIX A PHYSICAL PROPERTIES OF PROCESS STREAMS

In the sulfuric acid contact plant, there are four streams in the whole process. These are the low-pressure gases (SO_2, SO_3, O_2, and N_2), liquid sulfur, steam (compressed water and superheated vapor), and sulfuric acid liquid. Since the pressure of the gases is lower (range in 1 atm. to 1.4 atm.) throughout the whole process, they are considered as ideal gases. Their enthalpy and heat capacities are calculated by the regression equations from NASA Technical Memorandum 4513 (Mcbride et al., 1993). Also, the enthalpy for liquid sulfur is determined from the regression equation in the condensed state from NASA Technical Memorandum 4513 (Mcbride et al., 1993). However, the pressure of steam stream is as high as 640-730 psi, and the computation formulas of the enthalpy for steam are obtained by mean of a least square fit of the data from the ASME Steam Table (1977). The enthalpy for sulfuric acid liquid is obtained from a two variables (concentration and temperature) polynomial formula fit to the enthalpy-concentration chart (Ross, 1952).

I. The Physical Properties of Gases and Sulfur

For the ideal gases (O2, N2, SO2, SO3) and liquid sulfur, the data to calculate the heat capacity and sensible enthalpy is taken from NASA Technical Memorandum 4513 (Mcbride, et al., 1993). Tables A.1 and A.2 list the heat capacity coefficients for gases used in the balance equations as shown below. The heat capacity coefficients for liquid sulfur are given in Table A.3. The reference state for heat capacities and sensible enthalpies of the species is pressure at 1 Bar and temperature at 298.15 K.

Table A.1. The Coefficients of Heat Capacity and Enthalpy for Ideal Gases at the Temperature Range of 1000-5000 K

	SO2	SO3	O2	N2
a1	5.2451364	7.0757376	3.6609608	2.9525763
a2	1.97042e-3	3.17634e-3	6.56366e-4	1.39690e-3
a3	-8.03758e-7	-1.35358e-6	-1.41149e-7	-4.92632e-7
a4	1.51500e-10	2.56309e-10	2.05798e-11	7.86010e-11
a5	1.05580e-14	-1.79360e-14	-1.29913e-15	-4.60755e-15
b1	-3.75582e4	-5.02114e4	-1.21598e3	-9.23949e2
b2	-1.074049	-11.187518	3.4153618	5.8718925

Table A.2. The Coefficients of Heat Capacity and Enthalpy for Ideal Gases at the Temperature Range of 300-1000 K

	SO2	SO3	O2	N2
a1	3.2665338	2.5780385	3.7824564	3.5310053
a2	5.32379e-3	1.45563e-2	-2.99673e-3	-1.23661e-4
a3	6.84376e-7	-9.17642e-6	9.84740e-6	-5.02999e-7
a4	-5.28100e-9	-7.92030e-10	-9.68130e-9	2.43531e-9
a5	2.55905e-12	1.97095e-12	3.24373e-12	-1.40881e-12
b1	-3.69081e4	-4.89318e4	-1.06394e3	-1.04698e3
b2	9.6646511	12.265138	3.6576757	2.9674747
H_{298}/R	-3.57008e4	-4.75978e4	0.0	0.0

Table A.3. The Coefficients of Heat Capacity and Enthalpy for Liquid Sulfur

	T > 1000 K	T ≤ 1000 K
a1	3.500784	-7.27406e1
a2	3.81662e-4	4.81223e-1
a3	-1.55570e-7	-1.07842e-3
a4	2.72784e-11	1.03258e-6
a5	-1.72813e-15	-3.58884e-10
b1	-5.90873e2	8.29135e3
b2	-1.52117e1	3.15270e2
H_{298}/R	0.0	0.0

The empirical equations for heat capacity $C_P^i(T)$ and sensible enthalpy $h^i(T)$ for each species are:

$$\frac{C^i{}_P(T)}{R} = a_1 + a_2 T + a_3 T^2 + a_4 T^3 + a_5 T^4, \qquad i = SO_2, SO_3, O_2, N_2; \quad KJ/kmol - {}^oK \tag{A.1}$$

and

$$\frac{h^i(T)}{R} = -\frac{H_{298}}{R} + a_1 T + \frac{1}{2} a_2 T^2 + \frac{1}{3} a_3 T^3 + \frac{1}{4} a_4 T^4 + \frac{1}{5} a_5 T^5 + b_1 \qquad i = SO_2, SO_3, O_2, N_2, S(L); \quad KJ/kmol \tag{A.2}$$

where R is molar gas constant, 8.3145 KJ/kmol-^{0}K. T is the temperature in K. The reference state for enthalpy equation is the standard state, 298.15^{0}K and 1 bar. H_{298} is the absolute enthalpy at the standard state for each species given in NASA Technical Memorandum. It is zero for elements and the heat of formation for the species. Eq. A.2 is used to calculate the sensible enthalpy of a species with reference state as temperature 298.15 K and pressure at 1 Bar. The units of enthalpy and heat capacity are dependent on the units of the constant R.

II. The Physical Properties of Steam

The steam properties are divided into two groups, compressed water from stream SS1 to SS4 and superheated vapor in stream SS5 and SS7. For the compressed water, the variation of enthalpy in the operating pressure range is not significant. It is assumed that its enthalpy is only a function of temperature. The polynomial function of enthalpy for compressed water is regressed from ASME Steam Table data (Meyer, et al., 1977) shown as following:

$$h = 1.0861707T - 5.63134\times10^{-4}T^2 + 8.34491\times10^{-7}T^3 - \frac{1.14266\times10^4}{T} + \frac{1.01824\times10^6}{T^2}, \quad BTU/lb \tag{A.3}$$

where the unit of temperature T is ^{o}F, and the reference state of the enthalpy is 298.15 K and 1 atm. The regression ranges are 200-500 ^{o}F and 600-750 psi. The comparison of prediction and tabulated data is shown in Figure A.1. The symbol and solid line in the figure represent the tabulated data and formula prediction respectively. The largest relative difference between prediction value and tabulated data is 0.01%.

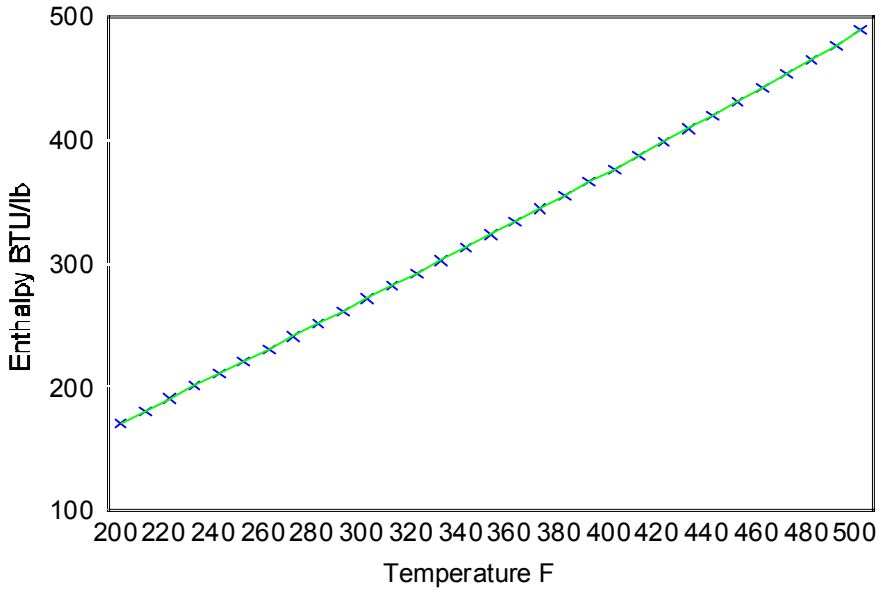

Figure A.1 The Comparison of Prediction and Tabulated Data
for the Enthalpy of Compressed Water

The superheated vapor is fit to a third order polynomial in temperature and second order polynomial in pressure with ASME steam table data (Meyer et al., 1977). The regression function is:

$$\begin{aligned} h = \; & 5.32661\,T - 0.2839015\,P - 7.352389\times10^{-3}\,T^2 \\ & + 3.581547\times10^{-6}\,T^3 - 7.289244\times10^{-5}\,P^2 \\ & + 4.595405\times10^{-4}\,TP, \; BTU/lb \end{aligned} \tag{A.4}$$

where the unit of temperature is ^{o}F and unit of pressure is psia. The reference state of the enthalpy is 298.15 K and 1 atm. The regression ranges are 200-500 F for temperature and 600-750 psia for pressure. The comparison of prediction and tabulated data is shown in Figure A.2. The symbol and solid line in the figure represent the

tabulated data and formula prediction respectively. The largest relative error between prediction and tabulated data is 0.15%.

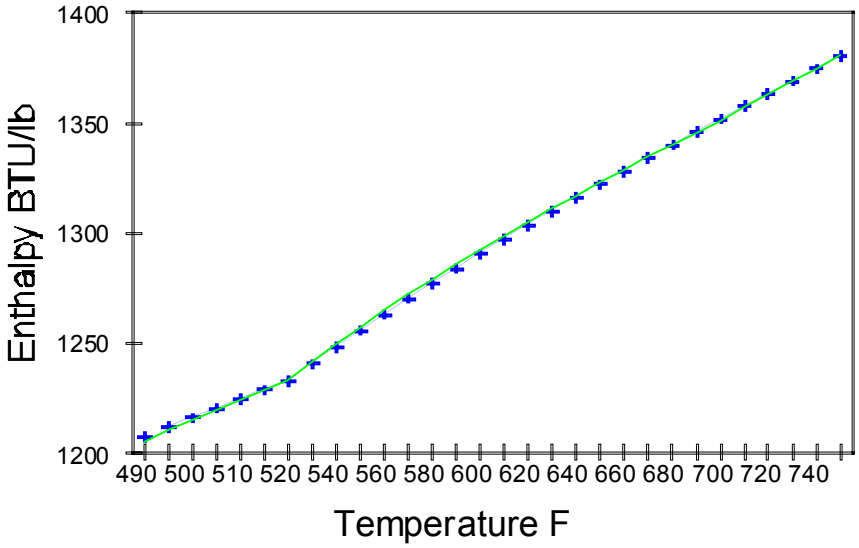

Figure A.2 The Comparison of Prediction and Tabulated Data for Enthalpy of Superheated Vapor at 600 psi

III. The Physical Properties of Sulfuric Acid

For the sulfuric acid stream, one of the difficulties in writing the energy equations is using the right thermodynamic model to calculate the enthalpy of the sulfuric acid system. One possible approach, which was, used by Crowe (1971), Doering (1976) and Richard (1987) is using RENON activity equation, which leads to relatively complicated equations. Also, the temperatures predicted by this method did not agree with the design data well (Zhang, 1993). Besides, the variations in temperature and concentration of the sulfuric acid system are very small in comparison to the range of application of the thermodynamic equation. Therefore, it was decided

that the enthalpy of sulfuric acid system could be regressed directly from enthalpy-concentration chart given by Ross (1952). By inspecting the data of the chart, it was found that the enthalpy at the same concentrations is almost a linear function of temperature. Therefore, the enthalpy data was regressed into a two-variable function, linear in temperature and second order in concentration. The regression result is:

$$h = -145.8407C + 9.738664e\text{-}3T + 8.023897e\text{-}3TC + 83.61468C^2 + 60.19207 \quad \text{(A.5)}$$

For $60^oC \le T \le 120^oC$; $0.90 \le C \le 1.00$

where the unit of T is °C, and C is the weight fraction of sulfuric acid. The unit of enthalpy, h, is kilogram calorie per gram mole, where one gram mole of solution is defined as:

$$80.06x+18.02(1-x) \text{ g}$$

and x is mole fraction of SO3 defined as:

$$x = \frac{\frac{C}{98.08}}{\frac{2C}{98.08}+\frac{1-C}{18.02}} \quad \text{(A.6)}$$

The standard states were chosen as h_{H2O}=0.0 kcal/gmol and $h_{100\%H2SO4}$=-1.70 kcal/gmol at T=16°C. The enthalpy calculated in Eq. A.5 is referenced to this standard state. The regressed prediction is compared with the chart data as shown in Figure A.3. The largest relative predicted error for this enthalpy is 3%.

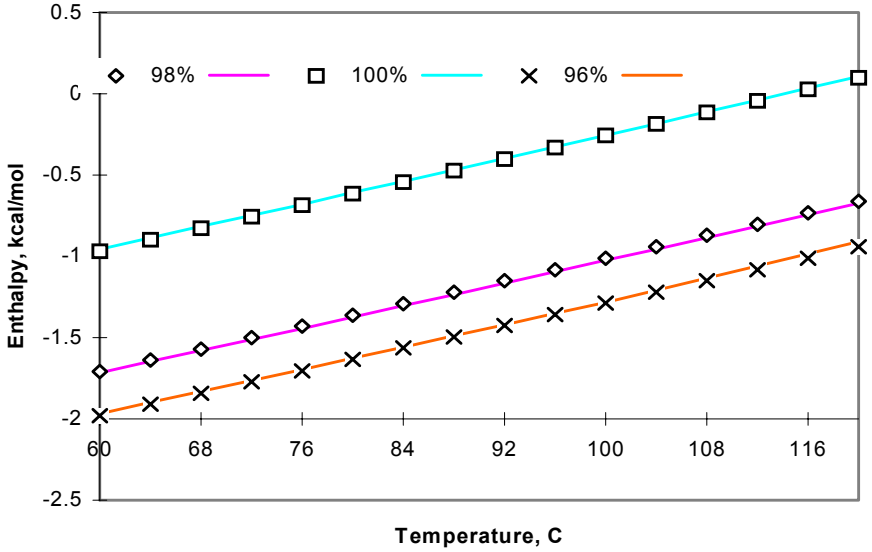

Figure A.3 The Comparison of Prediction and Tabulated Data
for Enthalpy of Sulfuric Acid solution

The information in this appendix is from the dissertation of Xueyu Chen (Chen, 1998). It is an integral part of this study and is included for that reason.

APPENDIX B. KINETIC MODEL FOR THE CATALYTIC OXIDATION OF SO_2 TO SO_3

Doering (1976) developed a kinetic model for the catalytic oxidation of sulfur dioxide to sulfur trioxide over vanadium pentoxide catalyst. This model was modified for the contact sulfuric acid plant design by Monsanto Enviro-Chem System, Inc. and is discussed below. The oxidation of SO_2 to SO_3,

$$SO_2 + \frac{1}{2}O_2 \rightleftharpoons SO_3 \qquad \text{(B.1)}$$

is carried out over a vanadium pentoxide catalyst promoted by potassium salts. Extensive efforts have been directed at correlating the reaction rate data for this reaction. Doering used Harris and Norman's rate equation for this reaction with Monsanto Type 11 and 210 catalysts. Also, this rate equation was applied to the new LP-110 and LP-120 vanadium pentoxide catalysts which are being used by IMC Agrico's Uncle Sam plants (Richard, 1987). The difference between the old and new catalysts is only their shapes, and the former had a cylindrical shape, while the latter utilizes the Rasching ring form. The difference in shape does not affect the intrinsic reaction rate equation; it only changes the diffusional effect. The new catalysts have 45% to 50% lower pressure drops with the same conversion performance as the old catalysts. The intrinsic rate equation given by Harris and Norman (1972) is:

$$r_{SO_2} = \frac{P^{o}_{SO_2} P^{o}_{O_2}{}^{1/2}}{(A + BP^{o}_{O_2}{}^{1/2} + CP^{o}_{SO_2} + DP_{SO_3})^2} \left[1 - \frac{P_{SO_3}}{K_p P_{SO_2} P_{O_2}{}^{1/2}} \right] \qquad \text{(B.2)}$$

where r_{SO2} is the intrinsic reaction rate with units of lb-mol of SO_2 converted per hour per lb catalyst, and K_p is the thermodynamic equilibrium constant with units of $atm^{-1/2}$. P_{O2}, P_{SO2}, and P_{SO3} are interfacial partial pressure of O_2, SO_2, and SO_3 in units of atm; and P^0_{O2} and P^0_{SO2} are interfacial partial pressures of oxygen and sulfur dioxide at zero conversion under the total pressure of reactor, in units of atm. The thermodynamic equilibrium constant can be calculated by:

$$Log_{10}K_P = 5129/T - 4.869, \quad T \text{ in K} \tag{B.3}$$

The parameters A, B, C and D in the rate equation, Eq. B.2, were derived from least square regression of the rate data by Harris and Norman (1972). They are the function of temperature in K as following:

Catalyst Type LP-110	Catalyst Type LP-120	
$A = \exp(-6.80 + 4960/T)$	$A = \exp(-5.69 + 4060/T)$	
$B = 0$	$B = 0$	(B.4)
$C = \exp(10.32 - 7350/T)$	$C = \exp(6.45 - 4610/T)$	
$D = \exp(-7.38 + 6370/T)$	$D = \exp(-8.59 + 7020/T)$	

The intrinsic rate equation is the rate under the conditions on the catalyst surface. To determine the real reaction rate from the conditions of bulk-gas stream, the following four transport phenomena need to be considered:

1) Diffusion of reactants and product through the pores within the catalyst.

2) Pellet internal temperature gradient.

3) Bulk-gas to pellet temperature gradient.

4) Bulk-gas to pellet concentration gradients.

Diffusion: The effect of diffusion through the catalyst pores is taken into account by multiplying the intrinsic reaction rate by an effectiveness factor, E_f, to get the actual rate, r_{SO3}, i.e.,

$$r_{SO3} = r_{SO2} E_f \qquad (B.5)$$

In Doering's work (1976), followed by Richard (1987) and Zhang (1993), the effectiveness factor for this reaction was calculated by the empirical formulas. After examining the formulas, some inaccuracy was found. Therefore, the model has been modified; and the effectiveness factor was changed to a process parameter to be estimated by plant data for each converter.

Pellet Temperature Gradients: The intraparticle heat conduction could cause a temperature gradient within the catalyst pellet if the heat conduction is slow relative to the rate of heat generation due to reaction. Based on the criterion developed by Carberry for determining temperature gradient within a catalyst particle, Doering (1976) concluded that a significant temperature gradient does not exist. Therefore, it is assumed that the temperature gradient within these catalyst particles has an insignificant effect on the reaction rate for this system.

Bulk Gas to Pellet Temperature Gradient: The bulk gas temperatures in the packed bed reactors are measured. The uniform pellet temperature can be determined if the temperature gradient across the external film of the catalyst surface can be calculated. Yoshida et al. (1962) presented a method of estimating the temperature gradient using the following equation:

$$\Delta T = \frac{r_{SO_3}\rho_B \Delta h_{rxn}^{SO_3} Pr^{2/3}}{a_v \phi C_p G j_H} \qquad \text{(B.6)}$$

where:

ΔT = temperature drop from a catalyst surface to the bulk gas, K

r_{SO3} = actual reaction rate of SO_2, lb-mol/hr-lb Cat.

$\Delta H_{rxn}^{SO3} = 1.827\times(-24{,}097-0.26T+1.69\times10^{-3}T^2+1.5\times10^{5}/T)$

= heat of reaction of SO_2, Btu/lb-mole

C_p = gas heat capacity, Btu/lb-^oK

Pr = Prandtl number = 0.83

$\rho_\beta = (1-\epsilon)\rho_{app}$, lb/ft^3 = Bulk density

ϕ = shape factor = 0.91

G = mass velocity of gas, lb/hr-ft^2

a_v = Specific surface of pellet = $6(1-\epsilon)/d_p$, FT^2/FT^3

$j_H = 0.91\ Re^{-0.51}$

$Re = G/(a_v\phi\mu)$

μ = gas viscosity, lb/ft-hr

The bulk density and spherical diameters of catalysts are given in Table B.1 (Zhang, 1993).

Table B.1 Catalyst Physical Properties

	L-110	L-120
Bulk Density, lb/ft^3	33.8	38.1
Spherical Diameter, ft	0.0405	0.054

The heat capacities of the gas streams are given in Appendix A. The critical gas viscosity were calculated by the following equations (Bird, et al., 1960):

$$\mu_c = 61.6\frac{(M_w T_c)^{1/2}}{V_c^{2/3}},\ Micropoise$$
$$= 0.0149\frac{(M_w T_c)^{1/2}}{V_c^{2/3}},\ lb_m/ft\text{-}hr \qquad \textbf{(B.7)}$$

where Mw is the molecular weight. Tc and Vc are the critical temperature in K and volume in CC per gram-mol respectively. The viscosity for temperature T can be calculated by (Zhang, 1993):

$$\mu = \sum \mu_c^i F_{Tr}^i y_i \qquad \textbf{(B.8)}$$

where y_i's are molar fractions of gas components, i= SO_2, SO_3, O_2, N_2. F_{tr}^{i}'s are temperature factors for gases which can be calculated by (Zhang, 1993):

$$F_{Tr}^i = 1.058 \times Tr_i^{0.645} - \frac{0.261}{(1.9\,Tr_i)^{0.9\log_{10}(1.9\,Tr_i)}} \qquad \textbf{(B.9)}$$

where Tri's are the relative temperature of gas components i.

Bulk-gas to pellet concentration gradients: Based on the work of Yoshida, et al. (1962), Doering(1976) concluded that the partial pressure gradients from the bulk gas to the pellet was sufficiently small to be neglected.

Summary: The kinetic model for the oxidation of SO2 to SO3 is given in this appendix. The equations required to determine the reaction rate are summarized in Figure B.1, and

$$\text{Reaction:} \qquad SO_2 + \frac{1}{2}O_2 \leftrightharpoons SO_3$$

SO_2 conversion rate equation:

$$r_{SO_2} = \frac{P^0_{SO_2}\, P^{0\,1/2}_{O_2}}{(A + BP^{0\,1/2}_{O_2} + CP^0_{SO_2} + DP_{SO_3})^2}\left[1 - \frac{P_{SO_3}}{K_p P_{SO_2} P_{O_2}^{1/2}}\right]$$

r_{SO_2} = rate of reaction, $\frac{lb\ mole\ of\ SO_2\ converted}{hr\text{-}lb\ catalyst}$

$P_{O_2}, P_{SO_2}, P_{SO_3}$ = interfacial partial pressures of O_2, SO_2, SO_3, atm

$P^0_{O_2}, P^0_{SO_2}$ = interfacial partial pressures of O_2 and SO_2 at zero conversion under the total pressure at the point in the reator, atm

K_p = thermodynamic equilibrium constant, $atm^{-\frac{1}{2}}$

$$Log_{10}K_P = 5129/T - 4.869, \qquad T \text{ in } {}^oK$$

A, B, C, D are function of temperature T:

Catalyst Type LP-110:

$$A = e^{-6.80+4960/T}, \quad B = 0, \quad C = e^{10.32-7350/T}, \quad D = e^{-7.38+6370/T}$$

Catalyst Type LP-120:

$$A = e^{-5.69+4060/T}, \quad B = 0, \quad C = e^{6.45-4610/T}, \quad D = e^{-8.59+7020/T}$$

Figure B.1 Rate Equation for the Catalytic Oxidation of SO_2 to SO_3 Using Type LP-110 and LP-120 Vanadium Pentoxide Catalyst

they are incorporated in GAMS program. This kinetic model precisely describes the relation of the reaction operation conditions, such as temperature, pressure, concentrations of gas components. In addition, the modification of reaction effectiveness factors determined from empirical formulas with the assumption of pseudo first order reaction to plant parameters improves the performance of the kinetic model in GAMS program.

The information in this appendix is from the dissertation of Xueyu Chen (Chen, 1998). It is an integral part of this study and is included for that reason.